WRDC-TR-90-3037
VOLUME III

Multivariable Methods for the Design, Identification, and Control of Large Space Structures

Vol. III. A Study of the Integrated Control/Structure Design Optimization Problem for Large Flexible Structures

M. D. McLaren
G. L. Slater

University of Cincinnati
Dept of Aerospace Engineering & Engineering Mechanics
Cincinnati, Ohio 45221-0070

DTIC
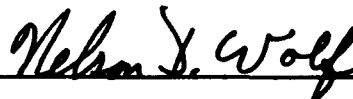ELECTE
SEP 18 1990
S B

AD-A226 526

NOTICE

When Government drawings, specifications, or other data are used for any purpose other than in connection with a definitely Government-related procurement, the United States Government incurs no responsibility or any obligation whatsoever. The fact that the Government may have formulated or in any way supplied the said drawings, specifications, or other data, is not to be regarded by implication, or otherwise as in any manner, as licensing the holder or any other person or corporation; or as conveying any rights or permission to manufacture, use, or sell any patented invention that may in any way be related thereto.

This report is releasable to the National Technical Information Service (NTIS). At NTIS, it will be available to the general public, including foreign nations.

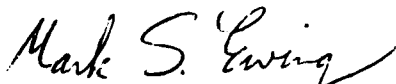This technical report has been reviewed and is approved for publication.

VICTORIA A. TISCHLER
Project Engineer
Design & Analysis Method. Group

NELSON D. WOLF, Technical Manager
Design & Analysis Methods Group
Analysis & Optimization Branch

FOR THE COMMANDER

MARK S. EWING, Maj, USAF
Chief, Analysis & Optimization Branch
Structures Division

"If your address has changed, if you wish to be removed from our mailing list, or if the addressee is no longer employed by your organization please notify WRDC/FIBRA, Wright-Patterson AFB OH 45433-6553 to help us maintain a current mailing list".

Copies of this report should not be returned unless return is required by security considerations, contractual obligations, or notice on a specific document.

REPORT DOCUMENTATION PAGE

Form Approved
OMB No. 0704-0188

1a. REPORT SECURITY CLASSIFICATION	1b. RESTRICTIVE MARKINGS
UNCLASSIFIED	

2a. SECURITY CLASSIFICATION AUTHORITY	3. DISTRIBUTION/AVAILABILITY OF REPORT
	Approved for public release;
2b. DECLASSIFICATION/DOWNGRADING SCHEDULE	distribution is unlimited.

4. PERFORMING ORGANIZATION REPORT NUMBER(S)	5. MONITORING ORGANIZATION REPORT NUMBER(S)
	WRDC-TR-90-3037, Volume III

6a. NAME OF PERFORMING ORGANIZATION	6b. OFFICE SYMBOL (If applicable)	7a. NAME OF MONITORING ORGANIZATION
University of Cincinnati		Flight Dynamics Laboratory (WRDC/FIBRA) Wright Research and Development Center

6c. ADDRESS (City, State, and ZIP Code)	7b. ADDRESS (City, State, and ZIP Code)
Cincinnati, Ohio 45221-0070	Wright-Patterson Air Force Base, Ohio 45433-6553

8a. NAME OF FUNDING/SPONSORING ORGANIZATION	8b. OFFICE SYMBOL (If applicable)	9. PROCUREMENT INSTRUMENT IDENTIFICATION NUMBER
		F33615-86-C-3216

8c. ADDRESS (City, State, and ZIP Code)	10. SOURCE OF FUNDING NUMBERS			
	PROGRAM ELEMENT NO.	PROJECT NO.	TASK NO.	WORK UNIT ACCESSION NO.
	61102F	2302	N5	04

11. TITLE (Include Security Classification) Multivariable Methods for the Design, Identification, and Control of Large Space Structures - Vol III. A Study of the Integrated Control/Structure Design Optimization Problem for Large Flexible Structures

12. PERSONAL AUTHOR(S)
M. D. McLaren and G. L. Slater

13a. TYPE OF REPORT	13b. TIME COVERED	14. DATE OF REPORT (Year, Month, Day)	15. PAGE COUNT
Final	FROM 87 July TO 89 Feb	1989, July	102

16. SUPPLEMENTARY NOTATION

17.	COSATI CODES		18. SUBJECT TERMS (Continue on reverse if necessary and identify by block number)
FIELD	GROUP	SUB-GROUP	Large Space Structures; Multi-Variable Control;
			Control Structure Interaction

19. ABSTRACT (Continue on reverse if necessary and identify by block number)

A comparison of optimal and suboptimal estimation applied to large flexible structures under perfect and imperfect model information conditions is presented. The filters estimate the modal positions and velocities of a simple pinned-pinned beam. Among the types of estimators investigated are full and reduced-order centralized estimators, reduced-order decentralized estimators, and one-mode and two-mode sensitivity-shaped estimators. The suboptimal estimators are shown to have lower position rms error values than the optimal estimator when 20% errors in the structural frequencies are present. The sensitivity-shaped estimators produce more accurate positon estimates when velocity sensors are used than any of the reduced-order Linear Quadratic (LQ) centralized or decentralized estimators. A method for choosing the gains of the sensitivity-shaped estimators is given. Robustness of the system is discussed using a proposed phase-shaping method and the Lyapunov method. The closed-loop system with the one-mode sensitivity-shaped filter is proven to be marginally stable with the former

(CONTINUED ON REVERSE)

20. DISTRIBUTION/AVAILABILITY OF ABSTRACT	21. ABSTRACT SECURITY CLASSIFICATION	
☒ UNCLASSIFIED/UNLIMITED ☐ SAME AS RPT. ☐ DTIC USERS	UNCLASSIFIED	
22a. NAME OF RESPONSIBLE INDIVIDUAL	22b. TELEPHONE (Include Area Code)	22c. OFFICE SYMBOL
Victoria A. Tischler	513-255-6992	WRDC/FIBRA

DD Form 1473, JUN 86   *Previous editions are obsolete.*   SECURITY CLASSIFICATION OF THIS PAGE

ITEM 19.   ABSTRACT (CONTINUED)

method and asymptotically stable with the latter method, provided controller gains
satisfy certain outlined requirements. A brief investigation of controller types
and resulting closed-loop system response is included. A numerical sensitivity
analysis with respect to variations in structural frequencies illustrates the
relative frequency insensitivity of the suboptimal estimators as compared with
the optimal estimators.

FOREWORD

This final report was prepared by the University of Cincinnati, Cincinnati, Ohio for the Analysis and Optimization Branch (FIBR) of the Wright Research and Development Center. The work was performed under Contract F33615-86-C-3216 which was initiated under Project No. 2032, "Structures", Task No. N5, "Structural Dynamics and Controls". The objective of this contract was to develop mathematical algorithms for the integration of structural dynamics and controls with particular reference to the design of large space structures. This report, which is Vol III of a three volume final report, is entitled "A Study of the Integrated Control/Structure Design Optimization Problem for Large Flexible Structures". The program manager was Dr G. L. Slater of the Aerospace Engineering Department. He was supported by Mr M. D. McLaren a graduate student in the same department. In FIBR V. A. Tischler was the project monitor while Dr V. B. Venkayya initiated the program and provided overall program direction.

DTIC
COPY
INSPECTED
6

Accession For	
NTIS GRA&I	☑
DTIC TAB	☐
Unannounced	☐
Justification	
By	
Distribution/	
Availability Codes	
Dist	Avail and/or Special
A-1	

iii

Acknowledgments

TABLE OF CONTENTS

LIST OF FIGURES

Chapter 1

Introduction

With the prospects of space travel so near, evaluation and design of structures suit-
able for a space environment is needed. These structures include satellites, the space
station, space antennas, and others, and are grouped in a category termed Large
Flexible Space Structures (LFSS). Since many LFSS are characterized by low damp-
ing, vibration control is required to achieve sufficiently accurate shape control. There
are many ways to approach vibration control, including passive damping and active
damping. In the case of active damping through modal control, specific modes which
contribute significantly to the unwanted motion are selectively damped through the
use of active controls. A sensor senses the motion and processes it through a filter,
and a controller sends the signal to an actuator in an effort to counterbalance the
undesired modes.

The difficulties encountered in the evaluation and design of LFSS control systems
stem from the attempts to accurately model such a structure. Using modal control
involves formulating the model in modal form. Technically, structural modes are
a mathematical representation of actual motion. The motion is actually composed
of an infinite number of modes, for which controllers are impossible to design or
to implement. Furthermore, retaining a large number of modes is not practical for
computational purposes. Nevertheless, a "truth" model of the LFSS must contain
a reasonable number of modes for accurate modelling of the dynamics and inherent

characteristics of the LFSS. This modelling process is easier said than done – these structures are difficult to test on earth due to their size and the lack of a suitable space environment. The structural frequencies of LFSS are generally low, hence easily excited, and closely spaced which creates difficulties in modelling due to the inability to distinguish the modes of the structure. Many experiments [1-3] are being executed on scaled-down models, some with zero gravity springs, to determine the characteristics of these structures – mainly, frequencies of the structural modes, mode shapes, and damping of the structure. Since these experiments contain errors, as well as the fact that the dynamics and characteristics of the structure may change with time, there are uncertainties in the parameters of these structures. Therefore, the truth model of the LFSS may not adequately represent the structure through all operational conditions.

One way to improve the truth model is to introduce adaptive estimation, which modifies the truth model through actual information obtained. Unfortunately, convergence to a solution is not always guaranteed. Also, adaptive estimation tends to be more complex and increases computational difficulties.

Another method is to design a control system to be "robust" to modelling uncertainties. In this manner, the closed-loop system will be asymptotically stable in the presence of these uncertainties. Two major problems are encountered with robust designs. The first is that so many assumptions are made that the reality of the LFSS hardware is evaded and the control system, under these circumstances, may not be robust. It is assumed in this study that the actuators and sensors are point masses, velocity sensors are employed, and the dynamics of the actuators and sensors are much faster than those of the dominant modes of the structure itself, allowing the higher frequencies to be filtered out. Also, all actuators and sensors are collocated – in this way, the force can be applied directly to the point where the measurement of motion was taken. Mathematically, this collocation ensures the plant "positive realness" and, hence, desirable stability properties [4]. One of these properties states that for a positive real plant, if the feedback design is strictly positive real, then the closed-loop system is robust. Thus, although the actuator and sensor pairs or groups of pairs may have mass and may have "lower" frequency dynamics, it is hoped that

2

the effects get washed out with the guarantees of robustness. Furthermore, the advancement of technology in space actuators and sensors will hopefully reduce many concerns. The second limitation with robust designs is that the control system may be designed to be so insensitive to parameter changes that performance is not optimal. There is indeed a tradeoff between sensitivity and performance, which is addressed in Chapter 4.

To implement modal control [5], estimates of the modal positions and velocities of the structure are required. Full and reduced-order centralized Kalman filters have been reviewed extensively in [6-8]. The stability and robustness of decentralized filters is discussed in [9- 14]. These studies do not emphasize Single-Input Multi-Output (SIMO) systems which are a subset of Multi-Input Multi-Output (MIMO) systems. This study focuses on the performance of optimal and suboptimal filters under such circumstances with perfect and imperfect structural frequency information. The estimators evaluated here include the optimal Kalman filter, which is a full-order centralized filter, centralized reduced- order Kalman filters, a decentralized filter in which error amplitude frequency-shaping occurs, and sensitivity-shaped filters designed to reduce sensitivities to variations in the structural frequencies. This investigation includes systems with and without modelled noise.

Chapter 2 introduces optimal and suboptimal estimators. Chapter 3 contains modal analysis, problem formulation, and perfect model information results for centralized and decentralized estimators. Section 4.1 proposes one-mode and two-mode sensitivity-shaped filters which are less sensitive to errors in the structural frequencies. The sensitivity-shaped filter performance is compared with the centralized and decentralized estimators of Chapter 3 under structural frequency variations of 20 %. Section 4.2 presents basic concepts of positivity [4]. The robustness of the system under structural frequency errors with the one-mode sensitivity-shaped estimator is analyzed using a phase-shaping method of Section 4.3 and the Lyapunov method of Section 4.4. The phase-shaping method is based on the principle of positivity [4] with collocated actuators and sensors. It is a conservative method which requires the phase of the feedback loop estimator transfer functions to lie between ± 90 degrees, along with conditions on the controller gains, for the closed-loop system to be asymptoti-

cally stable. The sensitivity-shaped filter is shown to be at least marginally stable by this method. The Lyapunov method requires the choice of a controller gain to satisfy the Lyapunov equations, given the filter gains. The sensitivity-shaped filter is guaranteed to be asymptotically stable by this method, as long as the controller gains are chosen accordingly. The problem is posed in this manner to evaluate the estimators relatively independently of the controllers. Section 4.5 contains a closed-loop system analysis using controller gains chosen via the Lyapunov method of Section 4.4. In section 4.6, a sensitivity analysis with respect to variations in the structural frequencies up to 20 % is included for each type of estimator. The performance criteria used is the root mean square (rms) of the error. The suboptimal filters are shown to be less sensitive in the position estimates. Chapter 5 summarizes the comparison of the performance of various estimator types under perfect and imperfect model information conditions. Suggestions for future research in the area of estimator types applied to LFSS are offered.

Chapter 2

Opitmal And Suboptimal Estimation Theory

2.1 Introduction to Estimator Types

Since not all desired parameters of a LFSS are known, it is necessary to estimate them. An introduction to different types of estimators is presented. Imagine a generic system in the real world, call it system G. Suppose it is composed of many different components with generic parameters, call them P, all varying in time and space. To be able to predict anything about system G, a mathematic model G_m representing the physics behind it must be formulated. Since the actual modelling of such a system may be difficult, if not impossible, many simplifications are made to enable realistic implementation into a computer. A mathematical set of equations now exists representing system G and its motion with respect to some reference point of view as it moves through time and space. Since the model G_m is simplified, eventually the dynamics of G_m will depart from the actual dynamics of system G; this may be corrected using some type of measuring devices and feeding the measurements to G_m. Perhaps parameters P are desired that are not directly measurable quantities. Perhaps more accurate information is needed of parameters P in between the measurement updates. It is for these reasons that estimation of system G parameters P is introduced.

5

The system G can often be represented as a finite-dimensional linear time-invariant system in state space form as

$$\dot{x}(t) = Ax(t) + Bu(t) \qquad (2.1)$$

$$y(t) = Cx(t) \qquad (2.2)$$

with x the state vector, u the input vector, and A, B and C the constant plant, control and measurement matrices, respectively. Here, the parameters P to be estimated are the states $x = [x_1, x_2, \ldots x_n]^T$. To estimate the states, a filter is formulated as

$$\dot{\hat{x}}(t) = A_F\hat{x}(t) + B_Fu(t) + K_F(y(t) - \hat{y}(t)) \qquad (2.3)$$

$$\hat{y}(t) = C_F\hat{x}(t) \qquad (2.4)$$

where $\hat{x}$ is the estimated state vector, A_F, B_F and C_F are the constant estimator plant, control and measurement matrices, respectively, $\hat{y}$ is the estimated measurement vector, and K_F is the filter gain. K_F may be, in general, time-varying but will be assumed time-invariant for this study.

The problem at hand is the choice of K_F which will determine the state estimate $\hat{x}$ and, hence, the performance of the filter. It is proposed to investigate several methods of determining K_F. The optimal filter, in the sense of minimizing the mean square value of the error $e = x - \hat{x}$ for a given set of known model parameters, is given by Kalman [6]. This is a full-order centralized filter whereby all information is processed centrally in the optimal manner stated above. Quite often, a full-order Kalman filter is too cumbersome and costly to implement on a computer. A reduced-order Kalman filter is much more practical in this case.

Suppose now that central processing is not desirable or possible, or that computation costs are to be minimized. Suppose system G exists in such a way as to form neat, concise subsets of the states, all combining to form the total system G. A separate filter could be designed for each subset of system G which would process information locally – information could then be contained within each subset without the need to feed information over the entire system G. Such a set of filters is a decentralized filter. Advantages of a decentralized filter include enforcement of a desired architecture, and usually a reduction in order of the filters needed to represent each subsystem. Because of this reduction in order, a decentralized filter is easier to design and implement; reduction in cost is an important factor here. Of course, the decentralized filter will not be optimal in the sense of minimizing the mean square error if compared to the centralized filter, but the above advantages may justify the degradation of performance.

The time-invariant filters described above are categorized as optimal (centralized full-order filters) or suboptimal (reduced-order filters and decentralized filters). Also to be considered are filters where K_F is not the Kalman gain, but rather is a gain used to shape filter responses or some other set of specified criteria.

2.2 Centralized Estimation Theory

The full-order centralized estimation equations are given by equations (2.3) and (2.4) where $\hat{x} = [\hat{x}_1, \hat{x}_2, ..., \hat{x}_n]^T$ and n is the order of the modelled system G_m. The optimal gain, in the sense of minimizing the mean square error, given a set of model parameters, is the Kalman gain [6]

$$K_F = \hat{P}C_F\hat{R}^{-1} \tag{2.5}$$

where $\hat{P}$ is the solution to the Riccati equation

$$A_F \hat{P} + \hat{P} A_F^T - \hat{P} C_F^T \hat{R}^{-1} C_F \hat{P} + \hat{Q} = 0 \qquad (2.6)$$

and $\hat{Q}$ and $\hat{R}$ are the covariance matrices of the state and measurement noises. Equation (2.6) assumes a steady state filter exists, which implies $[A_F, B_F]$ and $[A_F, C_F]$ are controllable and observable pairs, respectively. An example of a centralized system is given in Figure 2.1.

The reduced-order Kalman filter is similar to the full-order case with corresponding reduced-order matrices

$$\dot{\hat{x}}_r = A_{F_r} \hat{x}_r + B_{F_r} u_r + K_F(y_r - \hat{y}_r) \qquad (2.7)$$

$$\hat{y}_r = C_{F_r} \hat{x}_r \qquad (2.8)$$

where $\hat{x}_r$ is the reduced-order state estimate vector and A_{F_r}, B_{F_r} and C_{F_r} are the reduced-order filter plant, control and measurement matrices, respectively. The input and the measurement vectors may or may not be reduced-order, depending on the existing substructures – it may be desirable to control a certain part of a LFSS using only local measurements and actuators. The reduced-order matrices are formed by retaining only the estimated states which make up the reduced-order filter. It is up to the discretion of the designer to decide which states are most important to retain. Many techniques of model reduction applied to LFSS exist [15-20] and will not be discussed in this study. K_F is the reduced-order Kalman gain determined by

$$K_F = \hat{P}_r C_{F_r} \hat{R}_r^{-1} \qquad (2.9)$$

where $\hat{P}_r$ is the solution to equation (2.6) with the appropriate reduced-order matrices substituted. $\hat{Q}_r$ and $\hat{R}_r$ are the reduced-order covariance matrices. This reduced-order

filter is now a suboptimal filter. Error has been introduced because certain states of the system have been neglected. While the filter is no longer optimal, it is still the "best" filter for a system of the same order as the reduced-order model, in the sense of minimizing the mean square error.

Suppose K_F is now chosen to shape the filter response of equations (2.7) and (2.8). It may be advantageous to have the magnitude of the filter frequency response peak in a given frequency range. It may be desired to have the phase of the frequency response lie in a certain region. This K_F then has been chosen to "shape" the frequency response of the filter in some way and will be hereafter named a frequency-shaped gain. The resulting filter is a suboptimal filter since it is not optimal for a given set of model parameters.

2.3 Decentralized Estimation Theory

It is assumed that the system dynamics can be reduced to p decoupled subsets of n_k equations for $k = 1, ..., p$, where no further reduction within each of the p subsets is possible. Note that the sum of n_k over k is n, the order of the system. Each decentralized filter is formed from some combination of the p subsets where the equations for any two of the decentralized filters are not necessarily decoupled. The ith decentralized filter is given by

$$\dot{\hat{x}}_i = A_i \hat{x}_i + B_i u_i + K_{F_i}(y_i - \hat{y}_i) \qquad (2.10)$$

and

$$\hat{y}_i = C_i \hat{x}_i \qquad (2.11)$$

The ith estimated state vector is $\hat{x}_i$, the ith plant, control, and measurement matrices

are A_i, B_i, and C_i respectively, and the ith filter gain is K_{F_i}. The states of the decentralized filter subsets may be chosen using model reduction techniques. If the decentralization is spatial, different modes may be important at different locations along the LFSS. Or, decentralization may be used to reduce the overall number of filter computations. Each filter may be full-order but, by taking advantage of properties which usually exist with the subset architecture, each filter will most probably be reduced-order. The K_{F_i} may be chosen to be reduced-order Kalman filter gains or some criteria-shaped gains. These filters are suboptimal due to decentralization, reduction in order, and, if criteria-shaped gains are used, not minimizing the mean square error. An example of a decentralized system is shown in Figure 2.2.
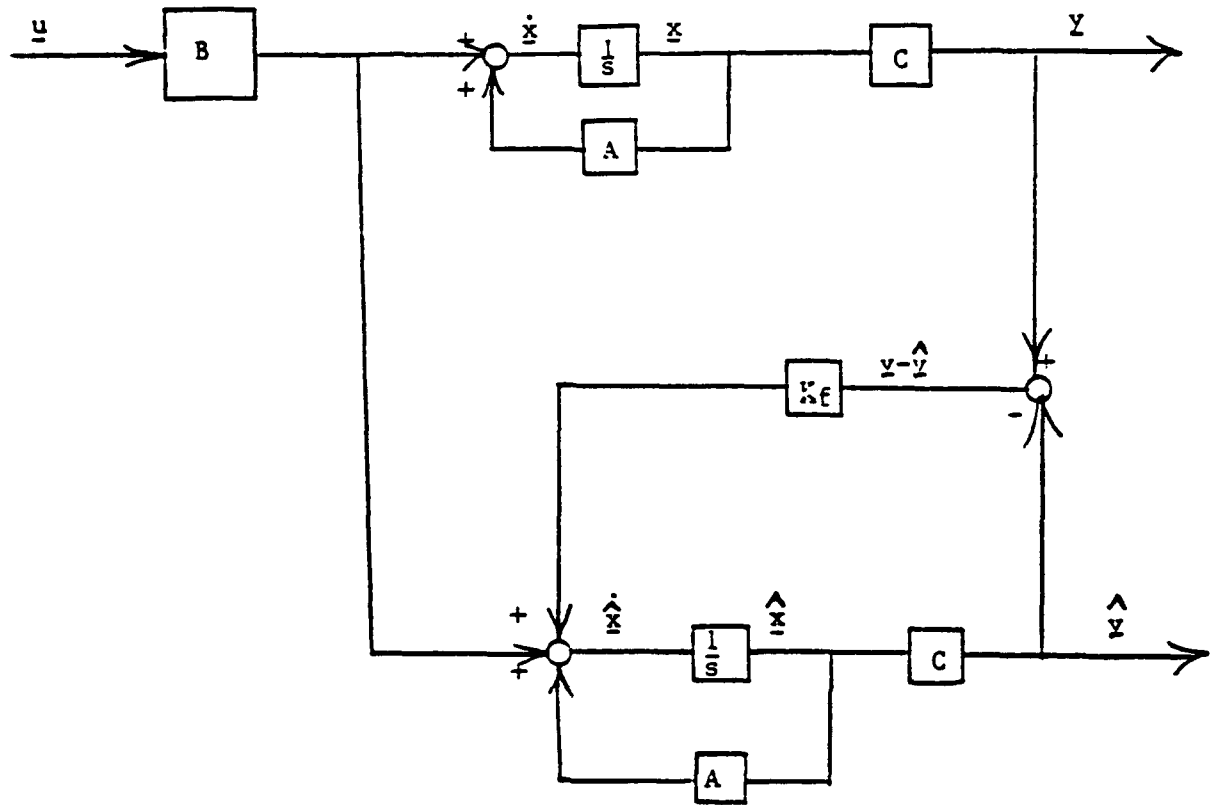
Figure 2.1: Open loop system with centralized filter
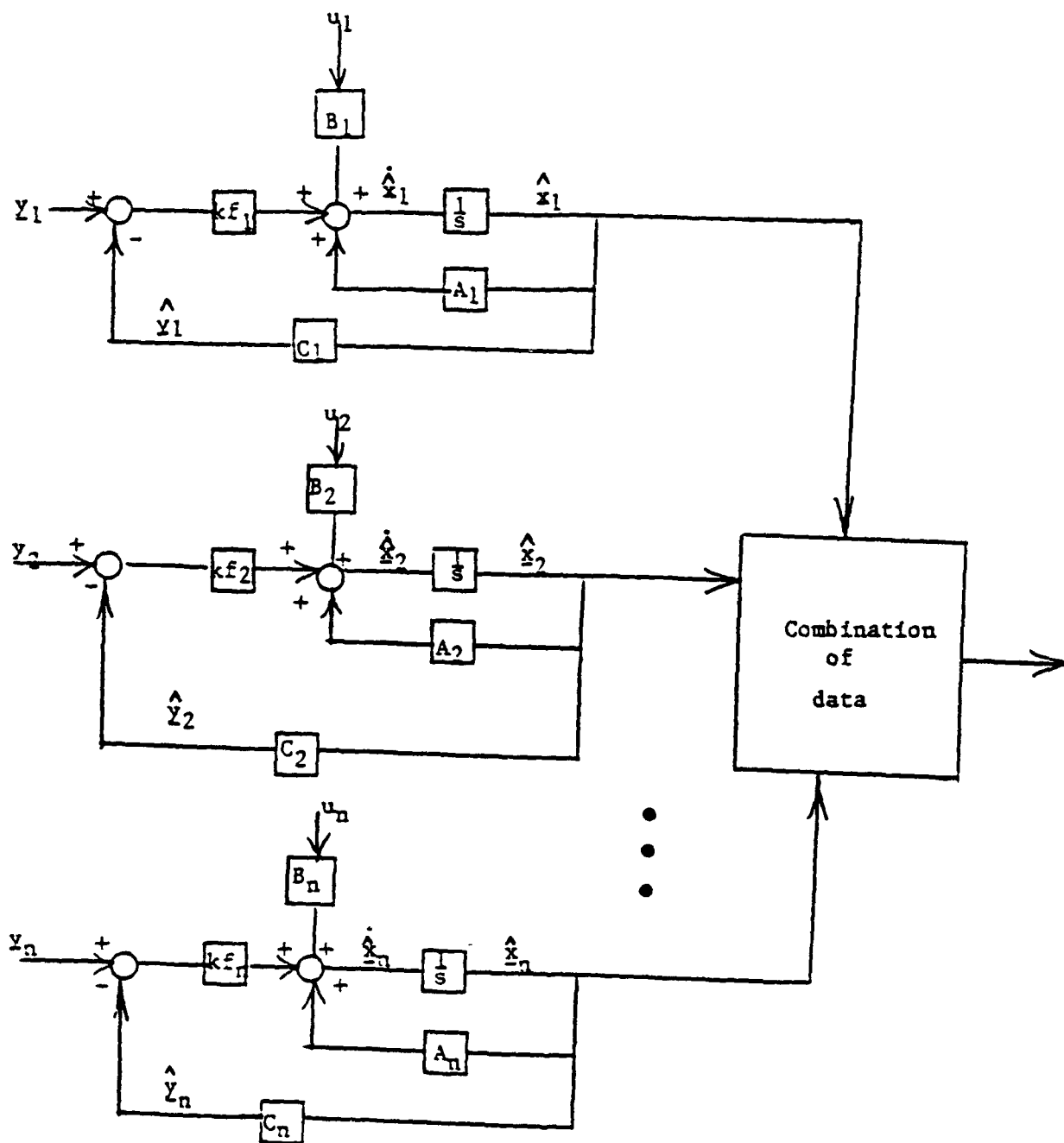
Figure 2.2: Decentralized filter

Chapter 3

Modal Analysis And Perfect Information Results

3.1 Modal Analysis Theory

To implement a control system for a flexible structure, a dynamic model of the structure must first be formed. It is advantageous to express the model in modal form, as modal control – the damping of selected modes of vibration – is often used. The basic equations of motion for a structure are

$$[M]\ddot{q} + [C]\dot{q} + [K]q = Q \tag{3.1}$$

where $[M]$, $[C]$ and $[K]$ are the mass, damping and stiffness matrices, respectively, q is the displacement vector of the structure, and Q is the generalized force vector acting upon the structure.

The equations of motion in the form of (3.1) are generally coupled. Implementing the method of modal analysis as given in [5] involves introducing the linear transformation

$$q(t) = [U]\eta(t) \tag{3.2}$$

where $[U]$ is the modal matrix and $\eta(t)$ is a generalized coordinate. Equation (3.1) then becomes

$$[M][U]\ddot{\eta} + [C][U]\dot{\eta} + [K][U]\eta = Q. \tag{3.3}$$

At this point, a justifiable assumption is made that $[C] \approx 0$. A term will be added at a later time to represent the small inherent damping in the LFSS without destroying the decoupled form of the equations. Then

$$[M][U]\ddot{\eta} + [K][U]\eta = Q. \tag{3.4}$$

Premultiplying equation (3.4) by $[U]^T$ yields

$$[U]^T[M][U]\ddot{\eta} + [U]^T[K][U]\eta = [U]^T Q. \tag{3.5}$$

The amplitude of the modal matrix $[U]$ is arbitrary. To simplify equation (3.5), introduce the normalizations

$$[U]^T[M][U] = [I] \tag{3.6}$$

$$[U]^T[K][U] = diag(\omega_i^2) \tag{3.7}$$

where $[M]$ and $[K]$ are positive-definite symmetric matrices, and ω_i are the eigenvalues. Letting $[U]^T Q = N$ results in

$$\ddot{\eta} + diag(\omega_i^2)\eta = N \tag{3.8}$$

or

$$\ddot{\eta}_i(t) + \omega_i^2 \eta(t) = N_i(t) \tag{3.9}$$

for the ith mode. A numerical example of normalizing $[U]$ will be given later.

As a representation of a large flexible structure, a pinned-pinned beam is considered, as shown in Figure 3.1. The equation for an Euler beam is

$$m\frac{\partial^2 y(x,t)}{\partial t^2} - EI\frac{\partial^4 y(x,t)}{\partial t^4} = f(x,t) \tag{3.10}$$

where m is the mass of the beam, EI is the stiffness of the beam, $y(x,t)$ is the displacement at location x and time t of the beam, and $f(x,t)$ is the force distribution applied to the beam. To solve equation (3.10), an assumption that free vibration occurs, i.e. $f(x,t) = 0$, is made. If $y(x,t)$ is separable in time and space as

$$y(x,t) = q(t)U(x), \tag{3.11}$$

then the solutions to equation (3.10) obey

$$q + \omega^2 q = 0 \tag{3.12}$$

and

$$U^{(4)} + (m\frac{\omega^2}{EI})U = 0. \tag{3.13}$$

Solving the pinned-pinned beam problem for the natural frequencies, ω_i, and the mode shapes, U_i, in equations (3.12) and (3.13) yields the values

$$\omega_i = (i\pi)^2 sqrt[\frac{EI}{(mL)^4}], \ i = 1, 2, ..., \infty \tag{3.14}$$

$$U_i(x) = A_i sin(\frac{i\pi x}{L}). \tag{3.15}$$

The mode shapes U_i are arbitrary in amplitude A_i. Normalizing such that

$$\int_0^L mU_i^2(x)dx = 1 \tag{3.16}$$

gives

$$U_i(x) = sqrt[\frac{2}{mL}]sin(\frac{i\pi x}{L}). \tag{3.17}$$

The total displacement and velocity of the beam at any point can be represented as the sum of the mode shapes multiplied by the generalized coordinates:

$$y(x, t) = \sum_{i=1}^{\infty} U_i(x)\eta_i(t) \tag{3.18}$$

16

$$\dot{y}(x,t) = \sum_{i=1}^{\infty} U_i(x)\dot{\eta}_i(t). \tag{3.19}$$

The dynamic model of the beam has now been expressed in modal form where $\eta_i(t)$ and $\dot{\eta}_i(t)$ are the modal positions and velocities of the ith mode, respectively.

3.2   Problem Formulation

The simple beam example used throughout this study is the pinned- pinned beam with an impulse force applied, as shown in Figure 3.1. Velocity sensors and collocated actuators and sensors are investigated here to maintain positive realness of the plant, as discussed in Chapter 4.

Let the state x be defined as

$$x = [\eta_1, \dot{\eta}_1 : \eta_2, \dot{\eta}_2 : ... : \eta_n, \dot{\eta}_n]^T \tag{3.20}$$

where η_i and $\dot{\eta}_i$ are the ith modal amplitude and velocity, respectively. The state space formulation then becomes

$$\dot{x} = Ax + Bu \tag{3.21}$$

$$y = Cx \tag{3.22}$$

with

$$A = diag(A_i) \text{ where } A_i = \begin{bmatrix} 0 & 1 \\ -\omega_i^2 & -2\zeta_i\omega_i \end{bmatrix} \tag{3.23}$$

$$B = [0, C_1 : ... : 0, C_n]^T \tag{3.24}$$

and

$$C = [0, C_1 : ... : 0, C_2]. \tag{3.25}$$

Note that the matrix C takes the above form for a velocity sensor and, since actuators and sensors are collocated, $B = C^T$. The damping term ζ_i is included in the dynamics matrix A here to represent the slight damping inherent in the structure without destroying the decoupled form of the equations. The structural model is now in state space form with the modal positions and velocities as the state elements.

Numerical values for the structural parameters are given in Appendix A.

3.3 Estimation Performance Results for Perfect Model Information

Now that a preferred model of the structure exists, estimation of the state is desired. Since modal control is to be implemented, the modal positions and velocities are required. These parameters are not readily available for measurement and must be estimated. The filter types to be considered are full and reduced-order centralized estimators, full and reduced-order decentralized estimators, and a reduced-order decentralized estimator with frequency-shaped gains. In this chapter, the estimator performances are compared assuming structural frequency model information is known exactly.

The basic centralized estimator is given by equations (2.3) and (2.4) and is presented again in equations (3.26) and (3.27):

$$\dot{\hat{x}} = A_F \hat{x} + B_F u + K_F (y - \hat{y}). \tag{3.26}$$

$$\hat{y} = C_F \hat{x} \tag{3.27}$$

where

$$x = [\eta_1, \dot{\eta}_1 : ... : \eta_n, \dot{\eta}_n]^T \tag{3.28}$$

$$A_F = diag(A_{F_i}) \text{ where } A_{F_i} = \begin{bmatrix} 0 & 1 \\ -\omega_i^2 & -2\zeta_i \omega_i \end{bmatrix} \tag{3.29}$$

$$B_F = [0, C_1 : ... : 0, C_n]^T \tag{3.30}$$

and

$$C_F = [0, C_1 : ... : 0, C_n]. \tag{3.31}$$

The optimal time-invariant gain, in the sense of minimizing the mean square error, given a set of model parameters, is the Kalman gain

$$K_F = \hat{P} C_F \hat{R}^{-1} \tag{3.32}$$

where $\hat{P}$ is the solution to the Riccati equation

$$A_F\hat{P} + \hat{P}A_F^T - \hat{P}C_F^T\hat{R}^{-1}C_F\hat{P} + \hat{Q} = 0 \qquad (3.33)$$

and $\hat{Q}$ and $\hat{R}$ are the covariance matrices of the state and measurement noises.

Two cases with identical filters but different system models are considered. The first uses noise in the model when calculating the Kalman gain, even though no noise is present in the system. The noise used when obtaining the Kalman gain is called pseudo-noise. The second case determines the Kalman gain assuming noise covariances that correspond to actual noise in the system. The same noise covariances are used in both cases and numerical values are presented in Appendix A. The first filter is actually not an optimal filter – the optimal steady state Kalman gains for a full-order filter with no noise in the system are zero. The second filter is the optimal time-invariant filter for the system with the modelled noise. The statistical noise information for each mode is given in Appendix A.

The results of the centralized estimation are shown, in conjunction with the actual motion, in Figures 3.2 to 3.3. The first six modes of the system model describe the actual motion of the system adequately. However, the motion *is* dominated by the first two modes. The six-mode centralized estimator is full-order, while the one-mode, two-mode and four-mode estimators are reduced-order. All the centralized estimators use the Kalman gains (full or reduced-order) as the filter gains and are termed Linear Quadratic (LQ) estimators. Note that the centralized estimate follows the actual motion closely for the two and higher-mode filters. The one-mode filter contains second mode and higher frequencies in the error, due to low damping and to the high frequency content of the measurement input which contains all of the modes. Since the beam motion is dominated by the first two modes, this phenomenon does not appear in the two-mode and higher-mode filters. Examining Figures 3.2 and 3.3, two facts of value are noted. The velocity estimates appear to be "better" than the position estimates – this is because velocity sensors are used. Also, the trends

appearing in the system without noise do not change when system noise is included.

For the decentralized case, the full-order decentralized estimator will be identical to the full-order centralized estimator if information is not combined in a suboptimal manner and if the Kalman gain is chosen. Hence, the results for this filter will not be presented. As an arbitrary reduced-order decentralized case, the identical example of Figure 3.1 is used, but with two velocity sensors located as shown in Figure 3.4. One sensor provides output for one estimator while a second sensor provides output for a second estimator. The first estimator models and estimates only the first mode of the system while the second estimator models and estimates only the second mode of the system. This case represents the worst scenario – here, the dominant modes of the motion are assumed to be unknown. Hence, the result is two single-mode decentralized estimators. The ith estimator is given as

$$\dot{\hat{x}}_i = A_{F_i}\hat{x}_i + B_{F_i}u_i + K_{F_i}(y_i - \hat{y}_i) \qquad (3.34)$$

$$\hat{y}_i = C_{F_i}\hat{x}_i \qquad (3.35)$$

with $B_{F_i} = [0, C_i]^T, C_{F_i} = [0, C_i]$, and $\hat{x}_i = [\hat{\eta}_i, \dot{\hat{\eta}}_i]^T$. The results of the two decentralized estimators can be combined through summation if there are no common states, or if there are common states, through any desired estimation algorithm [21] such as Mean Square Error estimate (MSE), Maximum Apriori estimate (MAP), or Maximum Likelihood estimate (MLE).

Using Kalman gains calculated with pseudo-noise in the model but with no noise present in the system, Figure 3.5 shows the oscillatory motion of the decentralized estimates about the actual motion. Examining the separated first and second mode estimates of the decentralized system, shown in Figure 3.6, it can clearly be seen that the error between the decentralized estimate and the actual motion oscillates at undesirably high frequencies. This is due to low damping and to the high frequency

measurement input – the same phenomenon that occured with the one-mode centralized filter. Since this oscillation causes large errors in the position and velocity estimates, it is advantageous to remove the high frequency error content from the decentralized estimate through the shaping of the Bode magnitude plots of the error transfer functions, called error amplitude shaping.

The error transfer functions for the decentralized estimates are derived from the relation

$$\dot{e} = H\dot{\hat{x}} - \dot{\hat{x}} \tag{3.36}$$

or

$$E(s) = [sI - A_{F_CL}]^{-1}[HA - A_{F_{CL}}H - K_FC]X(s) \tag{3.37}$$

where H is a matrix of ones and zeros that selects the elements of the reduced-order state from the actual state, and $A_{F_{CL}} = A_F - K_F C_F$ is the closed-loop filter dynamics matrix. By varying the gains in equation (3.37), the frequency response of the filters can be shaped to the desired response.

For the one-mode decentralized filter, the denominator of the transfer matrix is a second-order polynomial given by

$$s^2 + (2\zeta_1\omega_1 + K_2C_1)s + \omega_1^2(1 - K_1C_1). \tag{3.38}$$

Comparing equation (3.38) with the general equation for a second-order system

$$s^2 + (2\zeta\omega_n)s + \omega_n^2 \tag{3.39}$$

22

yields the natural frequency and damping ratio of the filter response as

$$\omega_n = \omega_1 sqrt(1 - K_1 C_1) \tag{3.40}$$

and

$$\zeta = \frac{2\zeta_1\omega_1 + K_2 C_1}{2\omega_n} \tag{3.41}$$

The designer can therefore choose the desired natural frequency and damping ratio of the filter via the gains K_1 and K_2. The transfer functions to be considered are the error in the first mode estimated position and velocity due to the actual second mode velocity, and the error in the second mode estimated position and velocity due to the actual first mode velocity. The Bode magnitude plots of these error transfer functions, shown in Figure 3.7, indicate second mode and higher frequencies in the first and second mode filters. By varying the gains in (3.18), the frequency response of the error transfer functions may be shaped as shown in Figure 3.8. Figure 3.9 shows the separated first and second estimated modes of motion with frequency-shaped filters. It can be seen that much of the high frequency error has now been removed. The total actual motion of the system and decentralized estimation results with both filters frequency-shaped are shown in Figure 3.10. Much improvement over Figure 3.5 is observed.

Note that the previous decentralized results correspond to a system with no noise present. Now that a set of satisfactory frequency-shaped gains has been chosen for the decentralized filter, these same gains are used in a system with noise as given in Figure 3.3. The results are shown in Figure 3.11.
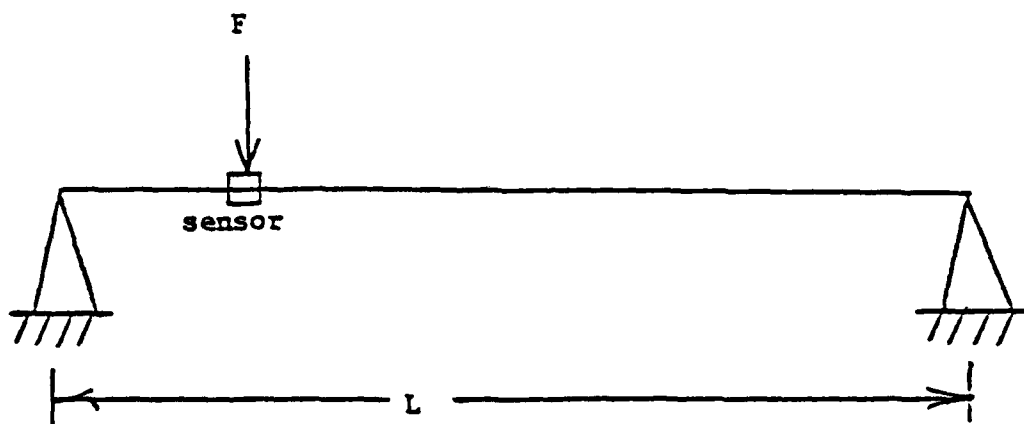
Figure 3.1: Pinned-pinned beam with impulse force applied
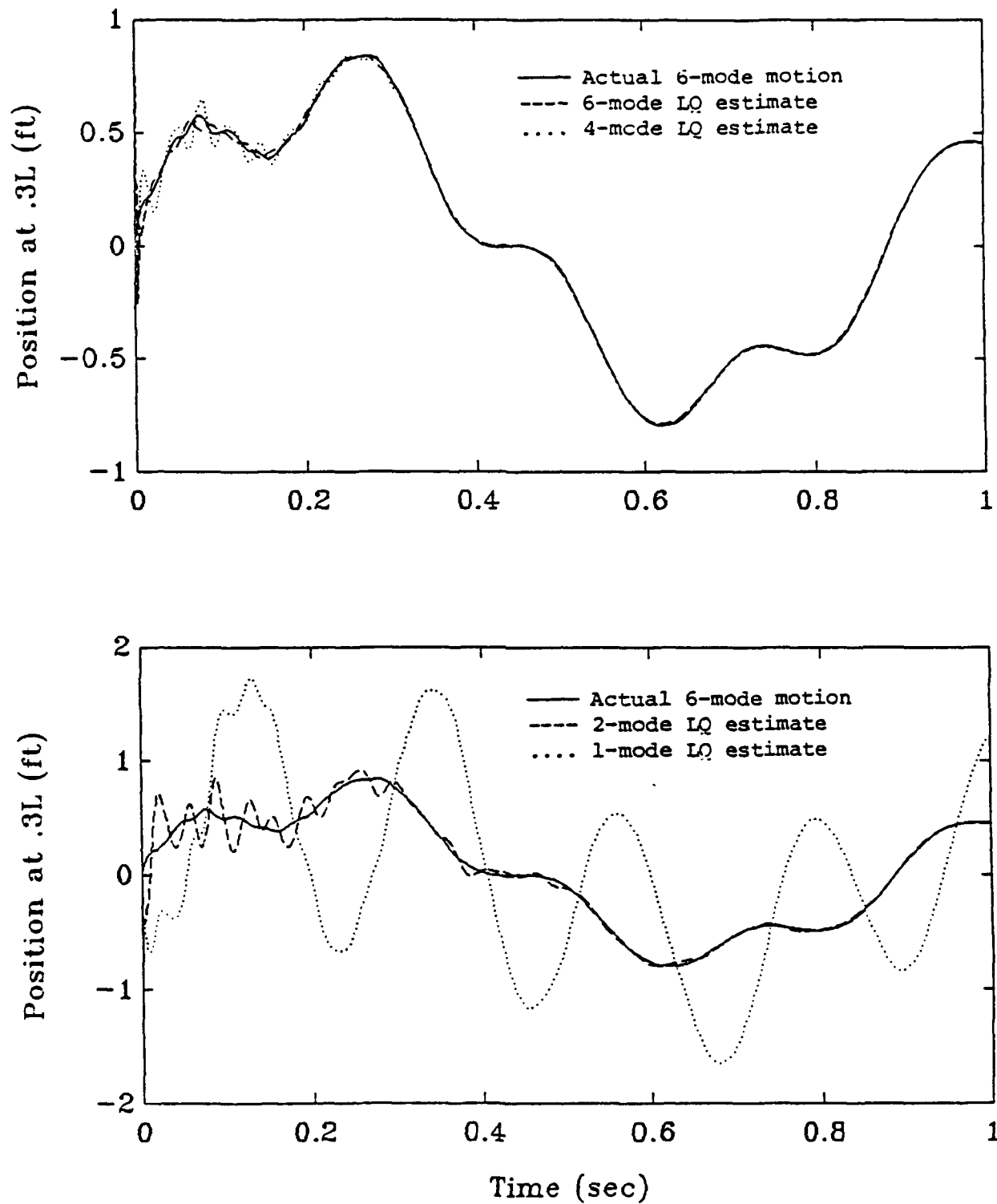
Figure 3.2a: Centralized position estimation results for the system with no noise (pseudo noise used to determine gains) and perfect model information
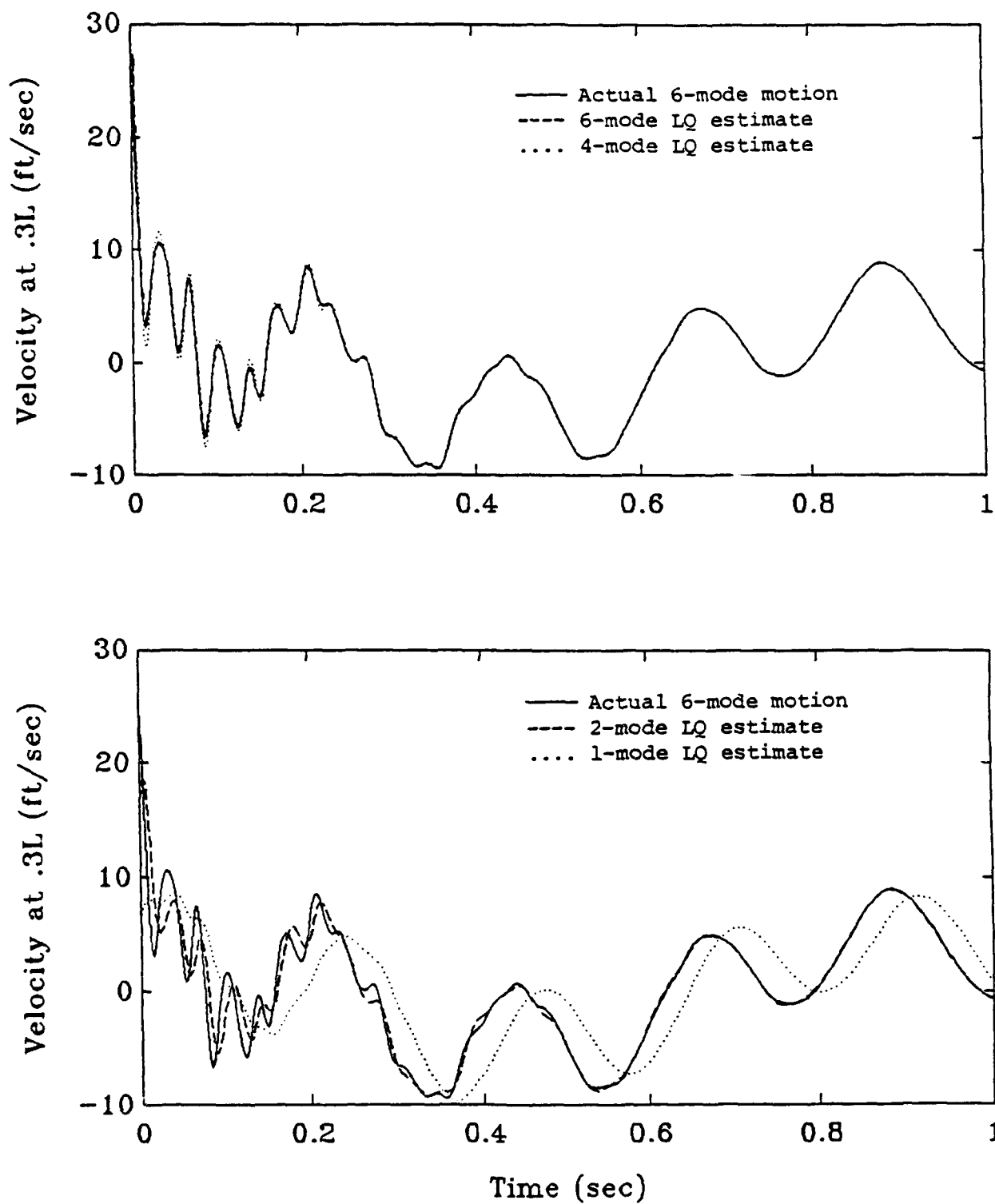
Figure 3.2b: Centralized velocity estimation results for the system with no noise (pseudo-noise used to determine gains) and perfect model information
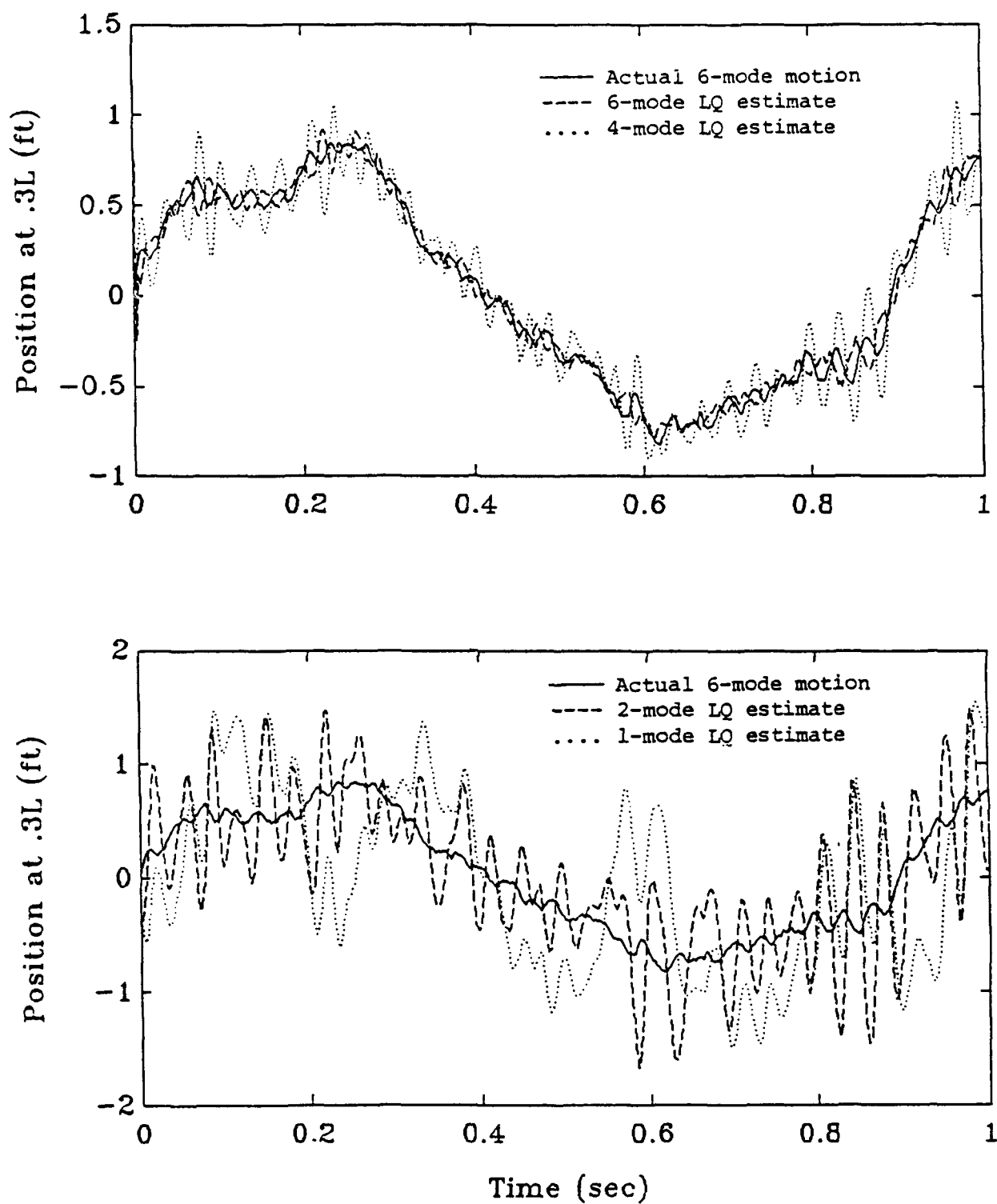
Figure 3.3a: Centralized position estimation results for system with noise and perfect information
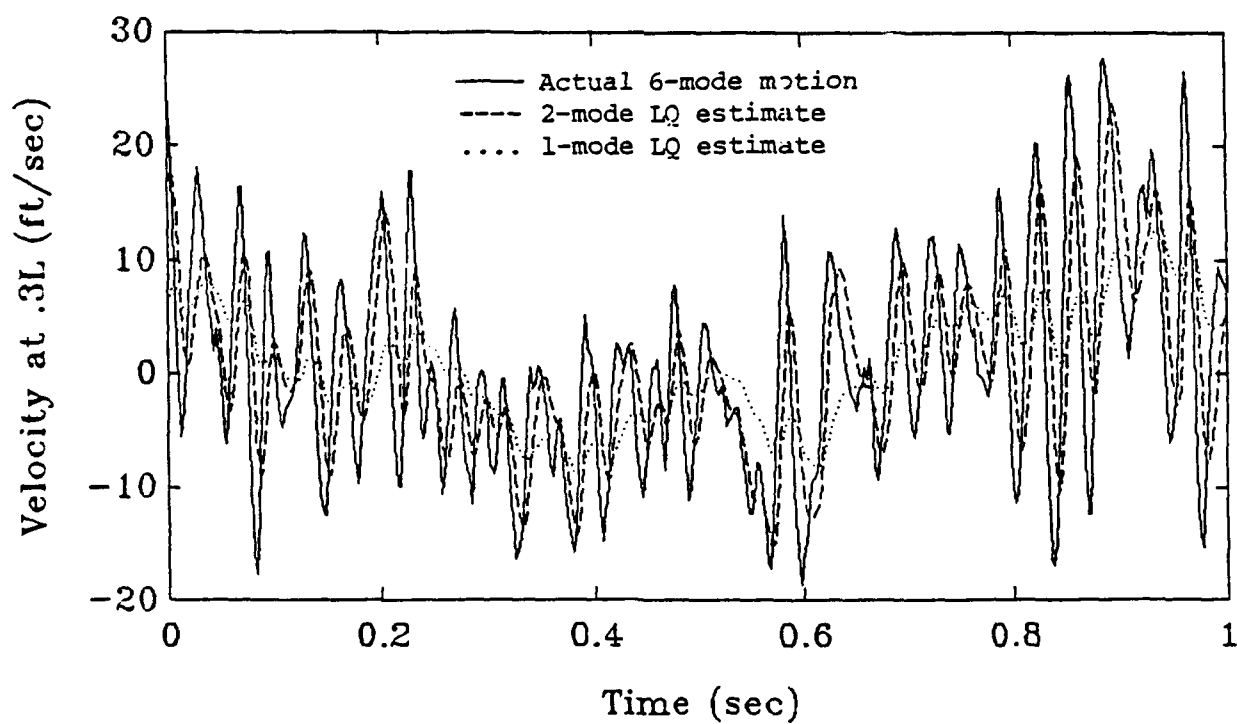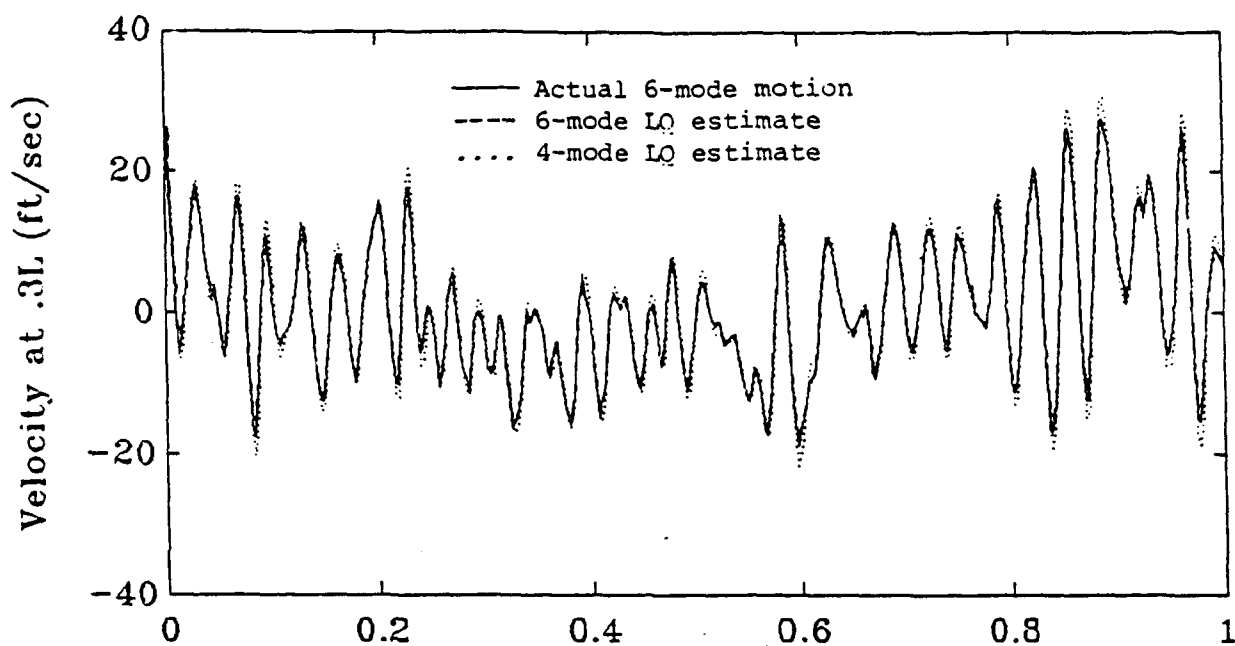
Figure 3.3b: Centralized velocity estimation results for system with noise and perfect information
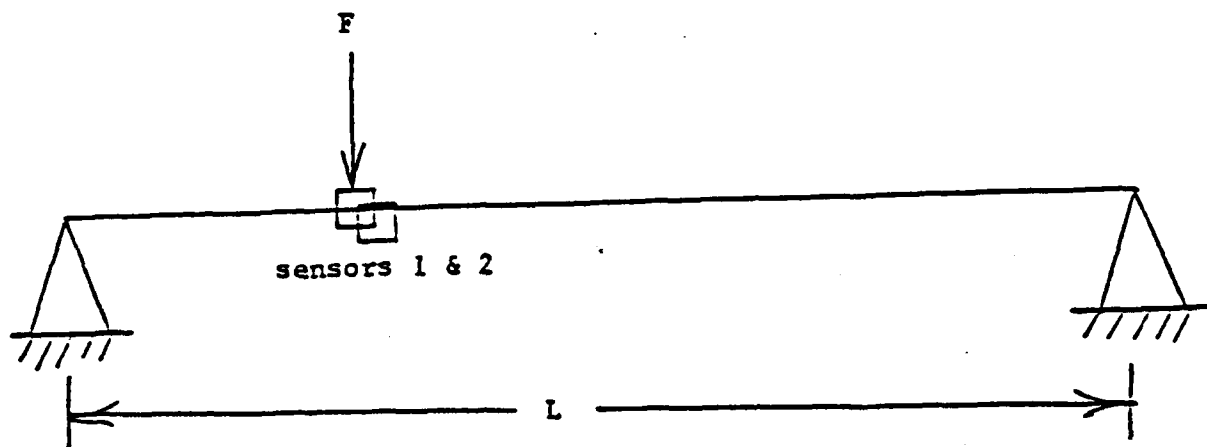
Figure 3.4: Pinned-pinned beam with impulse F applied ; Sensor 1 – Connected with estimator for 1st mode ; Sensor 2 – Connected with estimator for 2nd mode
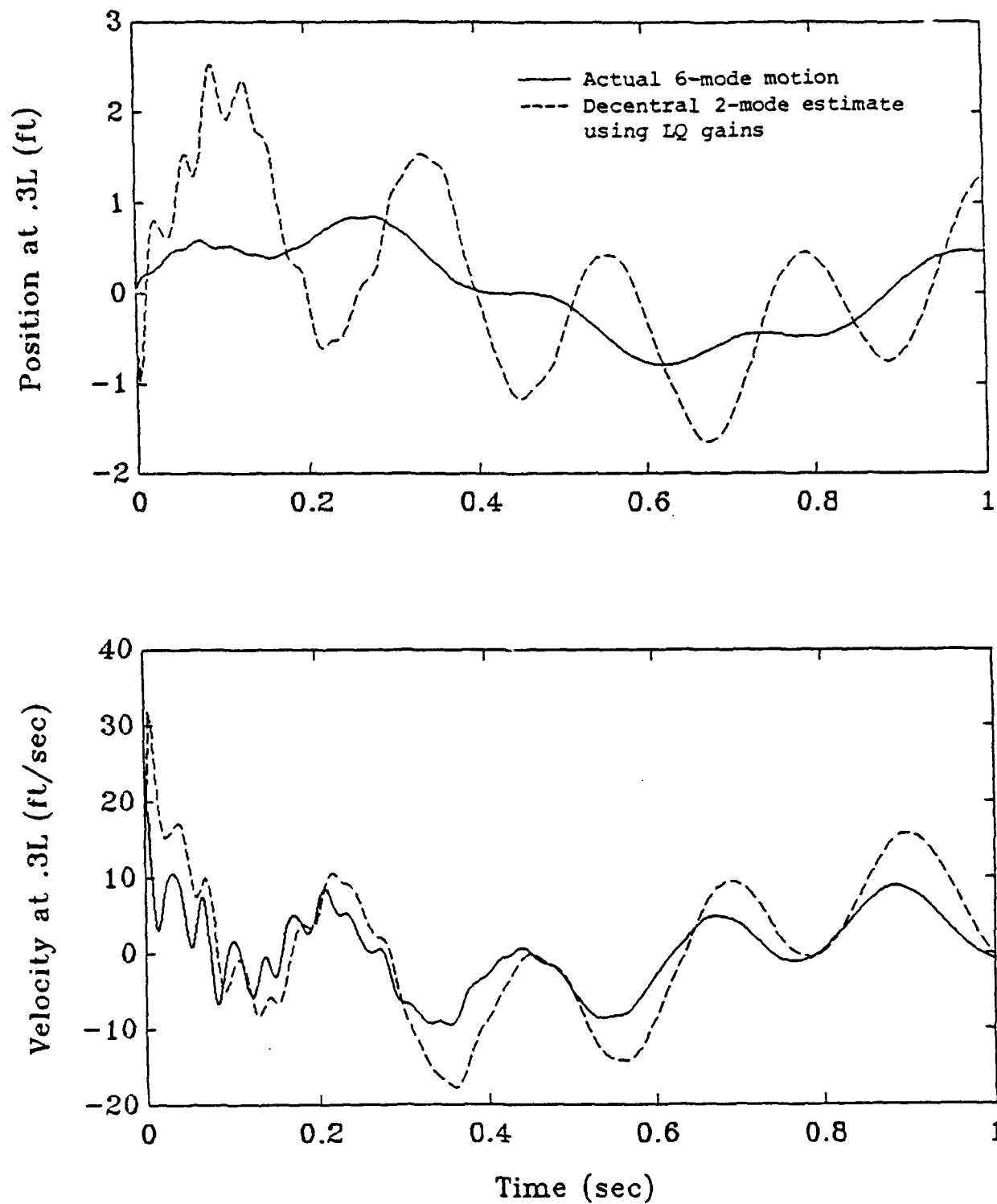
Figure 3.5: Total decentralized estimates using LQ gains for system with no noise and perfect information
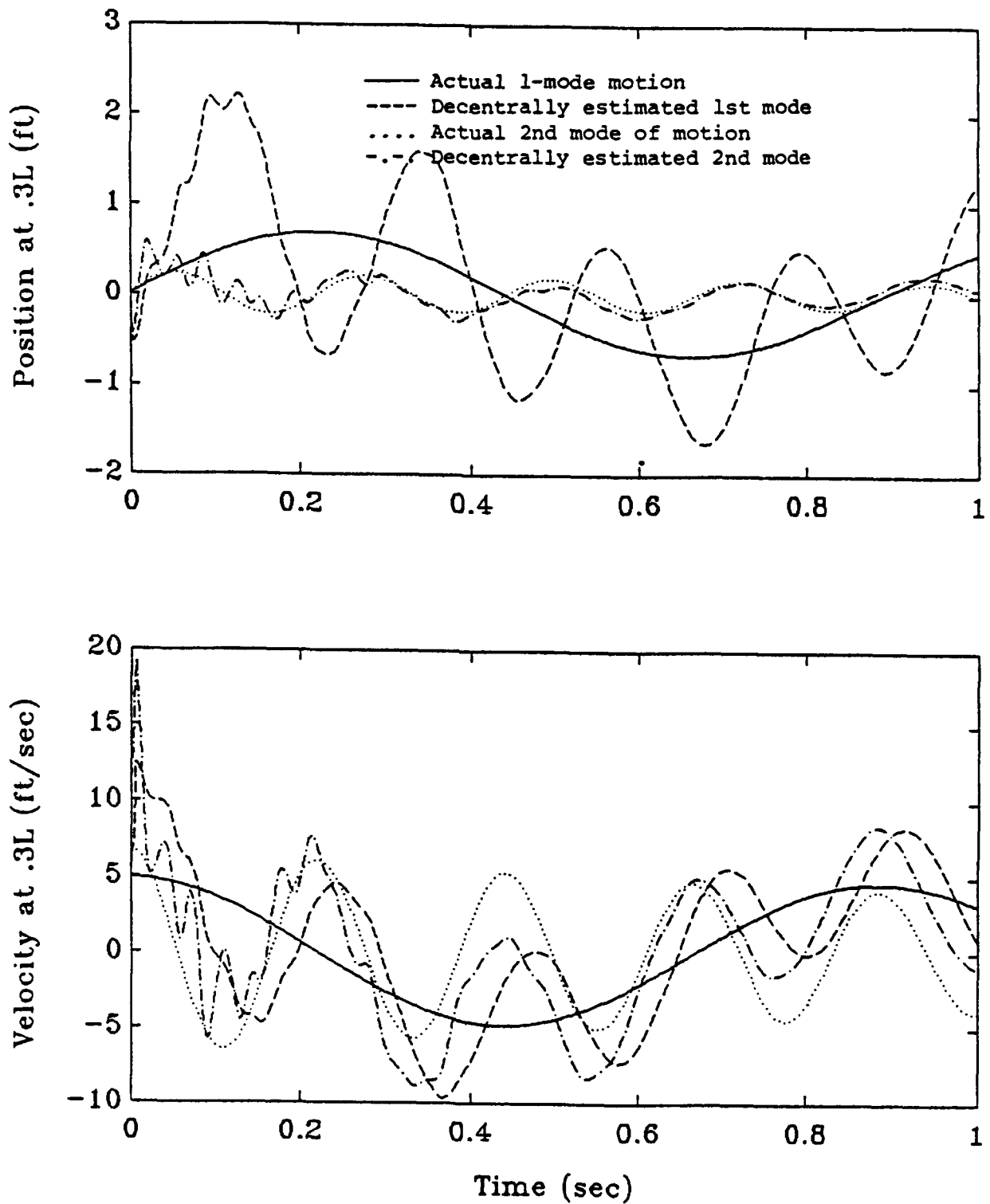
Figure 3.6: Decentralized estimates using LQ gains of the 1st and 2nd modes of motion for system with no noise and perfect information
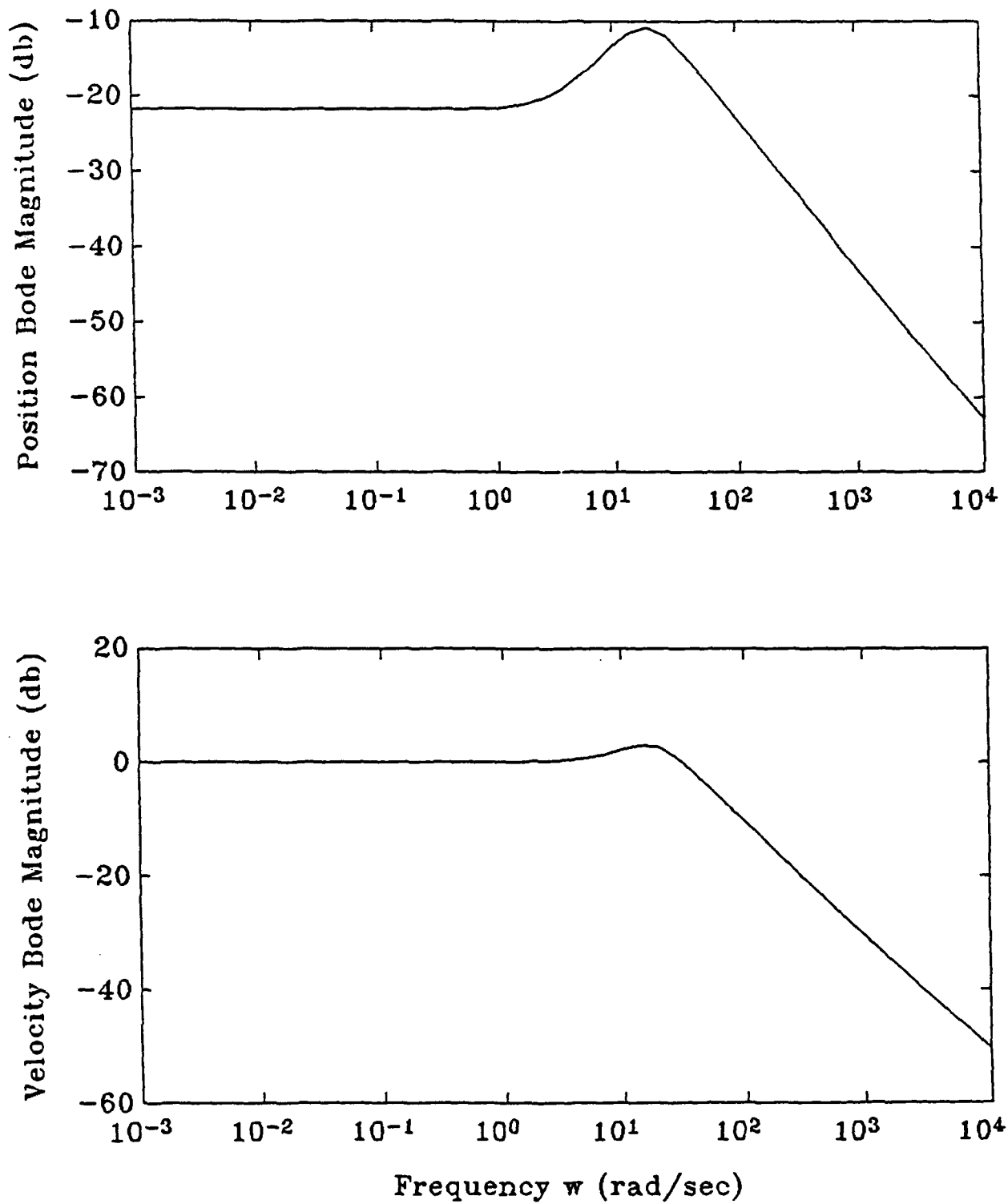
Figure 3.7a: Bode magnitude plots for error in first mode estimate due to second mode velocity. System has no noise and perfect model information. Filter is decentralized filter with LQ gains.
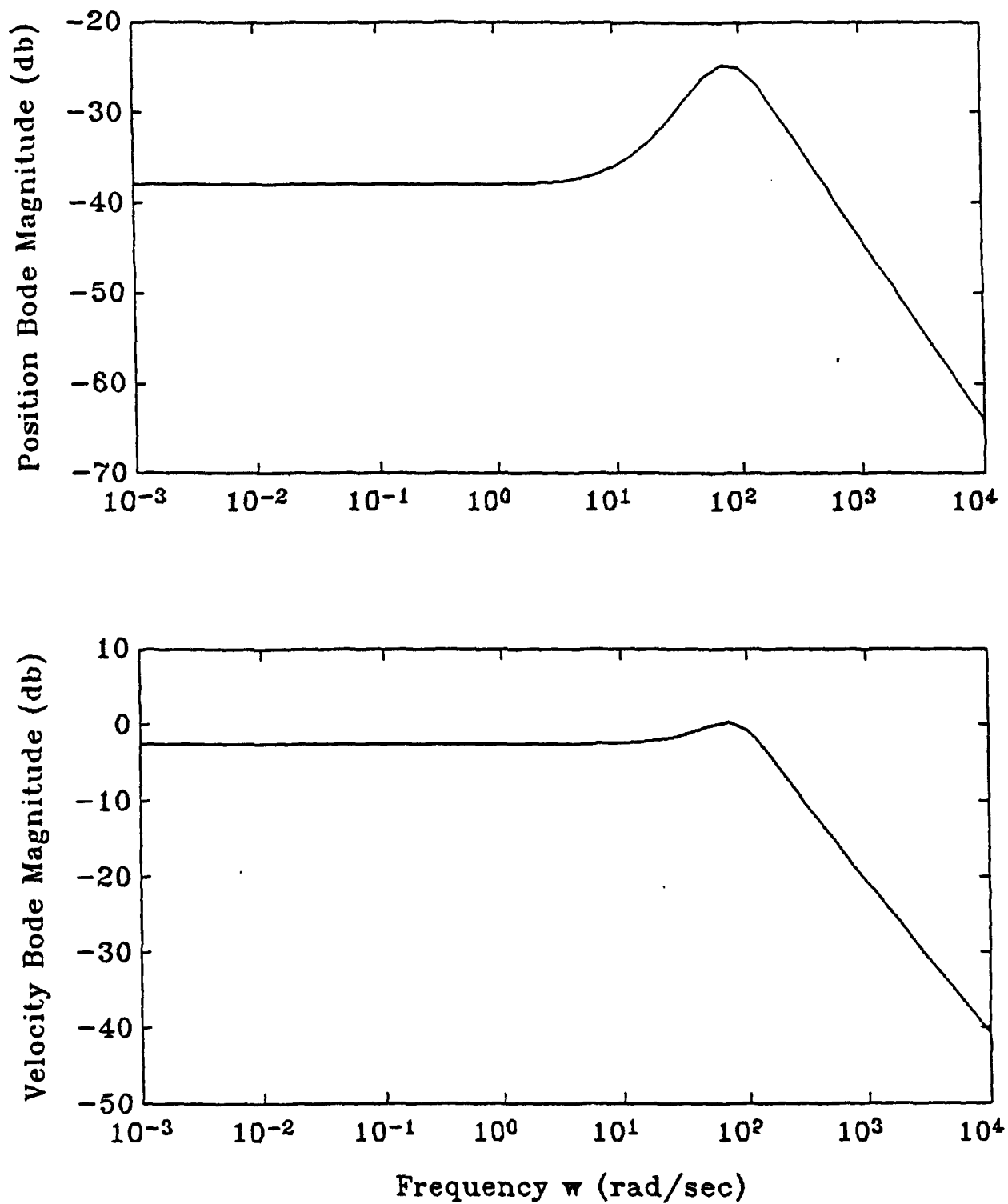
Figure 3.7b: Bode magnitude plots for error in second mode estimate due to first mode velocity. System has no noise and perfect model information. Filter is decentralized filter with LQ gains.

33
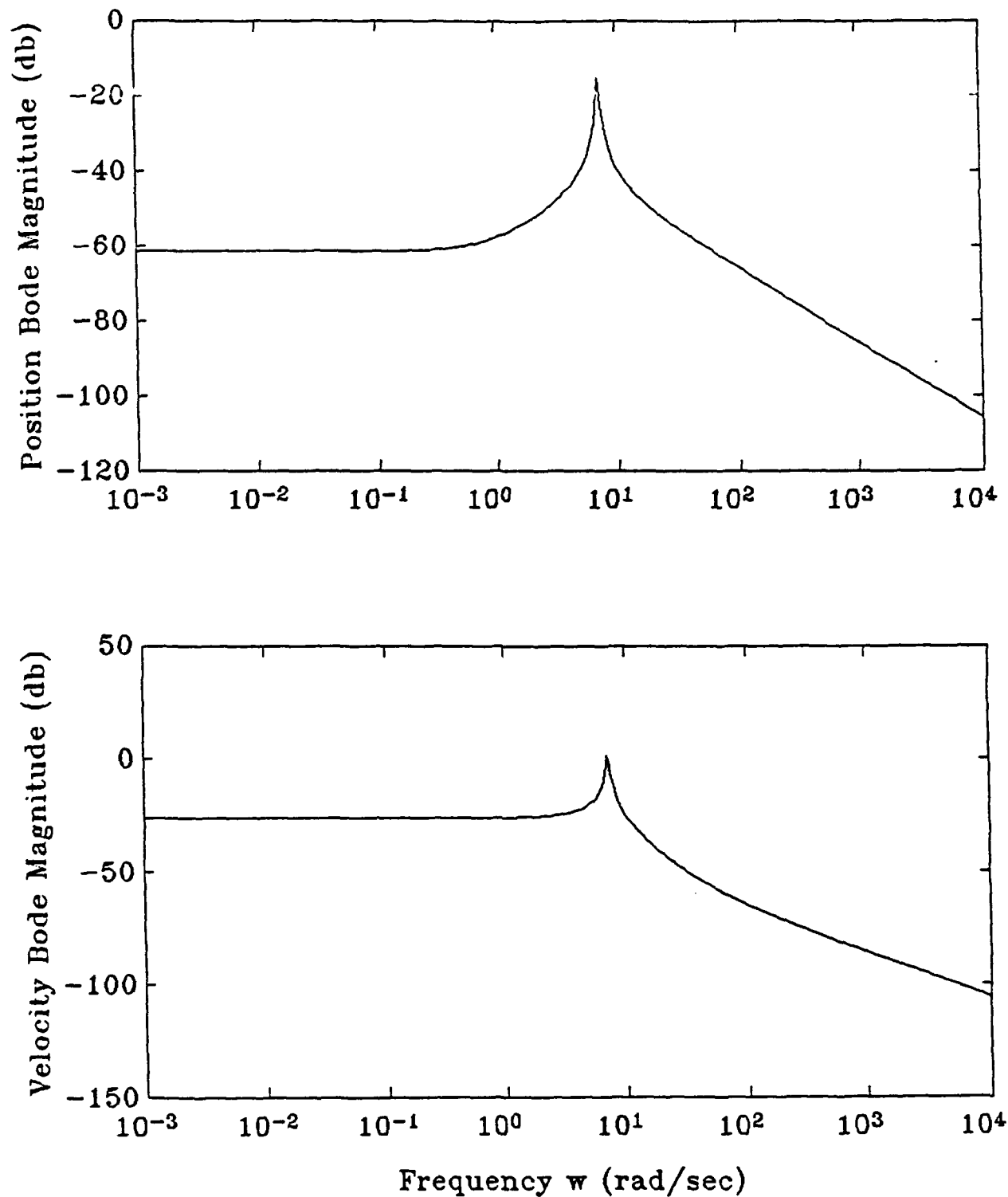
Figure 3.8a: Bode magnitude plots for error in first mode estimate due to second mode velocity. System has no noise and perfect model information. Filter is decentralized filter with shaped gains.
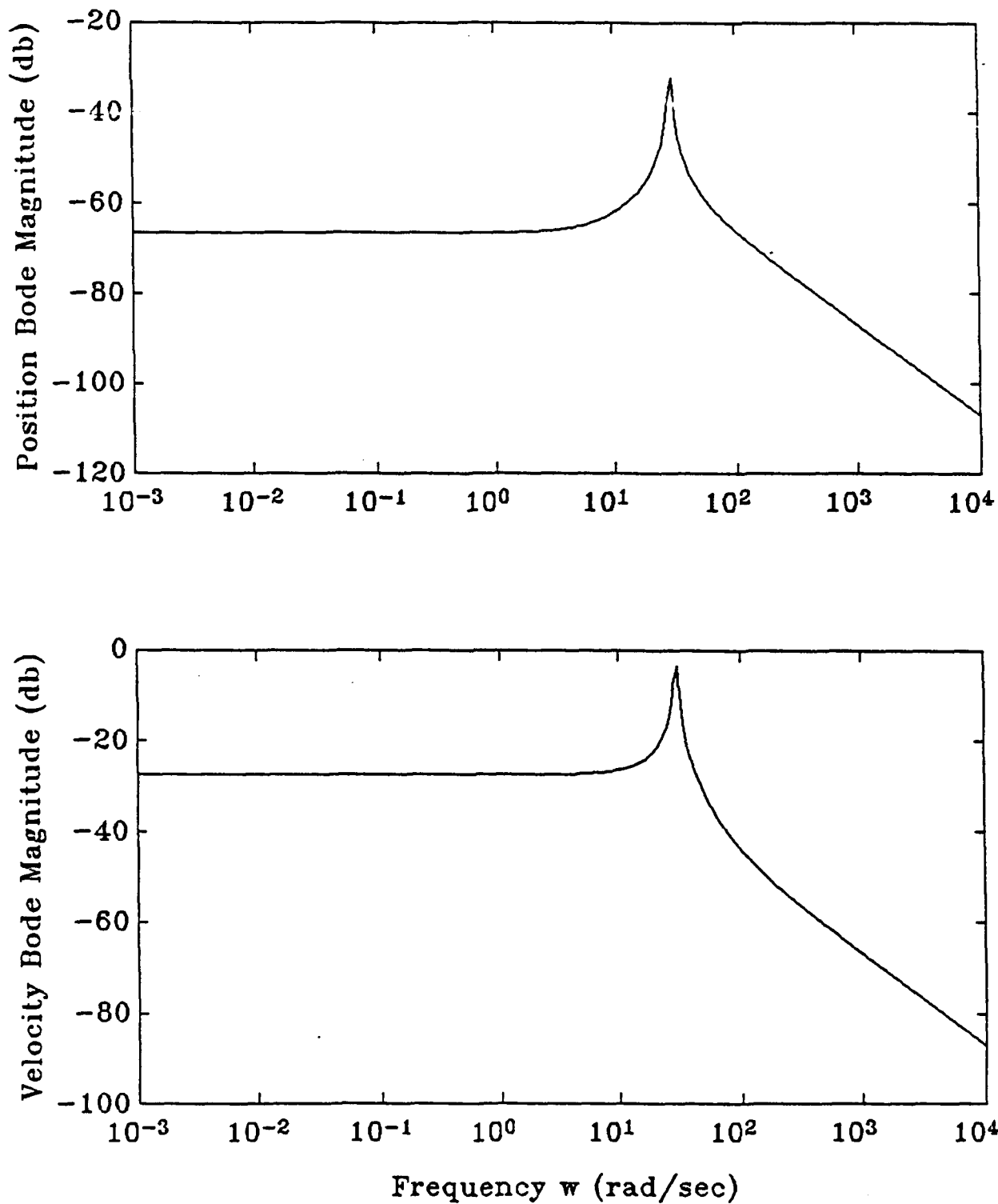
Figure 3.8b: Bode magnitude plots for error in second mode estimate due to second mode velocity. System has no noise and perfect model information. Filter is decentralized filter with shaped gains.
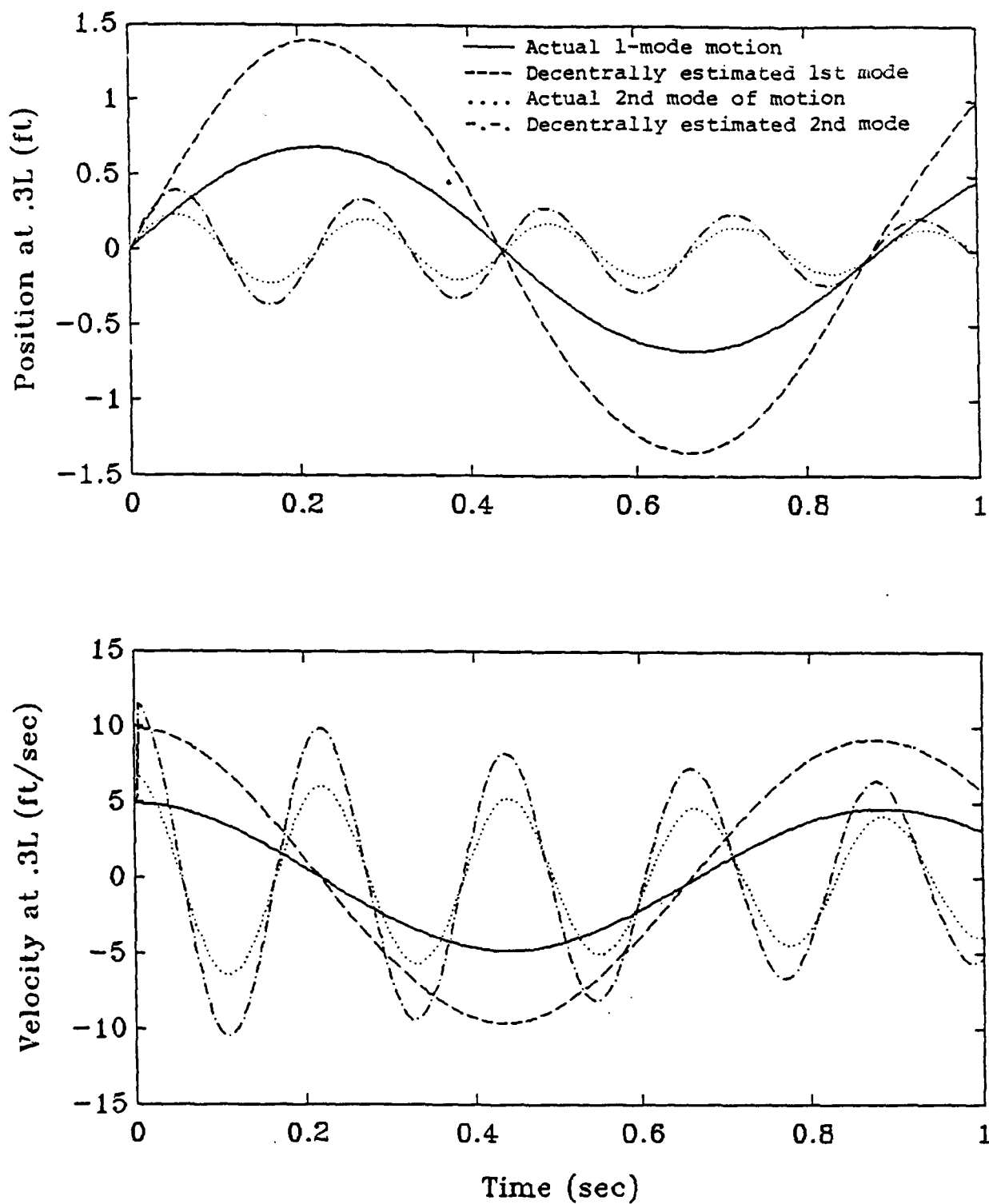
Figure 3.9: Shaped decentralized estimates of the 1st and 2nd modes of motion for system with no noise and perfect information
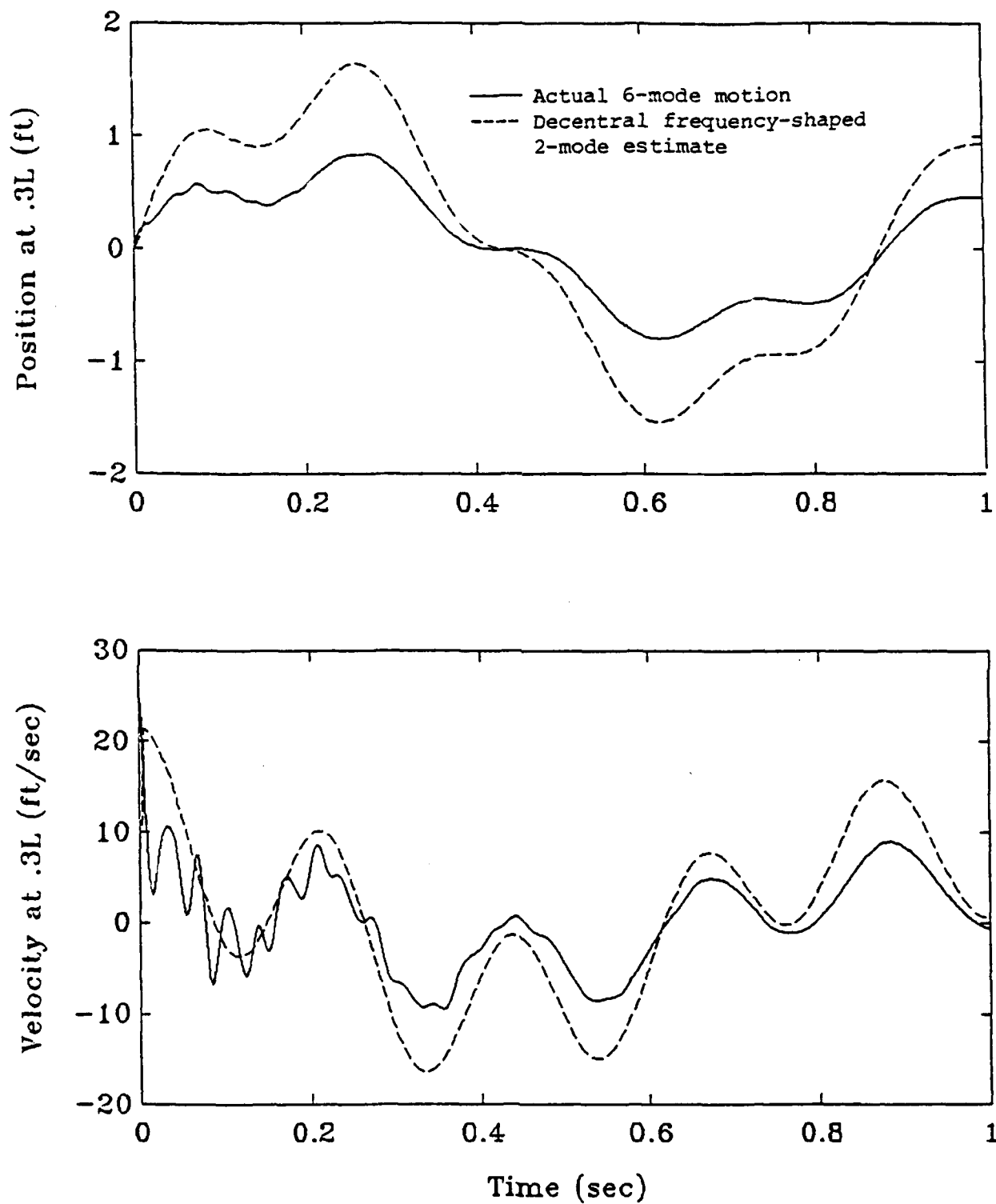
Figure 3.10: Total shaped decentralized estimates for system with no noise and perfect information
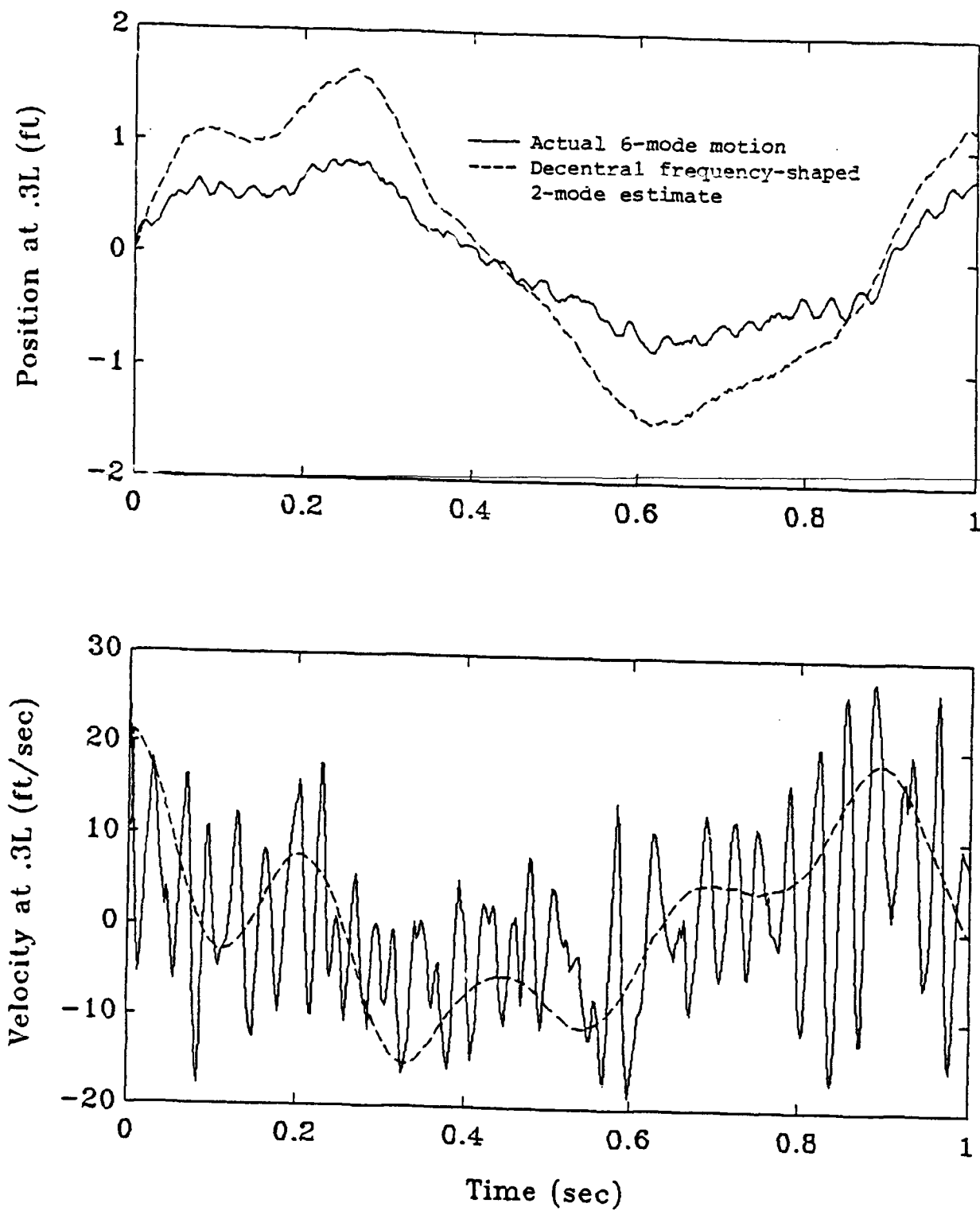
Figure 3.11: Total shaped decentralized estimates for system with noise but perfect information

Chapter 4

Robustness And Model Error Sensitivity Analysis

4.1 Sensitivity-Shaped Gains Selection

The previous analysis has been done for full and reduced-order linear quadratic (LQ) estimators and for a reduced-order decentralized estimator. No precautions have been taken to assure these filters give good performance in the presence of modelling errors. A sensitivity-shaped filter is now formulated to address this problem. A set of filter gains must be determined to ensure the system guaranteed asymptotic stability in the presence of modelling errors.

The modelling errors are chosen as errors in the structural frequencies ω of up to 20 %. This is felt to be representative of the actual uncertainties of the first few structural modes of a LFSS.

There is probably an inexhaustible supply of methods which will determine a satisfactory set of gains; this study will employ one method. The method is based upon minimizing the sensitivity of the filter to variations in the structural frequencies. The purpose of this method is to improve filter performance when imperfect knowledge of the system frequencies exists. While structural mode shape information is also uncer-

tain, it is assumed in this study that mode shapes are known exactly. The equations of motion, from equations (2.1) to (2.4), in state variable form are

$$\dot{x} = Ax + Bu \tag{4.1}$$

$$y = Cx \tag{4.2}$$

where A, B and C are the system plant, control and measurement matrices. The filter is represented by

$$\dot{\hat{x}} = A_F\hat{x} + B_Fu + K_F(y - \hat{y}) \tag{4.3}$$

$$\hat{y} = C_F\hat{x} \tag{4.4}$$

with A_F, B_F and C_F as the filter plant, control and measurement matrices and K_F as the filter gain matrix. The actual system plant matrix A will contain the actual frequencies $\bar{\omega}_i$, which may vary from the modelled frequencies by 20 %. The filter plant matrix A_F will contain the modelled frequencies ω_i. It is interesting, then, to note the transfer matrix between the actual state x and the estimated state $\hat{x}$. Since this relationship is Multi-Input Multi-Output (MIMO), the transfer matrix is composed of the individual transfer functions between the inputs and outputs. If the estimator was of the same order as the system plant, if noise was not taken into account, and if there were no modelling errors, then this transfer matrix *should* be the identity matrix. It is proposed to place emphasis on this point and to attempt to design a filter with this property.

Let $H_F(s)$ represent the filter transfer matrix between the filter output, $\hat{x}$, and the filter input, the state measurement y. Assuming that the number of actuators and

sensors are identical, or $dim(\boldsymbol{u}) = dim(\boldsymbol{y})$, an expression for $H_F(s)$ can be determined by defining the control vector $\boldsymbol{u}$ as

$$\boldsymbol{u} = [C(sI - A)^{-1}B]^{-1}\boldsymbol{y} \tag{4.5}$$

and substituting, with equation (4.4), into (4.3) to obtain equation (4.6). The result is

$$H_F(s) = [sI - A_F + K_F C_F]^{-1}[B_F\{C(sI - A)^{-1}B\}^{-1} + K_F]. \tag{4.6}$$

The system remains open-loop, but the feedback loop is driven by the same reference input as the system plant. A block diagram of this open-loop system is shown in Figure 4.1. Recall that the plant matrices A and A_F are partitioned into matrices with A_i and A_{F_i}, respectively, along the diagonals and zeros on the off-diagonals resulting in

$$A = diag(A_i) \text{ where } A_i = \begin{bmatrix} 0 & 1 \\ -\bar{\omega}_i^2 & -2\bar{\zeta}_i\bar{\omega}_i \end{bmatrix} \tag{4.7}$$

and

$$A_F = diag(A_{F_i}) \text{ where } A_{F_i} = \begin{bmatrix} 0 & 1 \\ -\omega_i^2 & -2\zeta_i\omega_i \end{bmatrix} \tag{4.8}$$

Through matrix partitioning, the plant and filter equations can be written as

$$\dot{\boldsymbol{x}}_i = A_i\boldsymbol{x} + B_i\boldsymbol{u}_i \tag{4.9}$$

41

$$y_i = C_i x_i \tag{4.10}$$

$$\dot{\hat{x}} = A_{F_i} \hat{x}_i + B_{F_i} u_i + K_{F_i}(y_i - \hat{y}_i) \tag{4.11}$$

$$\hat{y}_i = C_{F_i} \hat{x}_i \tag{4.12}$$

with $x_i = [\eta_i, \dot{\eta}_i]^T$, $B_i = B_{F_i} = [0, C_i]^T$, $C_i = C_{F_i} = [0, C_i]$, and $\hat{x}_i = [\hat{\eta}_i, \dot{\hat{\eta}}_i]^T$. The system control and measurement matrices B and C are affected by variations in the mode shapes, but not the structural frequencies. Hence, $\bar{\omega}_i$ terms do not appear in these matrices. In this study, it is assumed that mode shapes are perfectly known.

The transfer matrix $S(s)$ between the estimated state $\hat{x}$ and the actual state x is just

$$S(s) = H_F(s)C. \tag{4.13}$$

It is desired to force this matrix $S(s)$ as close to the identity matrix as possible. First, let it be noted that $S(s)$ will only be square if the system model has the same number of modes representing it as the filter model. Since the extra terms rendering the matrix non-square could just be forced to zero, the same number of modes will be used for simplicity. Starting with a one-mode representation of the system plant and filter, $S(s)$ has the elements

$$S(s) = \begin{bmatrix} \hat{\eta}_1/\eta_1 & \hat{\eta}_1/\dot{\eta}_1 \\ \dot{\hat{\eta}}_1/\eta_1 & \dot{\hat{\eta}}_1/\dot{\eta}_1 \end{bmatrix} \tag{4.14}$$

These elements can be analytically determined from equations (4.6) and (4.13) as

42

$$\hat{\eta}_1/\eta_1 = \frac{s^2 + (2\zeta_1\omega_1 + K_2C)s + \bar{\omega}_1^2(1 - K_1C)}{s^2 + (2\zeta_1\omega_1 + K_2C)s + \omega_1^2(1 - K_1C)} \qquad (4.15)$$

$$\hat{\eta}_1/\dot{\eta}_1 = \frac{1\zeta_1(K_1C - 1)(\omega_1 - \bar{\omega}_1)}{s^2 + (2\zeta_1\omega_1 + K_2C)s + \omega_1^2(1 - K_1C)} \qquad (4.16)$$

$$\hat{\dot{\eta}}_1/\eta_1 = \frac{s(\bar{\omega}_1^2 - \omega_1^2)}{s^2 + (2\zeta_1\omega_1 + K_2C)s + \omega_1^2(1 - K_1C)} \qquad (4.17)$$

$$\hat{\dot{\eta}}_1/\dot{\eta}_1 = \frac{s^2 + (2\zeta_1\bar{\omega}_1 + K_2C)s + \omega_1^2(1 - K_1C)}{s^2 + (2\zeta_1\omega_1 + K_2C)s + \omega_1^2(1 - K_1C)} \qquad (4.18)$$

where $K_{F_1} = [K_1, K_2]^T$ and $C_1 = [0, C]^T$. Note that if $\bar{\omega}_1 = \omega_1$, then equations (4.15) to (4.18) reduce to

$$\hat{\eta}_1/\eta_1 = 1 \qquad (4.19)$$

$$\hat{\eta}_1/\dot{\eta}_1 = 0 \qquad (4.20)$$

$$\hat{\dot{\eta}}_1/\eta_1 = 0 \qquad (4.21)$$

$$\hat{\dot{\eta}}_1/\dot{\eta}_1 = 1 \qquad (4.22)$$

In an attempt to drive the off-diagonal terms of equations (4.15) to (4.18) to zero and the diagonal terms to one, the value of $K_1 = \dfrac{1}{C}$ is chosen. Equations (4.15) to (4.18) become

43

$$\hat{\eta}_1 / \eta_1 = 1 \tag{4.23}$$

$$\hat{\eta}_1 / \dot{\eta}_1 = 0 \tag{4.24}$$

$$\hat{\dot{\eta}}_1 / \eta_1 = \frac{s(\bar{\omega}_1^2 - \omega_1^2)}{s(s + 2\zeta_1\omega_1 + K_2 C)} \tag{4.25}$$

$$\hat{\dot{\eta}}_1 / \dot{\eta}_1 = \frac{s(s + 2\zeta_1\bar{\omega}_1 + K_2 C)}{s(s + 2\zeta_1\omega_1 + K_2 C)} \tag{4.26}$$

Choosing a value for K_2 which shifts the pole $(-2\zeta_1\omega_1 + K_2 C)$ sufficiently to the left will ensure that the response due to that pole dies out quickly. Equations (4.23) to (4.26) then approach those of (4.19) to (4.22).

So far, the method used above seems to be rather specific. It assumes the number of modelled system plant modes is equal to the number of modelled filter modes. It assumes that only one mode, the same mode for the system plant and filter, is modelled. In the 2-mode case, using the first two modes as an example, the values of the filter gains are much more difficult to ascertain. No easy choices are immediately seen from the equations. With the aid of a symbolic manipulator, the transfer matrix between $\hat{x}$ and x is

$$S = \frac{1}{Z} \begin{bmatrix} J & K & L & M \\ N & O & P & Q \\ R & S & T & U \\ V & W & X & Y \end{bmatrix} \tag{4.27}$$

where

$$J = s^4 + [2\zeta_1\omega_1 + 2\zeta_2\omega_2 + C_2K_4 + C_1K_2]s^3 +$$
$$[4\zeta_1\omega_1\zeta_2\omega_2 + 2C_1K_2\zeta_2\omega_2 + 2K_4C_2\zeta_1\omega_1 + \bar{\omega}_1^2\{1 - C_1K_1\} + \omega_2^2\{1 - C_2K_3\}]s^2 +$$
$$[C_1K_2\omega_2^2 + C_2K_4\bar{\omega}_1^2 + 2\zeta_2\omega_2\bar{\omega}_1^2\{1 - C_1K_1\} + 2\zeta_1\omega_1\omega_2^2\{1 - C_2K_3\}]s +$$
$$\omega_1^2\omega_2^2\{1 - C_1K_1 - C_2K_3\}. \tag{4.28}$$

$$K = [\bar{\omega}_1^2 - \omega_1^2]s^3 + [\{\bar{\omega}_1^2 - \omega_1^2\}\{C_2K_4 + 2\zeta_2\omega_2\}]s^2 + [\omega_2^2\{1 - C_2K_3\}\{\bar{\omega}_1^2 - \omega_1^2\}]s \tag{4.29}$$

$$L = [C_1K_3\{\omega_1^2 - \bar{\omega}_1^2\}]s^2 + [\{\omega_1^2 - \bar{\omega}_1^2\}\{2C_1K_3\zeta_2\omega_2 + C_1K_4\}]s \tag{4.30}$$

$$M = [C_1K_4\{\omega_1^2 - \bar{\omega}_1^2\}]s^2 + [C_1K_3\omega_2^2\{\bar{\omega}_1^2 - \omega_1^2\}]s \tag{4.31}$$

$$N = [2\zeta_1\{1 - C_1K_1\}\{\bar{\omega}_1 - \omega_1\}]s^2 + [\{\bar{\omega}_1 - \omega_1\}\{4\zeta_1\zeta_2\omega_2(1 - C_1K_1) + 2C_2K_4\zeta_1\}]s +$$
$$2\{\bar{\omega}_1 - \omega_1\}\{\zeta_1\omega_2^2(1 - C_1K_1 - C_2K_3)\} \tag{4.32}$$

$$O = s^4 + [2\zeta_1\bar{\omega}_1 + 2\zeta_2\omega_2 + C_2K_4 + C_1K_2]s^3 +$$
$$[4\zeta_1\omega_1\zeta_2\omega_2 + 2C_1K_2\zeta_2\omega_2 + 2K_4C_2\zeta_1\bar{\omega}_1 + \omega_1^2\{1 - C_1K_1\} + \omega_2^2\{1 - C_2K_3\}]s^2 +$$
$$[C_1K_2\omega_2^2 + C_2K_4\omega_1^2 + 2\zeta_2\omega_2\omega_1^2\{1 - C_1K_1\} + 2\zeta_1\bar{\omega}_1\omega_2^2\{1 - C_2K_3\}]s +$$
$$\omega_1^2\omega_2^2\{1 - C_1K_1 - C_2K_3\}. \tag{4.33}$$

$$P = [2C_1K_3\zeta_1\{\omega_1 - \bar{\omega}_1\}]s^2 + [\{\omega_1 - \bar{\omega}_1\}2\zeta_1C_1\{2K_3\zeta_2\omega_2 + K_4\}]s \tag{4.34}$$

$$Q = [2C_1K_4\zeta_1\{\omega_1 - \bar{\omega}_1\}]s^2 - [2C_1K_3\zeta_1\omega_2^2\{\omega_1 - \bar{\omega}_1\}]s \tag{4.35}$$

$$R = [C_1K_1\{\omega_2^2 - \bar{\omega}_2^2\}]s^2 + [\{\omega_2^2 - \bar{\omega}_2^2\}\{2C_2K_1\zeta_1\omega_1 + C_2K_2\}]s \tag{4.36}$$

$$S = [C_2K_2\{\omega_2^2 - \bar{\omega}_2^2\}]s^2 + [C_2K_1\omega_1^2\{\bar{\omega}_2^2 - \omega_2^2\}]s \tag{4.37}$$

$$\begin{aligned}
T \;=\; & s^4 + [2\zeta_1\omega_1 + 2\zeta_2\omega_2 + C_2K_4 + C_1K_2]s^3 + \\
& [4\zeta_1\omega_1\zeta_2\omega_2 + 2C_1K_2\zeta_2\omega_2 + 2K_4C_2\zeta_1\omega_1 + \omega_1^2\{1 - C_1K_1\} + \bar{\omega}_2^2\{1 - C_2K_3\}]s^2 + \\
& [C_1K_2\bar{\omega}_2^2 + C_2K_4\omega_1^2 + 2\zeta_2\omega_2\omega_1^2\{1 - C_1K_1\} + 2\zeta_1\omega_1\bar{\omega}_2^2\{1 - C_2K_3\}]s + \\
& \omega_1^2\bar{\omega}_2^2\{1 - C_1K_1 - C_2K_3\}. \tag{4.38}
\end{aligned}$$

$$U = [\bar{\omega}_2^2 - \omega_2^2]s^3 + [\{\bar{\omega}_2^2 - \omega_2^2\}\{C_1K_2 + 2\zeta_1\omega_1\}]s^2 + [\omega_1^2\{1 - C_1K_1\}\{\bar{\omega}_2^2 - \omega_2^2\}]s \tag{4.39}$$

$$V = [2C_2K_1\zeta_2\{\omega_2 - \bar{\omega}_2\}]s^2 + [\{\omega_2 - \bar{\omega}_2\}2\zeta_2C_2\{2K_1\zeta_1\omega_1 + K_2\}]s \tag{4.40}$$

$$W = [2C_2K_2\zeta_2\{\omega_2 - \bar{\omega}_2\}]s^2 + [\{\omega_2 - \bar{\omega}_2\}2\zeta_2C_2K_1\omega_1^2\zeta_2]s \tag{4.41}$$

$$\begin{aligned}
X \;=\; & [2\zeta_2\{1 - C_2K_3\}\{\bar{\omega}_2 - \omega_2\}]s^2 + [\{\bar{\omega}_2 - \omega_2\}\{4\zeta_1\zeta_2\omega_1(1 - C_2K_3) + 2C_1K_2\zeta_2\}]s + \\
& 2\{\bar{\omega}_2 - \omega_2\}\{\zeta_2\omega_1^2(1 - C_1K_1 - C_2K_3)\} \tag{4.42}
\end{aligned}$$

46

$$Y = s^4 + [2\zeta_1\omega_1 + 2\zeta_2\bar{\omega}_2 + C_2K_4 + C_1K_2]s^3 +$$

$$[4\zeta_1\omega_1\zeta_2\bar{\omega}_2 + 2C_1K_2\zeta_2\bar{\omega}_2 + 2K_4C_2\zeta_1\omega_1 + \omega_1^2\{1 - C_1K_1\} + \omega_2^2\{1 - C_2K_3\}]s^2 +$$

$$[C_1K_2\omega_2^2 + C_2K_4\omega_1^2 + 2\zeta_2\bar{\omega}_2\omega_1^2\{1 - C_1K_1\} + 2\zeta_1\omega_1\omega_2^2\{1 - C_2K_3\}]s +$$

$$\omega_1^2\omega_2^2\{1 - C_1K_1 - C_2K_3\}. \tag{4.43}$$

$$Z = s^4 + [2\zeta_1\omega_1 + 2\zeta_2\omega_2 + C_2K_4 + C_1K_2]s^3 +$$

$$[4\zeta_1\omega_1\zeta_2\omega_2 + 2C_1K_2\zeta_2\omega_2 + 2K_4C_2\zeta_1\omega_1 + \omega_1^2\{1 - C_1K_1\} + \omega_2^2\{1 - C_2K_3\}]s^2 +$$

$$[C_1K_2\omega_2^2 + C_2K_4\omega_1^2 + 2\zeta_2\omega_2\omega_1^2\{1 - C_1K_1\} + 2\zeta_1\omega_1\omega_2^2\{1 - C_2K_3\}]s +$$

$$\omega_1^2\omega_2^2\{1 - C_1K_1 - C_2K_3\}. \tag{4.44}$$

Trying to force S to the identity matrix is not as obvious as in the one-mode case. However, choosing $K_1 = \dfrac{1}{C_1}$ and $K_2 = 30$ as in the one-mode case, and $K_3 = \dfrac{1}{C_2}, K_4 = 70$, yields a two-mode sensitivity-shaped filter which produces more accurate velocity estimates than the one-mode sensitivity-shaped filter. Since the pinned-pinned beam is dominated by the first two modes of motion, it is not necessary to produce a filter of three modes or higher. However, it is conjectured that the gains for the n-mode sensitivity-shaped filter can be determined via

$$K_{2i-1} = \frac{1}{C_i}$$
and
$$K_{2i} \geq \omega_{i+1} \tag{4.45}$$

for $i = 1, ..., n$.

Using the six-mode model for the system plant, as outlined in Chapter 3, the time response of the sensitivity-shaped estimators, the central LQ estimators, and

the decentral frequency-shaped estimator are compared. The estimators all contain the modelled frequencies ω_i. Systems with and without noise present are included. For the case with no system noise, given in Figure 4.2, the sensitivity-shaped filters estimate position more accurately, in the root mean square (rms) error sense, than the LQ filters with pseudo-noise or the decentral filter. The fact that the sensitivity-shaped filters perform better than the full-order LQ filter is due to the fact that pseudo-noise was introduced to obtain the LQ gains. The optimal time-invariant filter of zero gains is just the model with nominal frequencies, and is also included in Figure 4.2. The velocity estimates of the one-mode and two-mode sensitivity-shaped filters are comparable to the two-mode and four-mode LQ filters, respectively. For the system including noise, given in Figure 4.3, the one-mode sensitivity-shaped filter performs comparable to the four-mode and two-mode LQ filters for position and velocity estimates, respectively. Increasing the sensitivity-shaped gain k_2 above the given value will yield even better velocity estimates. Thus, the one-mode sensitivity-shaped filter is at least preferred over a filter of two modes – a saving in computations is achieved here. The two-mode sensitivity-shaped filter estimates position more accurately than any other filter investigated. The fact that the sensitivity-shaped position rms error values are lower than those of the optimal full-order filter is due to the fact that the optimal filter is time-invariant and also to the statistical anomaly in generating noise in the simulation. The two-mode sensitivity-shaped filter accuracy of the velocity estimates lies between the two-mode and four-mode LQ filters. It is important to note that these results are independent of sensor position. Regardless of the sensor position, the same trends in performance of the filters are recognized.

4.2 Positive Real Systems

A set of filter gains to decrease filter frequency sensitivity has been chosen on the basis of estimation performance. Is the resulting filter going to yield a robust closed-loop system? Before analyzing the robustness of the system, it is important to introduce positivity concepts. The following Definitions 1 and 2 and Theorems 1 and 2 are presented in [4].

Definition 1: A square transfer matrix $H(s)$ is called positive real if

(a) $H(s)$ has real elements for real s, and

(b) $H(s)$ has elements which are analytic for $\Re[s] > 0$, and

(c) $H^*(s) + H(s)$ is positive semidefinite for $\Re[s] > 0$, where * denotes the complex conjugate transpose.

Definition 2: A square transfer matrix H(s) is strictly positive real if

(a) $H(s)$ has real elements for real s, and

(b) $H(s)$ has elements that are analytic for $\Re[s] \geq 0$, and

(c) $H^*(j\omega) + H(j\omega)$ is positive definite for all real ω.

Theorem 1:

Given the square transfer matrices $G(s)$ and $H(s)$ in the feedback system of Figure 4.4, the system is asymptotically stable if at least one of the transfer matrices is positive real and the other transfer matrix is strictly positive real. If both transfer matrices $G(s)$ and $H(s)$ are only positive real, then the feedback system will be at least marginally stable.

In order to satisfy the sufficient condition of Theorem 1, it must be determined whether $G(s)$ or $H(s)$ is strictly positive real – the other will be constrained to be positive real. Normally, conditions ensuring a strictly positive real transfer matrix $G(s)$ are too restrictive on the model. Hence, $G(s)$ will be considered the positive real transfer matrix. $G(s)$ is not, however, positive real in general and the system must be modelled in a certain form to attain this.

Theorem 2:

For the system described in state variable form in equations (4.1) and (4.2), the transfer matrix $G(s) = C(sI - A)^{-1}B$ is positive real if and

49

only if there exists a symmetric positive definite matrix P and a symmetric positive semi-definite matrix Q such that

$$PA + A^T P = -Q \qquad (4.46)$$

$$C^T = PB. \qquad (4.47)$$

The equations of motion of the LSS in terms of modal variables is

$$\ddot{\eta} + [2\zeta\omega]\dot{\eta} + [\omega^2]\eta = N. \qquad (4.48)$$

Equation (4.48) can be written for n modes in the state space form, with

$$x = [\eta_1, \dot{\eta}_1 : \dots : \eta_n, \dot{\eta}_n] \qquad (4.49)$$

and

$$B = [0, C_1 : \dots : 0, C_n]^T. \qquad (4.50)$$

Now, from Theorem 2, for a positive real transfer matrix $G(s)$, conditions (4.46) and (4.47) must hold. Because of the form of the A matrix in equation (4.7), it can be shown that (4.46) will be satisfied for

$$P = diag(P_i) \text{ with } P_i = \begin{bmatrix} \omega_i^2 & 0 \\ 0 & 1 \end{bmatrix} \qquad (4.51)$$

$$Q = diag(Q_i) \text{ with } Q_i = \begin{bmatrix} 0 & 0 \\ 0 & 4\zeta_i\omega_i \end{bmatrix} \qquad (4.52)$$

Substitution of (4.50) and (4.51) into (4.47) yields

$$C^T = B. \tag{4.53}$$

The matrix B defined in (4.50) operates on the control vector $\boldsymbol{u}$ to indicate how the input signals act on the system states. It holds the information on the actuator locations and orientations through the generalized force vector $\boldsymbol{N}$. The matrix C operates on the state vector to give the outputs. It will therefore hold the information on the sensor locations and orientations. Therefore, using $C^T = B$ implies that the system has collocated actuators and sensors, and the above analysis indicates that this system configuration guarantees a positive real system transfer matrix $G(s)$. Note that the form of C given by (4.50) and (4.53) restricts the system sensors to rate sensors only. A positive real $G(s)$ may exist for non-collocated actuators and sensors and/or sensors other than rate sensors. However, these limitations have been adhered to here since they guarantee $G(s)$ positive real.

4.3   Phase-shaping Method to Test Robustness

Theorem 1 is a sufficient condition for guaranteed asymptotic stability in the presence of modelling errors. For collocated actuators and rate sensors, the system transfer matrix $G(s)$ is positive real. Attempts will now focus on finding a feedback transfer matrix $H(s)$ which is strictly positive real as given by Definition 2. This can undoubtedly be examined in numerous ways. One approach is termed the "phase-shaping" method, which is outlined below.

A sufficient condition for $H(s)$ to be strictly positive real is given in Theorem 3.

Theorem 3:

If the phase of each transfer function element of the filter transfer matrix

51

$H_F(s)$ lies between ± 90 degrees, and if the controller gains K are positive, then $H(s) = KH_F(s)$ is strictly positive real. Note that if the endpoints ± 90 degrees are included, then $H(s)$ is positive real. A proof of this theorem is contained within Appendix B.

The focus of this study is on the performance of the optimal and suboptimal filters. The open-loop case will be presented here, as well as the closed-loop case with generic controllers. It is assumed that the state-feedback controller gain K must be chosen to ensure that Theorem 3 is satisfied. In this way, filter performance can be evaluated as independently as possible of the controller used.

Referring to Figure 4.5, the feedback transfer matrix $H(s)$ is the combination of the estimator transfer matrix, $H_F(s)$, and the controller gain matrix, K. $H(s)$ is written as

$$H(s) = KH_F(s). \qquad (4.54)$$

The dimensions of these matrices are as follows: K is the number of measurements by twice the number of filter plant modelled modes; $H_F(s)$ is twice the number of filter plant modelled modes by the number of measurements; and $H(s)$ is the number of measurements by the number of measurements.

In the case of the one-mode sensitivity-shaped filter of Section 4.1, there is a phase shift of -90 degrees. This indicates positive realness rather than strict positive realness. The Bode phase plots for the transfer function elements of the transfer matrix between the filter output (estimated state) and the filter input (measurement) are given in Figures 4.6 to 4.7.

While these results do not guarantee asymptotic stability, two things must be remembered. For the one-mode sensitivity-shaped filter, $H(s)$ is guaranteed to be positive real by the **sufficient** condition of the phase-shaping method – this in turn

guarantees the closed-loop system at least marginal stability by the **sufficient** condition of Theorem 1. In other words, a conservative constraint has been imposed on top of another conservative constraint. The phase-shaping method guarantees that the system using the sensitivity-shaped filter is at *least* marginally stable. These results rely upon the choice of K to satisfy Theorem 3.

4.4 Lyapunov Method to Test Robustness

The phase-shaping method, based on the sufficient condition of Theorem 3, does not indicate whether or not the system is guaranteed asymptotic stability in the presence of modelling errors. Another approach is to investigate Theorem 2 as a necessary and sufficient condition. A form of Theorem 2 is given by

$$PA_{cl} + A_{cl}^T P = -(Q - K^T C - C^T K) \tag{4.55}$$

$$A^{cl} = (A - BK) \tag{4.56}$$

$$K^T = PK_F \tag{4.57}$$

where P is a symmetric positive definite matrix and Q is a symmetric positive semidefinite matrix. For the sensitivity-shaped gains of Section 4.1, $H(s)$ is strictly positive real if a K, P and Q can be found to satisfy equations (4.55) to (4.57).

Looking at the one-mode sensitivity-shaped filter, the matrices become

$$P = \begin{bmatrix} p_{11} & p_{12} \\ p_{12} & p_{22} \end{bmatrix} \tag{4.58}$$

53

$$Q = \begin{bmatrix} q_{11} & q_{12} \\ q_{12} & q_{22} \end{bmatrix} \qquad (4.59)$$

$$K_F = [kf_1, kf_2]^T \qquad (4.60)$$

$$K = [k_1, k_2]. \qquad (4.61)$$

The constraints are

$$q_{11} = -2p_{12}(\tilde{\omega}_1^2 + k_1 C_1) \qquad (4.62)$$

$$q_{12} = k_1 C_1 + p_{11} - p_{12}(2\zeta_1 \bar{\omega}_1 + k_2 C_1) - p_{22}(\bar{\omega}_1^2 + k_1 C_1) \qquad (4.63)$$

$$q_{22} = 2k_2 C_1 + 2(p_{12} - p_{22}[2\zeta_1 \bar{\omega}_1 + k_2 C_1]) \qquad (4.64)$$

$$k_1 = p_{11} kf_1 + p_{22} kf_2 \qquad (4.65)$$

$$k_1 = p_{12} kf_1 + p_{22} kf_2 \qquad (4.66)$$

$$P > 0 \qquad (4.67)$$

$$Q \geq 0. \qquad (4.68)$$

Choosing $P = \begin{bmatrix} 1 & -.0038 \\ -.0038 & .0522 \end{bmatrix}$ and $Q = \begin{bmatrix} 1 & .4893 \\ .4893 & 13.99 \end{bmatrix}$ yields the controller gain matrix $K = [.1108, 1.5654]$ which will satisfy equations (4.55) to (4.57). For the set of sensitivity-shaped gains, then, it is possible to choose P, Q, and K to ensure $H(s)$ is strictly positive real. In actuality, there are many different choices of P, Q, and K which will ensure this, and Section 4.5 deals with this topic.

4.5   Closed-Loop System Analysis

A brief analysis of the effect of P and Q on the controller gain matrix K and, hence, the closed-loop system performance, is presented. Six cases are chosen to represent possible variations in k_1 and k_2 and are listed below as Cases 1 through 6 in equations (4.69) to (4.74).

$$
\begin{aligned}
P &= \begin{bmatrix} 1 & -.0038 \\ -.0038 & .05 \end{bmatrix}, Q = \begin{bmatrix} 1 & .49 \\ .49 & 13.95 \end{bmatrix} \\
K &= \begin{bmatrix} .1108 & .5 \end{bmatrix}
\end{aligned}
\tag{4.69}
$$

$$
\begin{aligned}
P &= \begin{bmatrix} 1 & -.0038 \\ -.0038 & .05 \end{bmatrix}, Q = \begin{bmatrix} 1 & .49 \\ .49 & 13.95 \end{bmatrix} \\
K &= \begin{bmatrix} .1108 & 1.5654 \end{bmatrix}
\end{aligned}
\tag{4.70}
$$

$$
\begin{aligned}
P &= \begin{bmatrix} 1 & -.0038 \\ -.0038 & .8 \end{bmatrix}, Q = \begin{bmatrix} 1 & .49 \\ .49 & 14.73 \end{bmatrix} \\
K &= \begin{bmatrix} .1108 & 24 \end{bmatrix}
\end{aligned}
\tag{4.71}
$$

$$
\begin{aligned}
P &= \begin{bmatrix} 1 & .16 \\ .16 & .051 \end{bmatrix}, Q = \begin{bmatrix} 1 & .65 \\ .65 & 13.98 \end{bmatrix} \\
K &= \begin{bmatrix} 5 & 1.5654 \end{bmatrix}
\end{aligned}
\tag{4.72}
$$

$$
P = \begin{bmatrix} 1 & -.0038 \\ -.0038 & .166 \end{bmatrix}, Q = \begin{bmatrix} 1 & .49 \\ .49 & 14.1 \end{bmatrix}
$$

$$K = \begin{bmatrix} 5 & 5 \end{bmatrix} \tag{4.73}$$

$$P = \begin{bmatrix} 1 & .105 \\ .105 & .05 \end{bmatrix}, Q = \begin{bmatrix} 1 & .545 \\ .545 & 13.99 \end{bmatrix}$$

$$K = \begin{bmatrix} 3.37 & 1.5654 \end{bmatrix} \tag{4.74}$$

The closed-loop time response for each of these cases is given for the system with no noise present in Figures 4.8 to 4.9. Note that the larger the control forces, the faster the actual positions and velocities are damped, as is expected. Referring back to Section 4.3, do the controller gains chosen via the Lyapunov method also satisfy the controller gain requirements of the phase-shaping method? Since all of the controller gains are positive, then Theorem 3 guarantees $H(s)$ positive real which, in turn, guarantees marginal stability by the phase-shaping method of Section 4.3.

4.6   Sensitivity to Model Error Analysis

The system using the one-mode sensitivity-shaped filter of Section 4.1 and the controller gains of Section 4.4 has been shown to be robust for structural frequency variations of 20 %. How does the performance of this filter compare with those using LQ estimation theory? This is related to the sensitivity of the estimates to changes in the model parameters, namely, the structural frequencies. It is stated in [7] that optimal filters are more sensitive to model errors, as shown in Figure 4.10.

The sensitivity-shaped filters of Section 4.1, the LQ one, two, four and six-mode filters, and the reduced-order decentralized filter with frequency-shaped gains are considered here. The structural frequencies vary from the modelled frequencies by $\pm$ 20 % in 5 % increments. Figure 4.11 shows the sensitivity to variations in the frequencies ω of each of these filters in the position and velocity estimates with no noise modelled in the system. Model reduction among the LQ filters indicates that the lower the order of the filter, the higher the rms errors, and the less sensitive to changes in ω. This corresponds to the trends shown in Figure 4.10. For the position estimates,

the sensitivity-shaped filters perform the best under structural frequency variations. Once again, the one-mode and two-mode sensitivity-shaped results are comparable to the two-mode and four-mode LQ filters, respectively, for the velocity estimates. Figure 4.12 shows the sensitivity to variations in ω of the sensitivity-shaped, LQ and decentralized filters for the system with modelled noise included. The sensitivity-shaped filters' position estimates are less sensitive to frequency variations. Although the velocity estimate sensitivity plot no longer contains a minimum, due to statistical anomalies in the noise, the same relative performace of the filters is noted, and the one-mode and two-mode sensitivity-shaped filters again perform comparable to the two-mode and four-mode LQ filters, respectively.

In general, the accuracy of the position estimates of the sensitivity-shaped filters are superior to the velocity estimates. This is because the entries in the S matrix of equations (4.14) and (4.27) corresponding to position are identically one and zero while the entries in the S matrix corresponding to velocity are determined by how much the gain k_{2i} shifts the corresponding pole to the left, causing its effects to die out at different rates. The gain k_{2i} should be chosen large enough to yield acceptable velocity estimates; if there is a bound on k_{2i}, then the velocity estimate performance is defined via this bound.
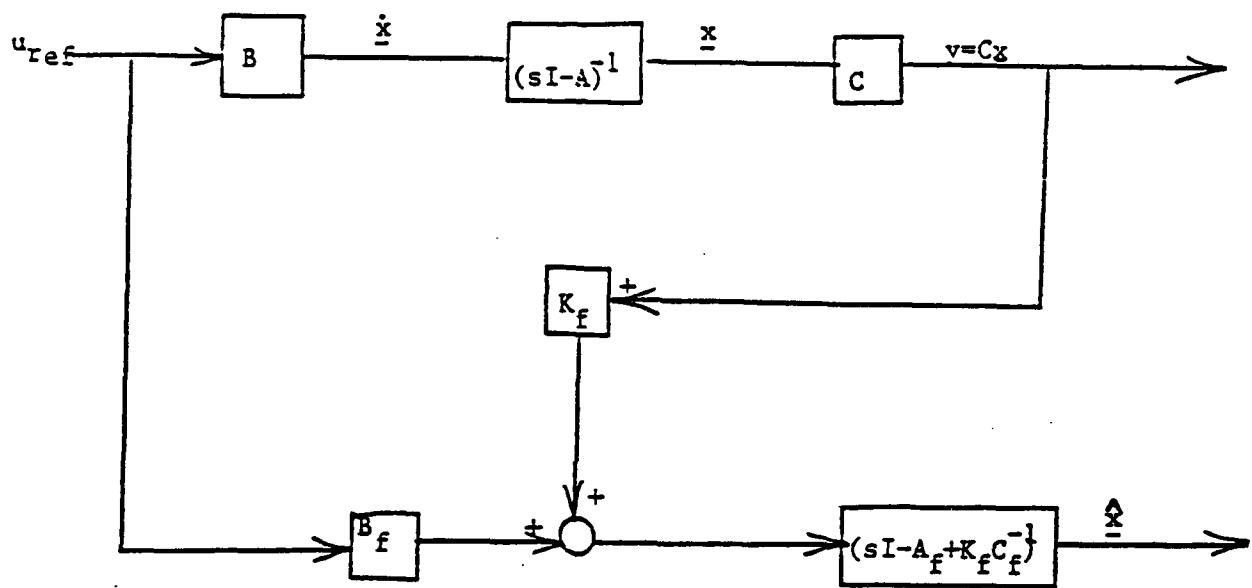
Figure 4.1: Open loop system with SIMO estimator
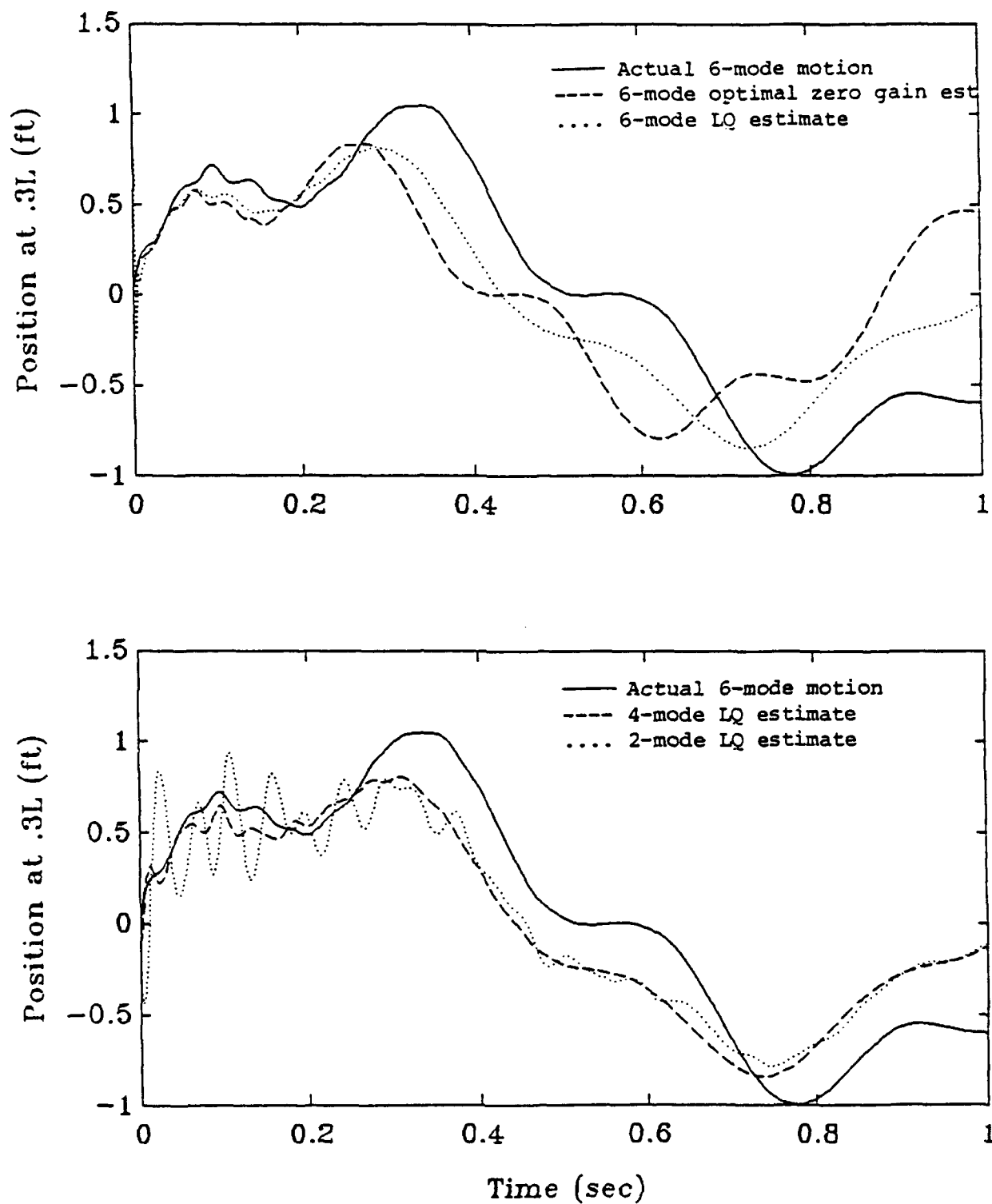
Figure 4.2a: Position estimation results for various filters with no noise in the system and structural frequency variations of 20 %
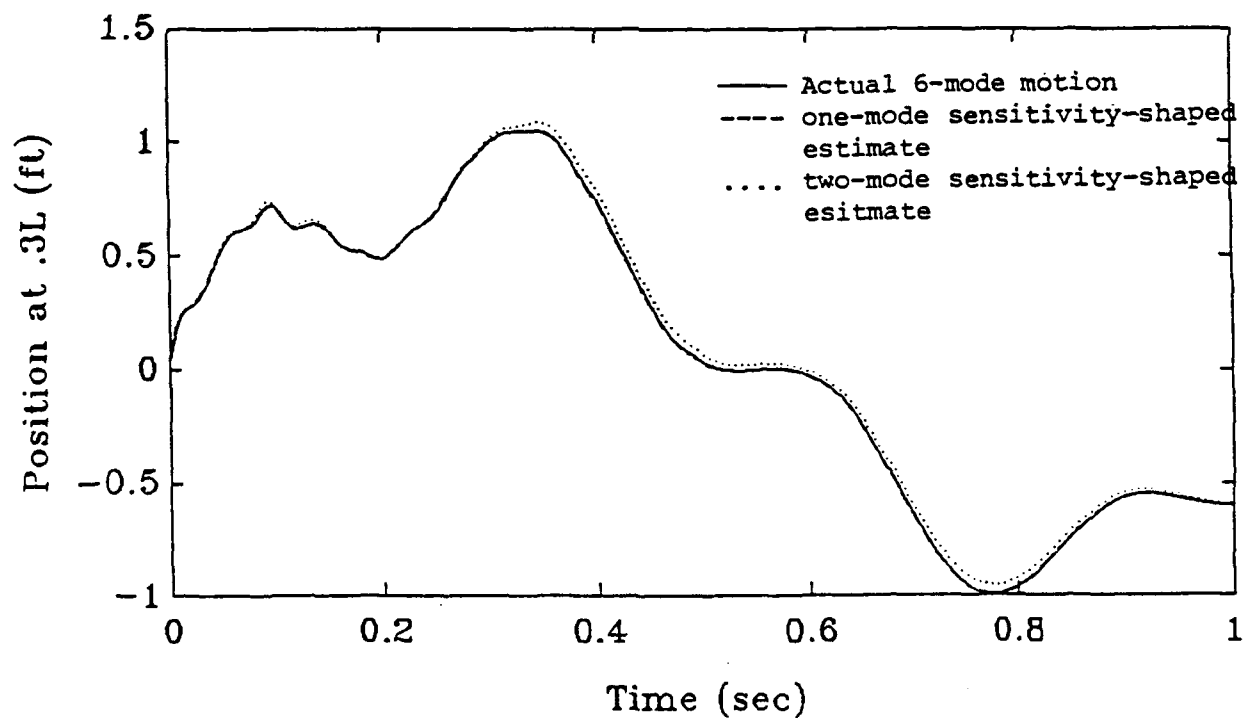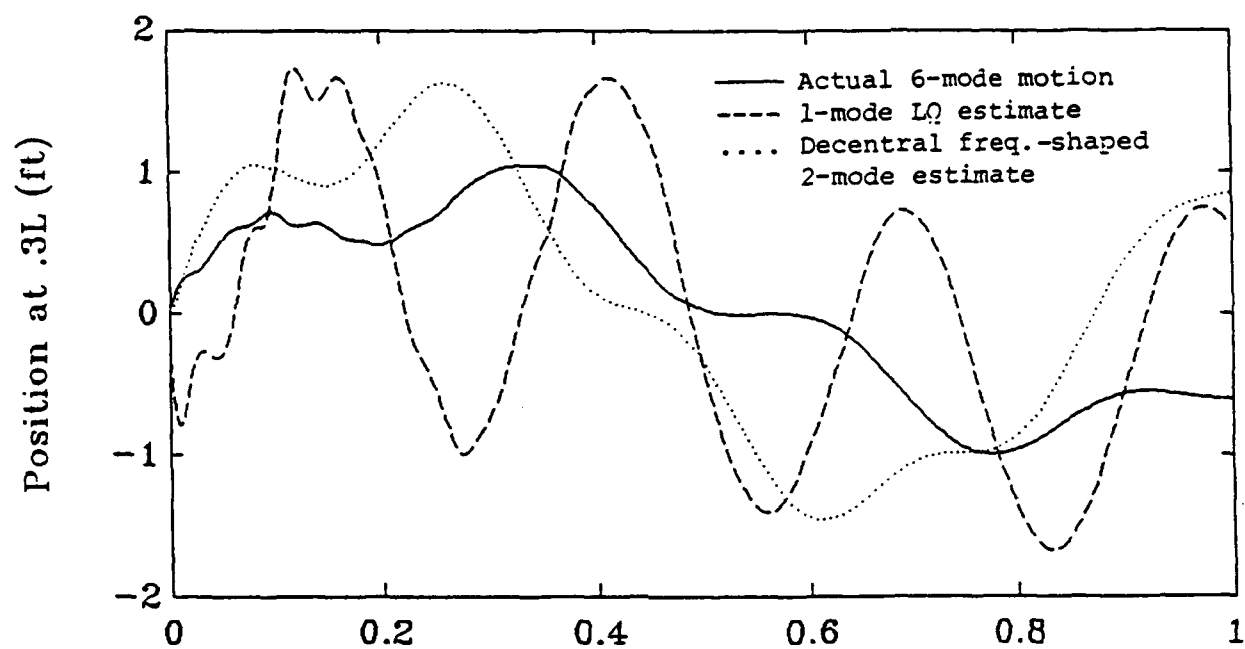
Figure 4.2b: Position estimation results for various filters with no noise in the system and structural frequency variations of 20 %
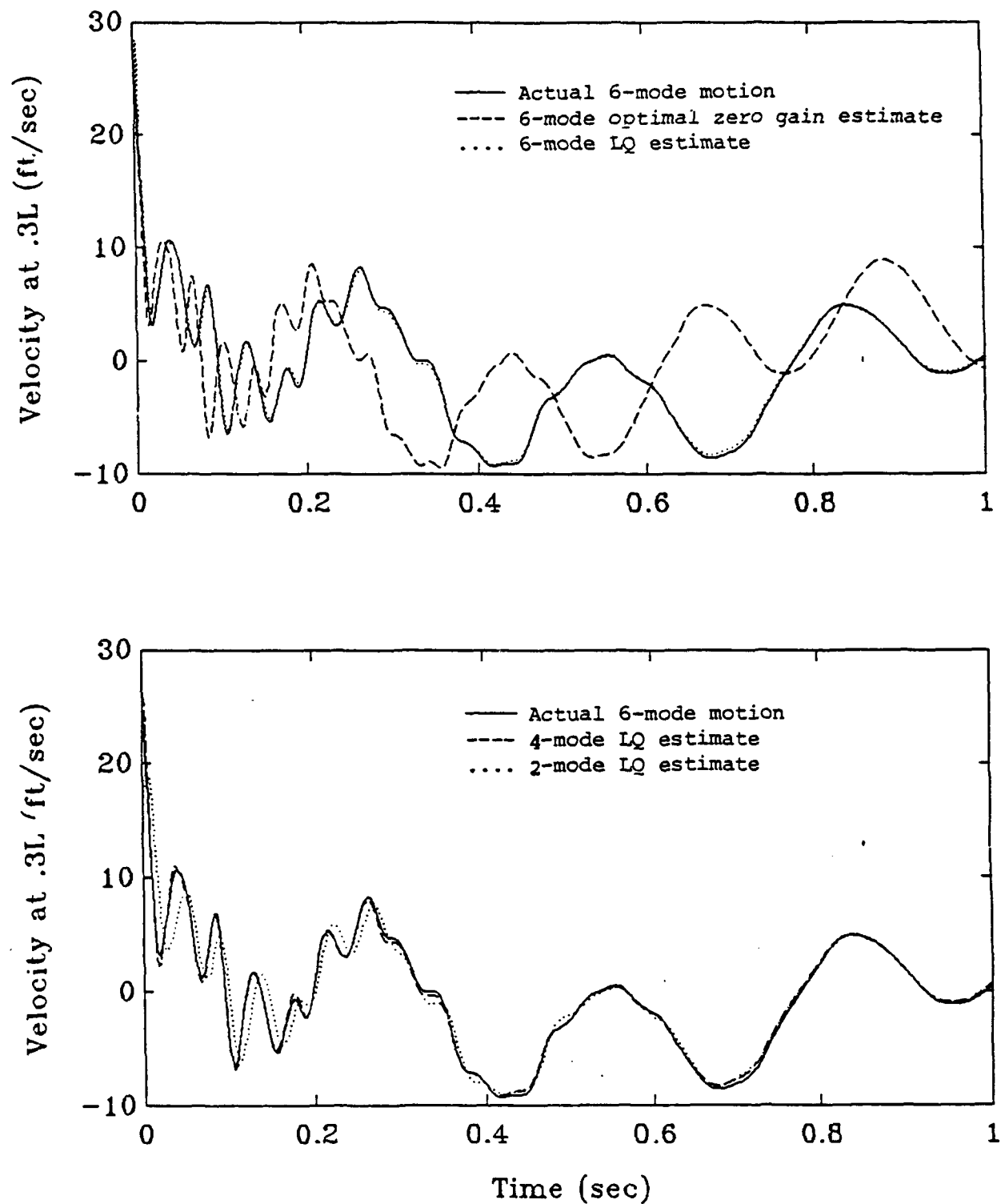
Figure 4.2c: Velocity estimation results for various filters with no noise in the system and structural frequency variations of 20 %
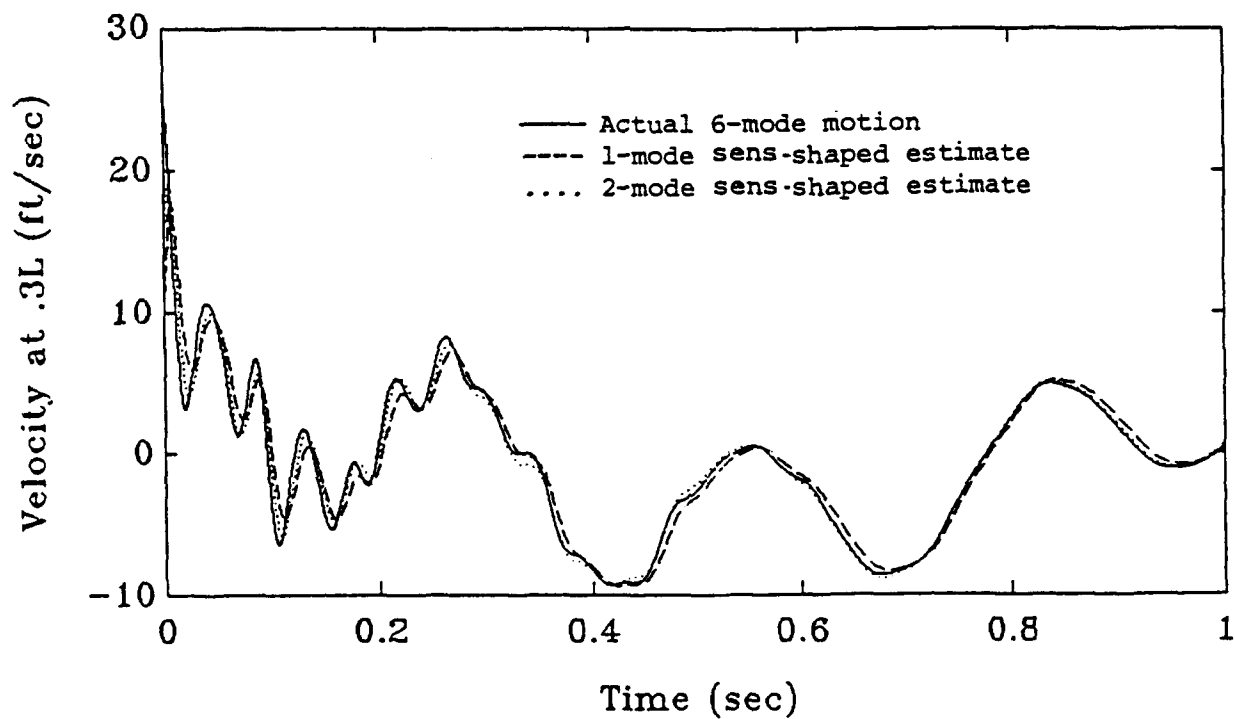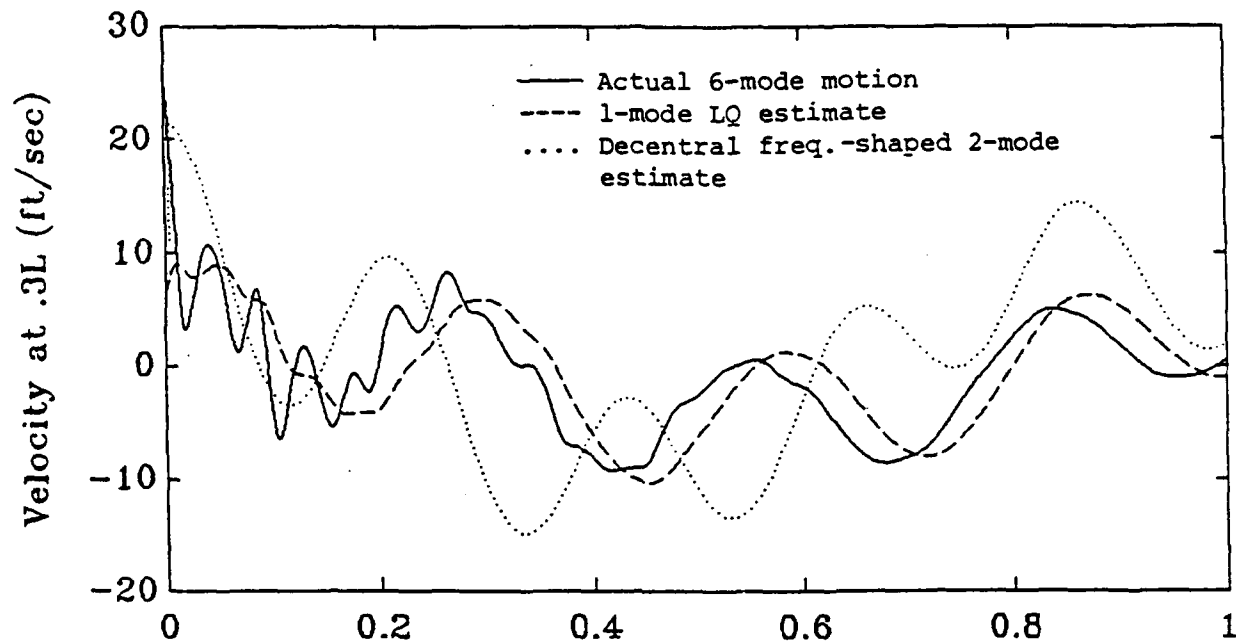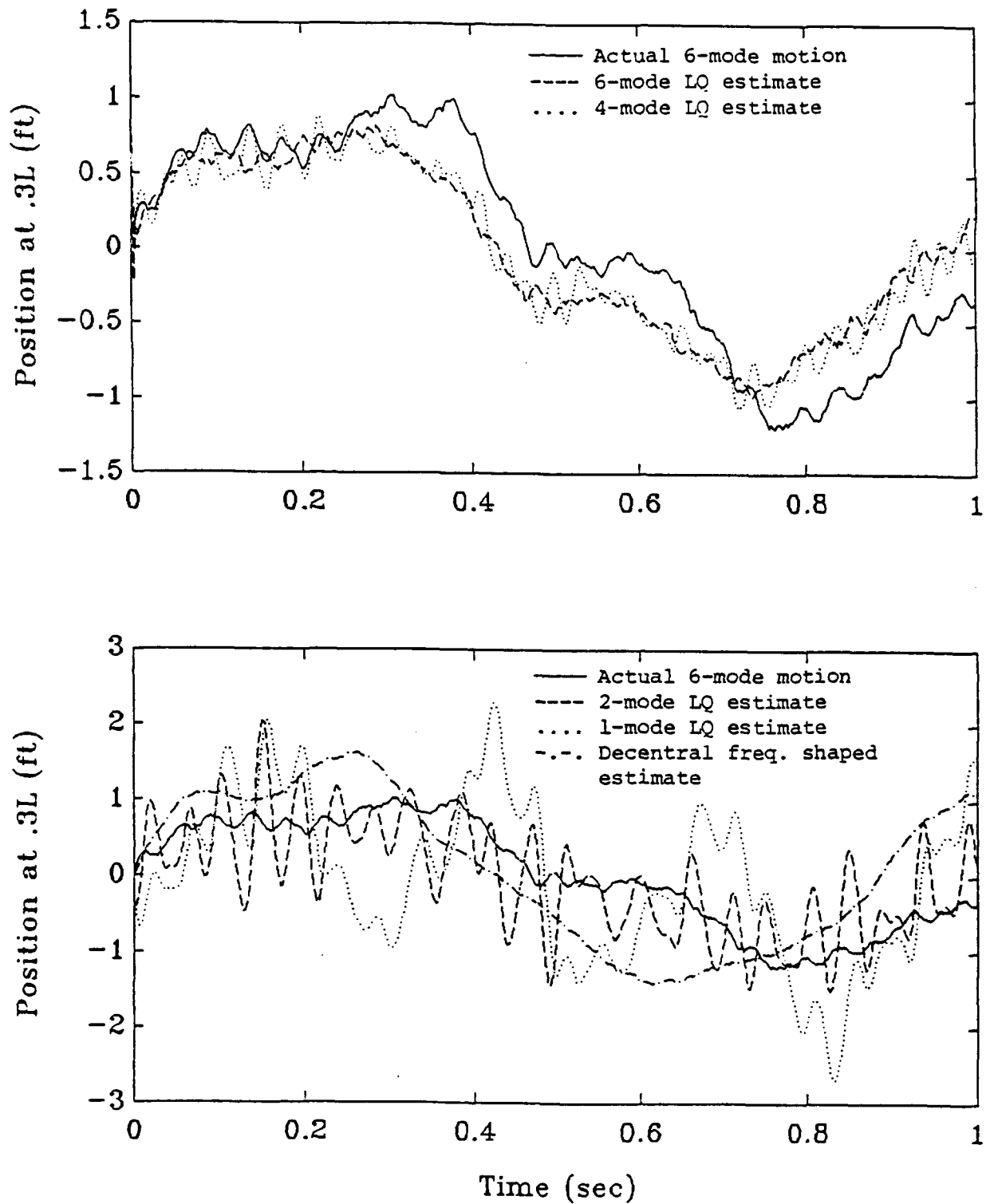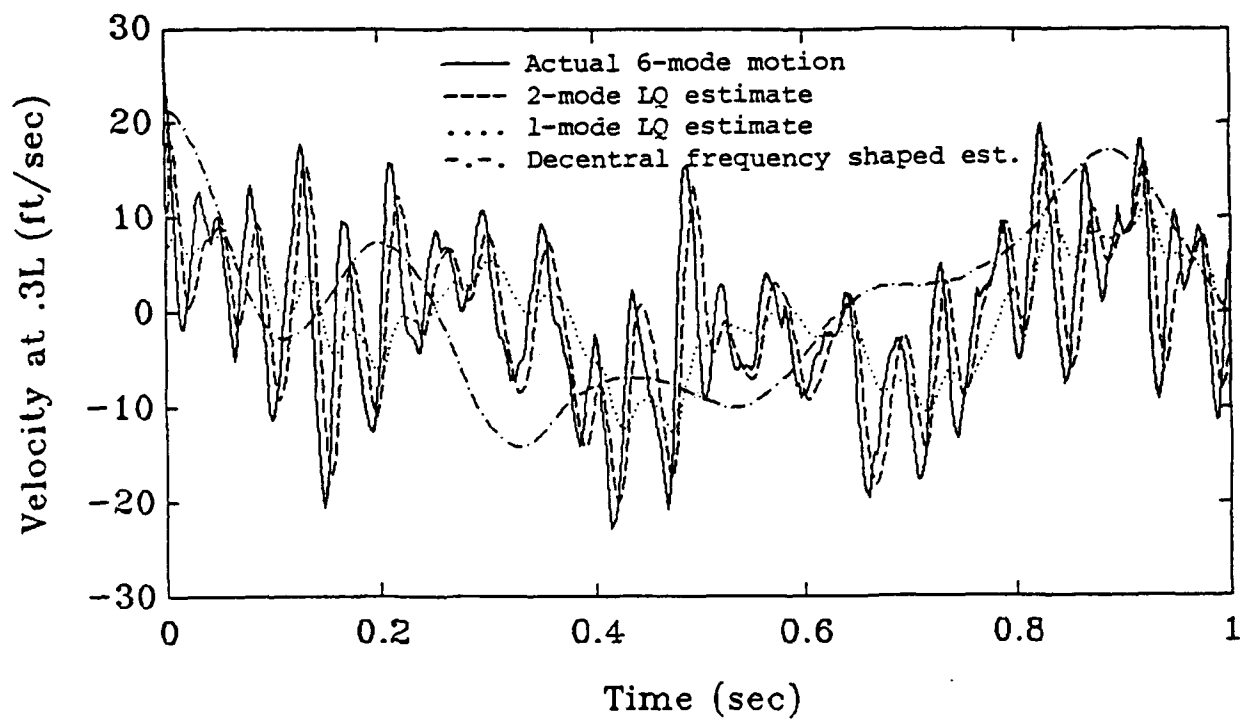
Figure 4.2d: Velocity estimation results for various filters with no noise in the system and structural frequency variations of 20 %

Figure 4.3a: Position estimation results for various filters with modelled noise included and structural frequency variations of 20 %
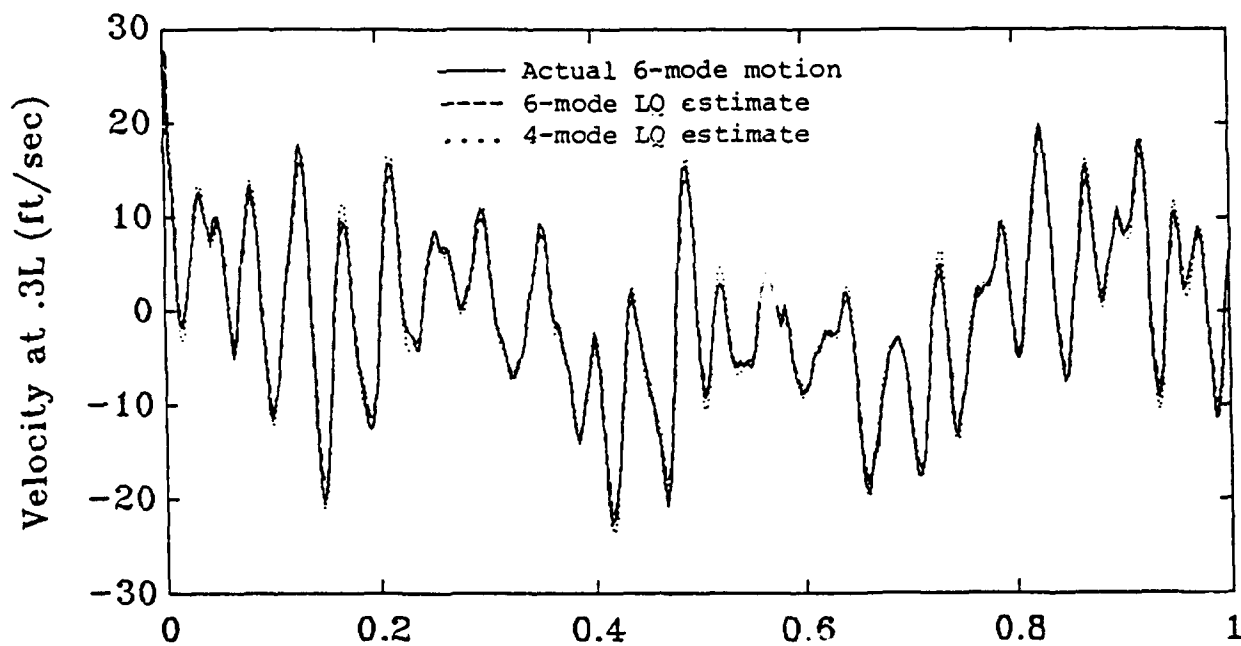
Figure 4.3b: Velocity estimation results for various filters with modelled noise included and structural frequency variations of 20 %
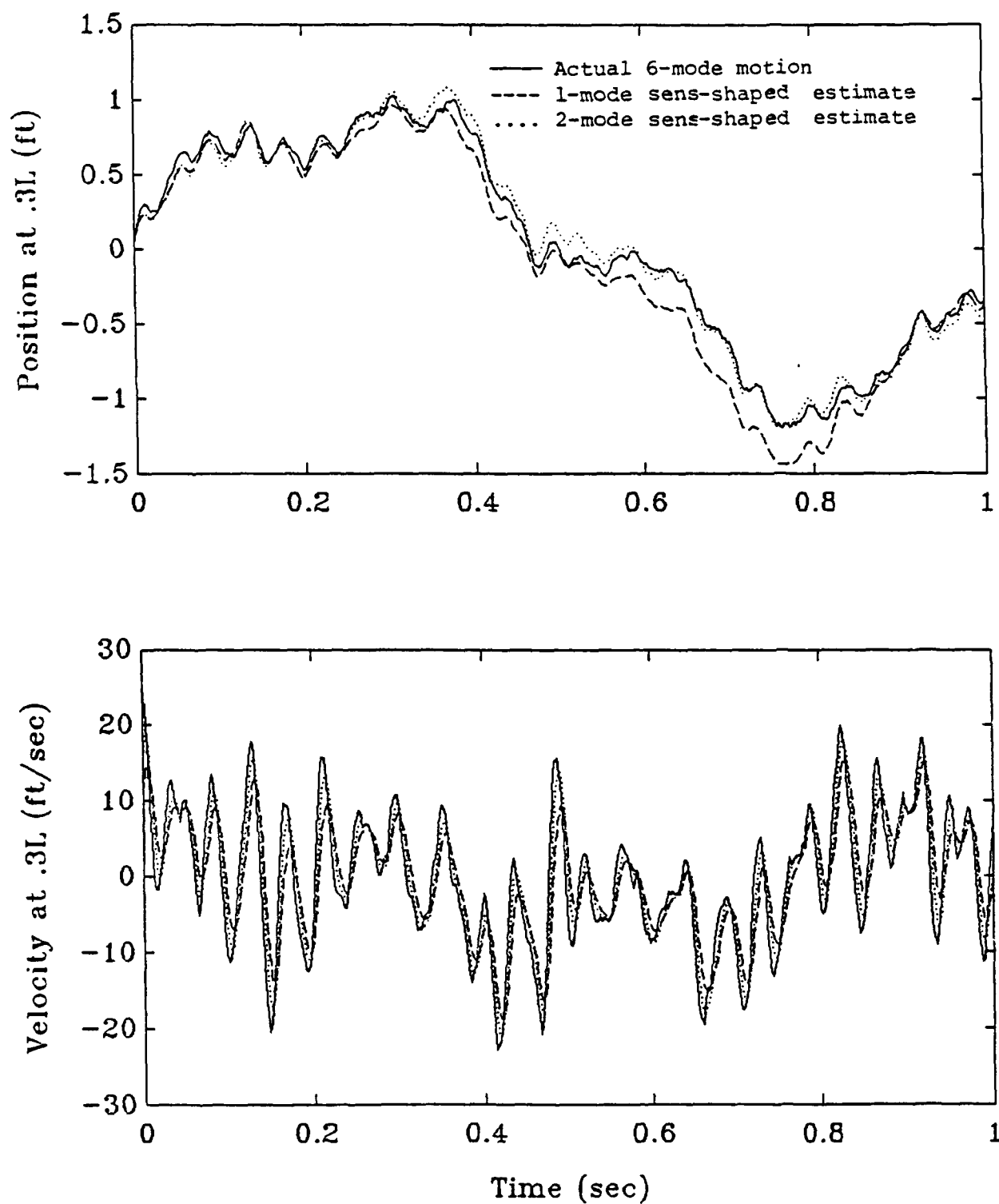
Figure 4.3c: Estimation results for the 1-mode sensitivity-shaped filter. Noise is included with structural frequency variations of 20 %
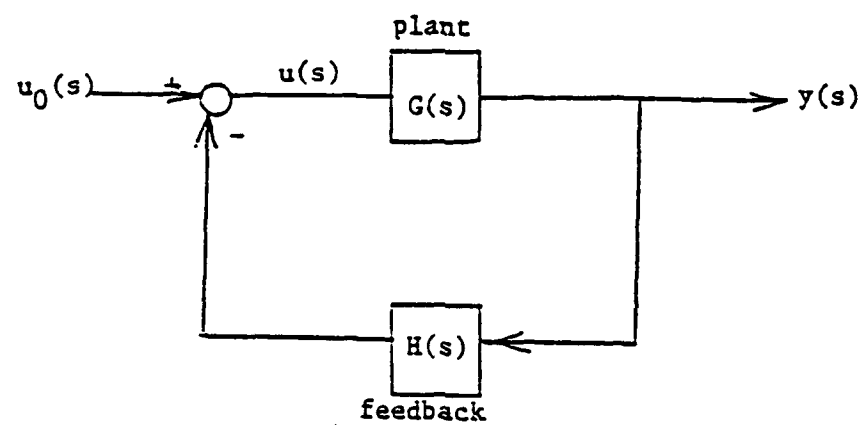
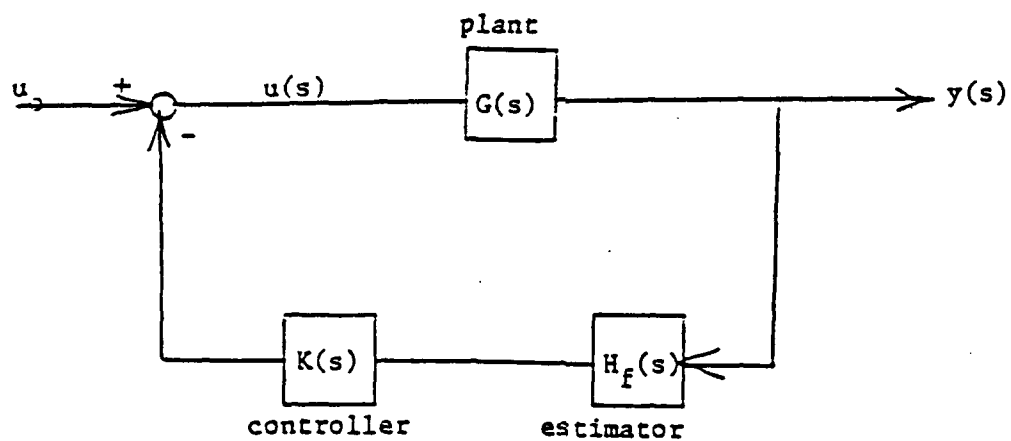Figure 4.4: General feedback control concept

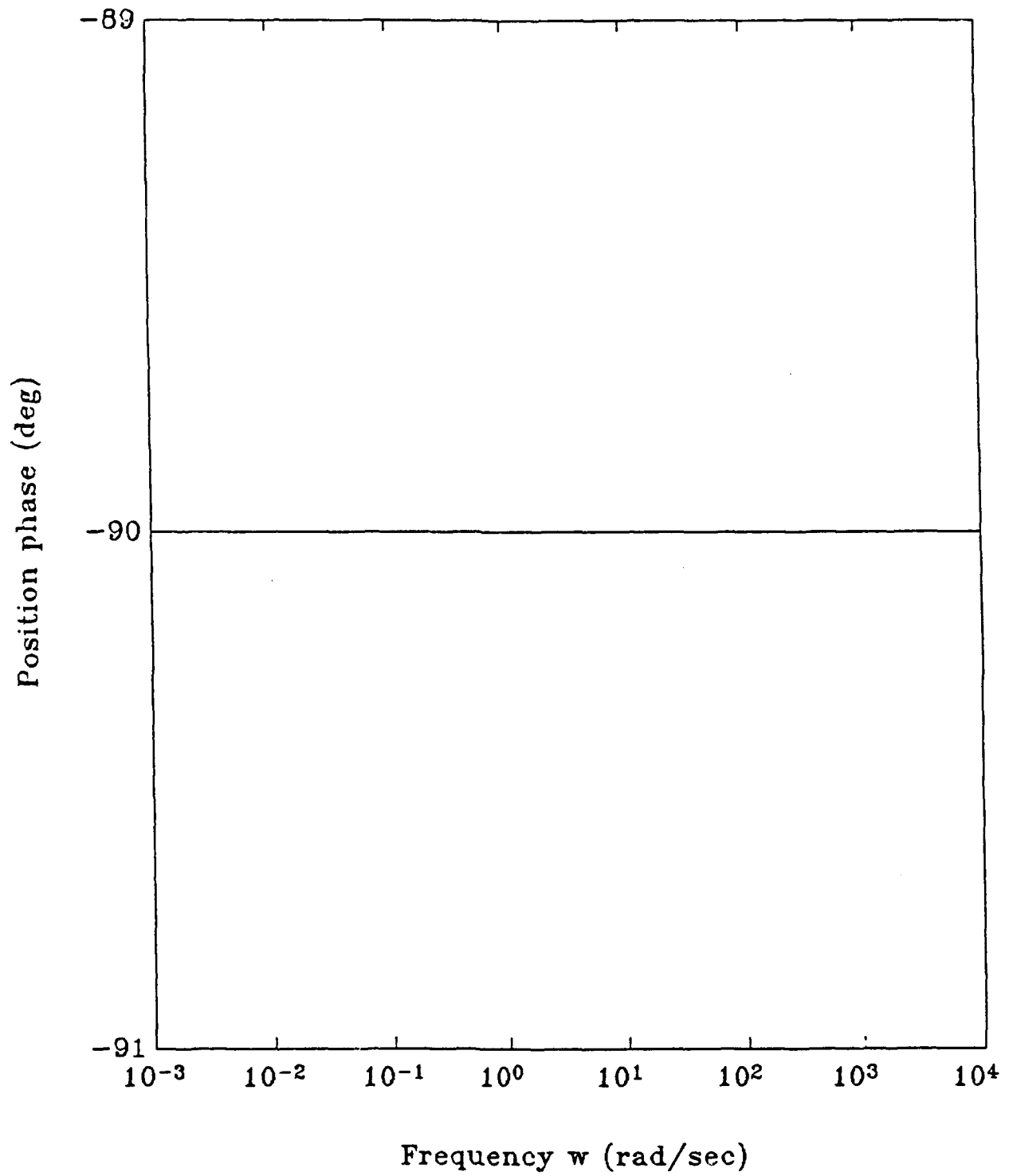Figure 4.5: General feedback control concept with estimator and controller in feedback loop

Figure 4.6: Bode phase diagram of output (sensitivity-shaped filter position esti-mate) to input (measurement y). System has no noise but has structural frequency variations of 20 %
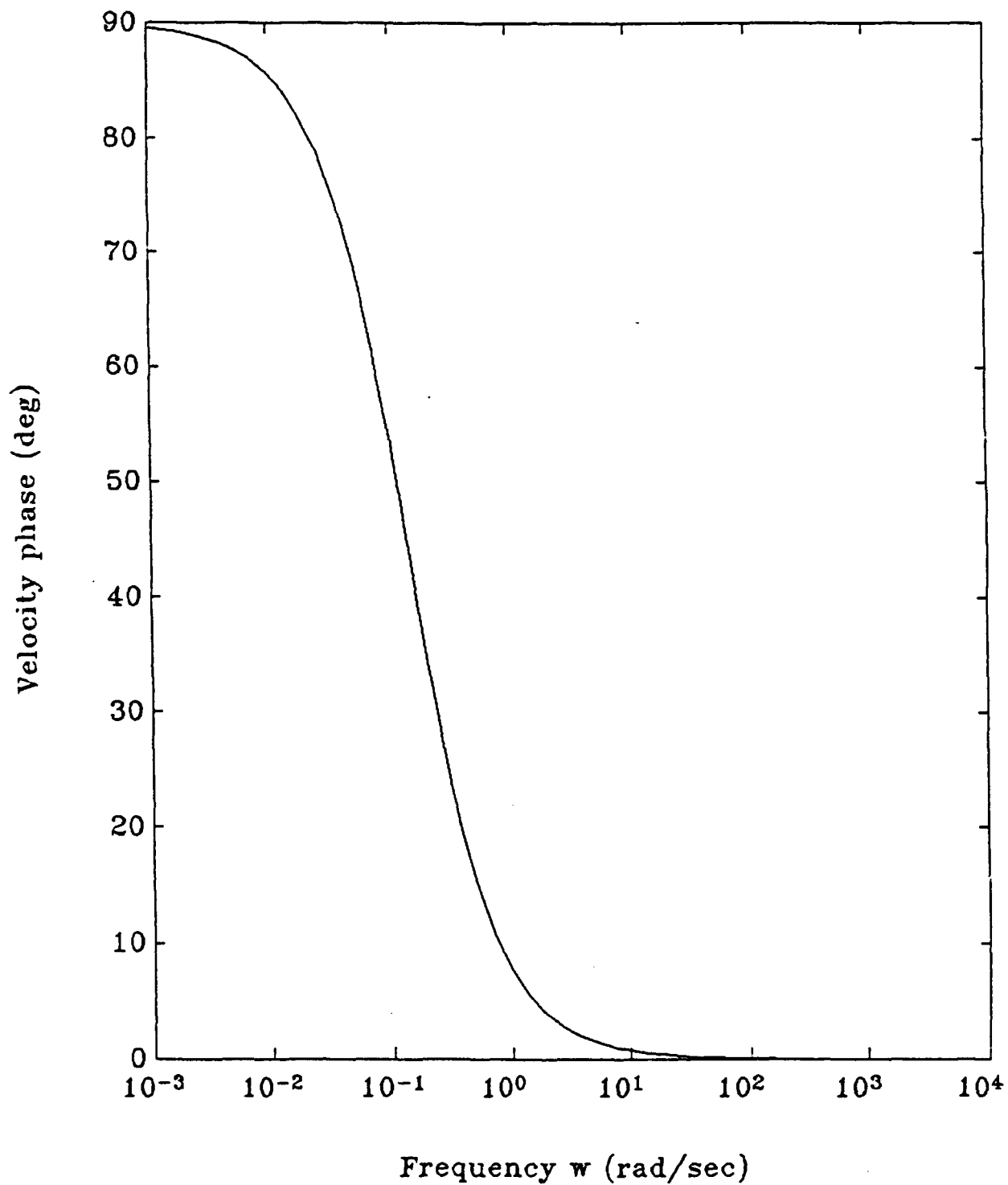
Figure 4.7: Bode phase diagram of output (sensitivity-shaped filter velocity estimate) to input (measurement y). System has no noise but has structural frequency variations of 20 %
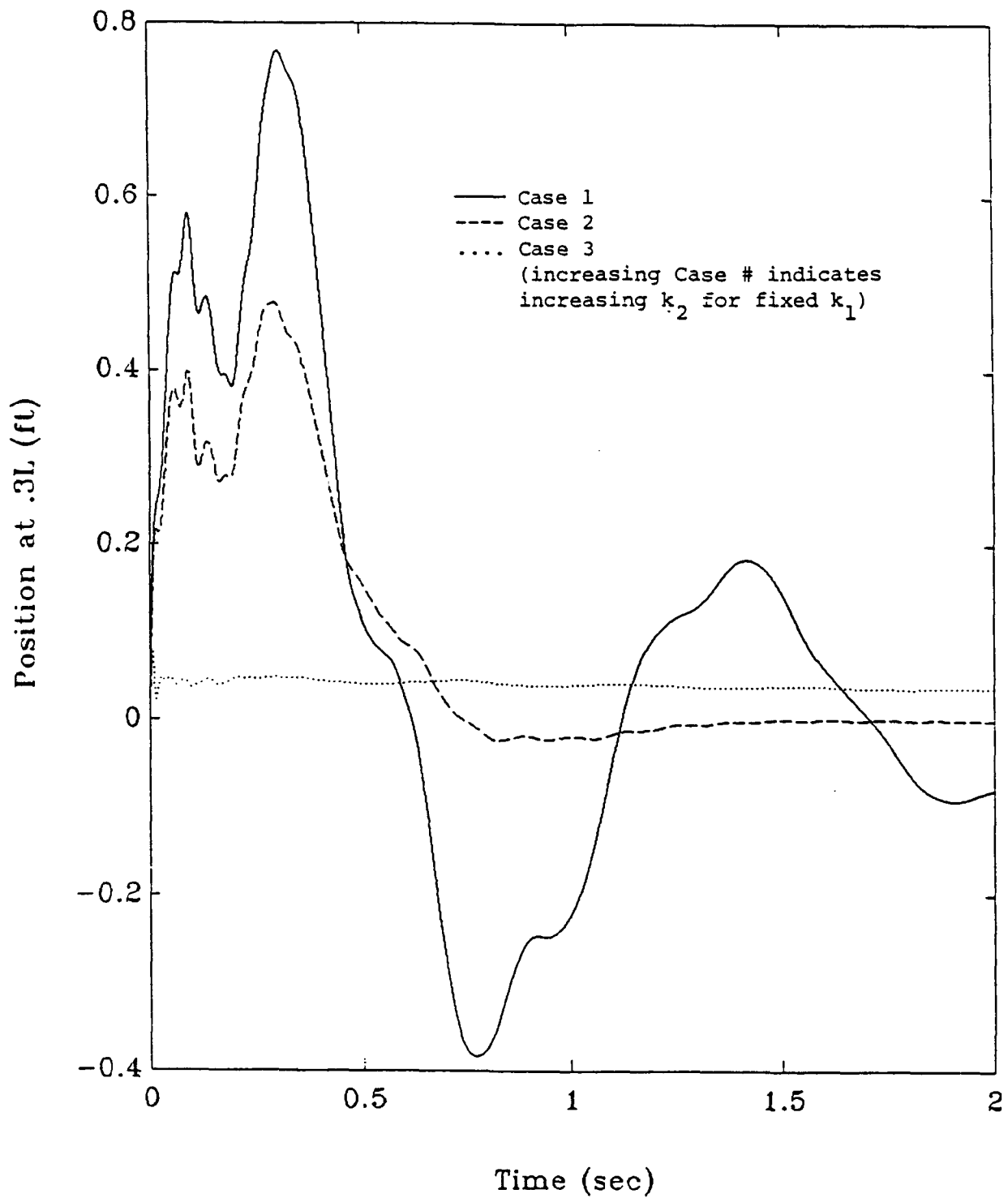
Figure 4.8a: Closed-loop system position response using various controllers and the 1-mode sensitivity-shaped estimator with no noise in the system and structural frequency variations of 20 %

Figure 4.8b: Closed-loop system velocity response using various controllers and the 1-mode sensitivity-shaped estimator with no noise in the system and structural frequency variations of 20 %

Figure 4.9a: Closed-loop system position response using various controllers and the 1-mode sensitivity-shaped estimator with no noise in the system and structural frequency variations of 20 %
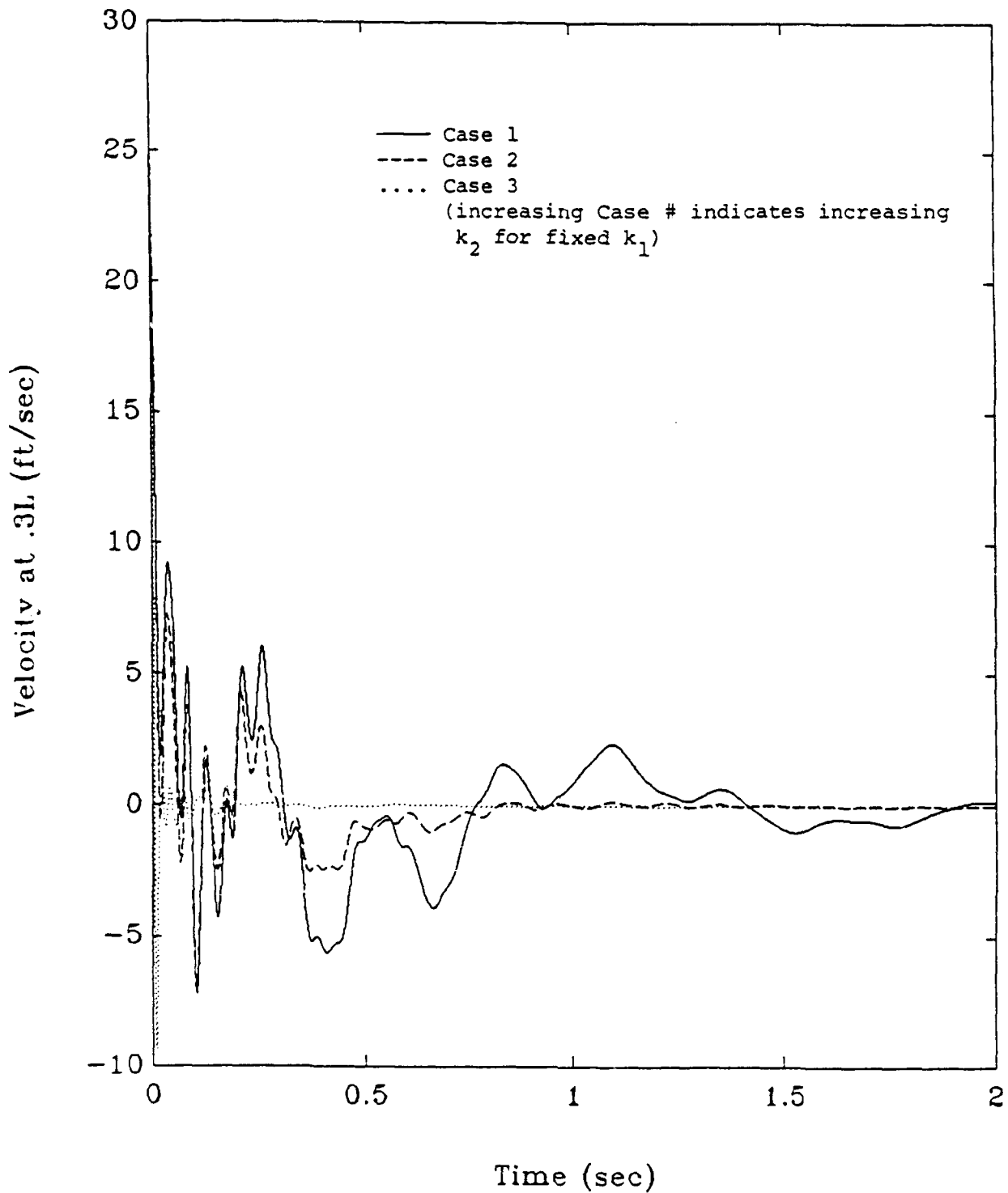
Figure 4.9b: Closed-loop system velocity response using various controllers and the 1-mode sensitivity-shaped estimator with no noise in the system and structural frequency variations of 20 %

Figure 4.9c: Closed-loop system position response using various controllers and the 1-mode sensitivity-shaped estimator with no noise in the system and structural frequency variations of 20 %
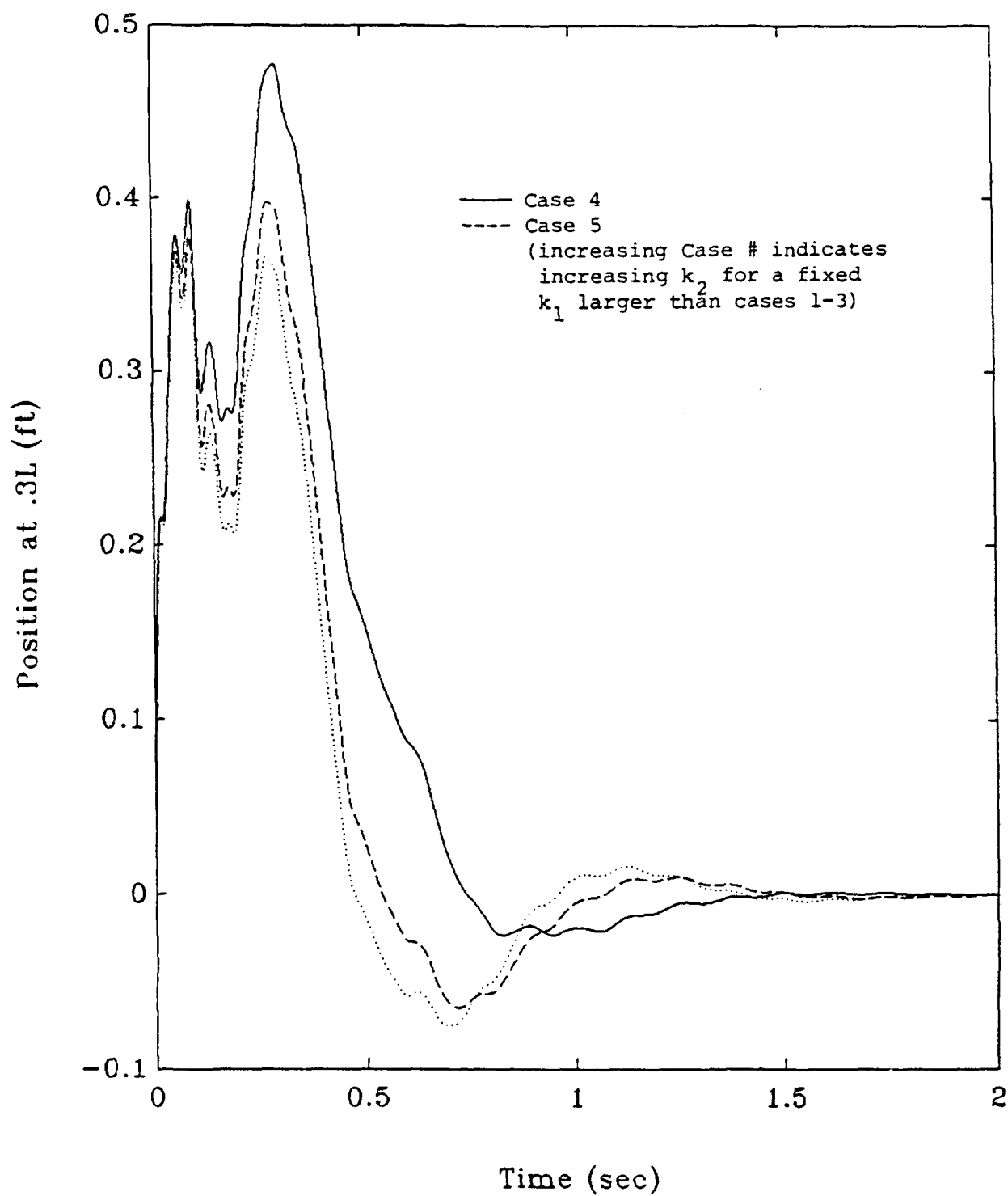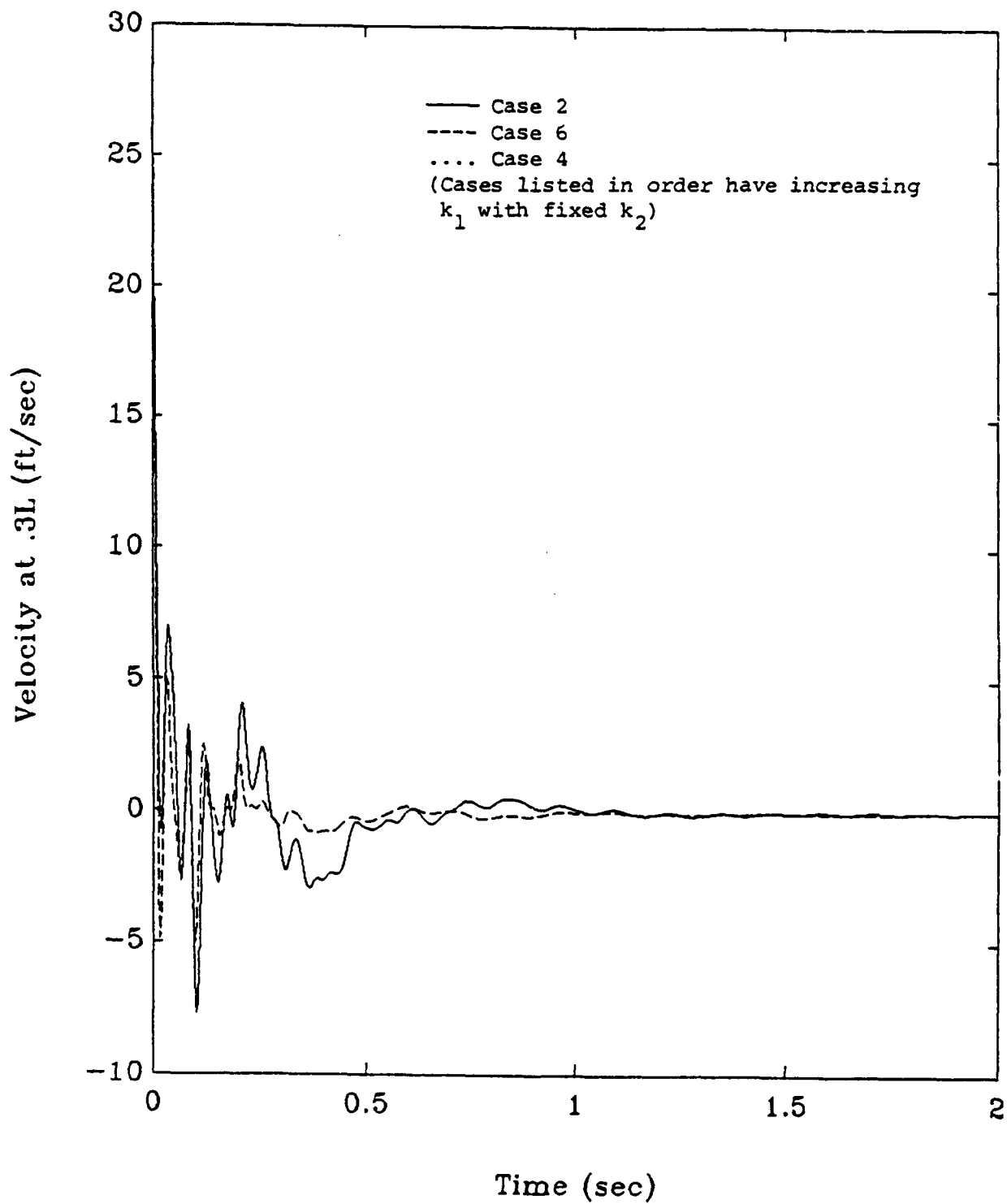
Figure 4.9d: Closed-loop system velocity response using various controllers and the 1-mode sensitivity-shaped estimator with no noise in the system and structural frequency variations of 20 %
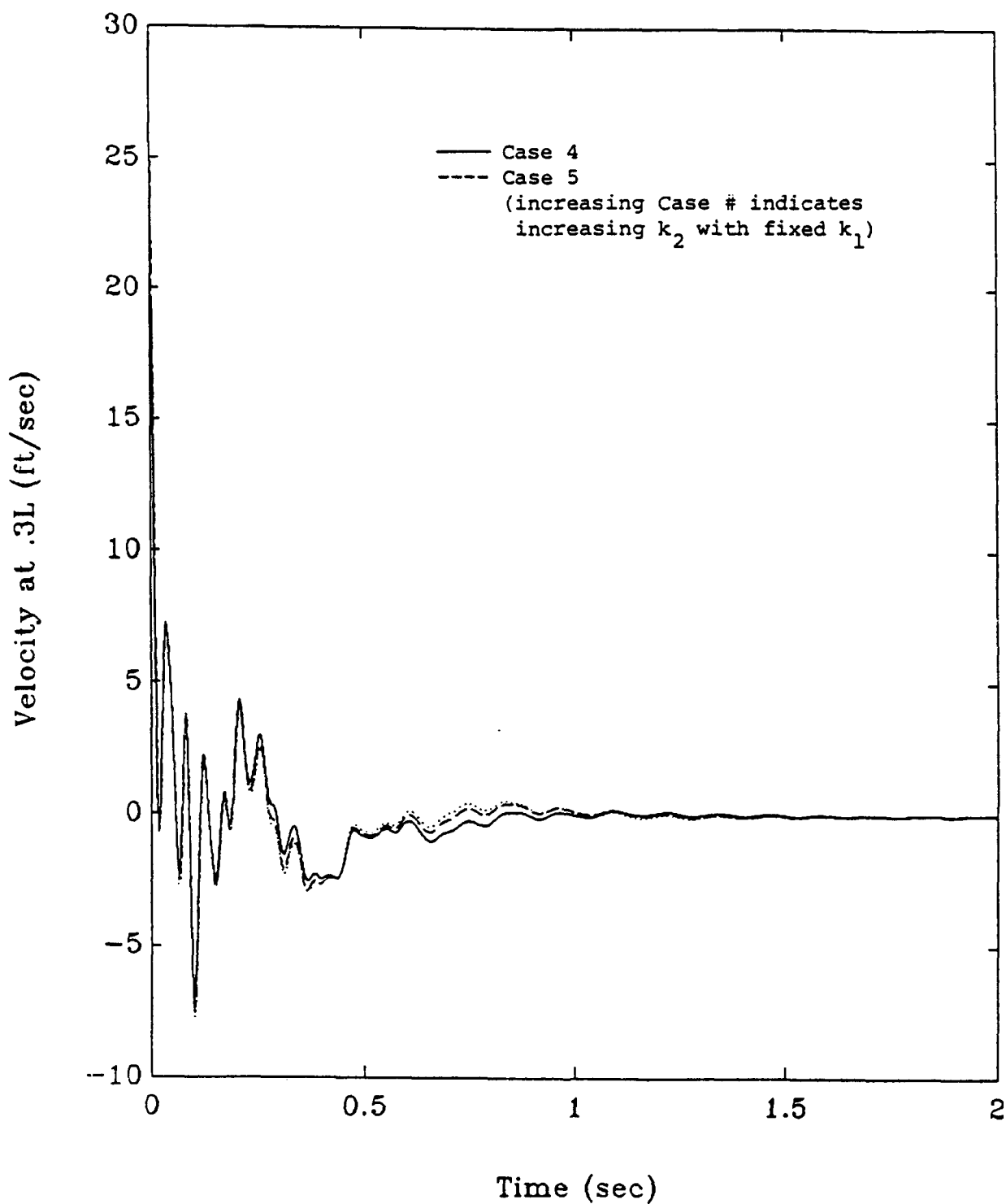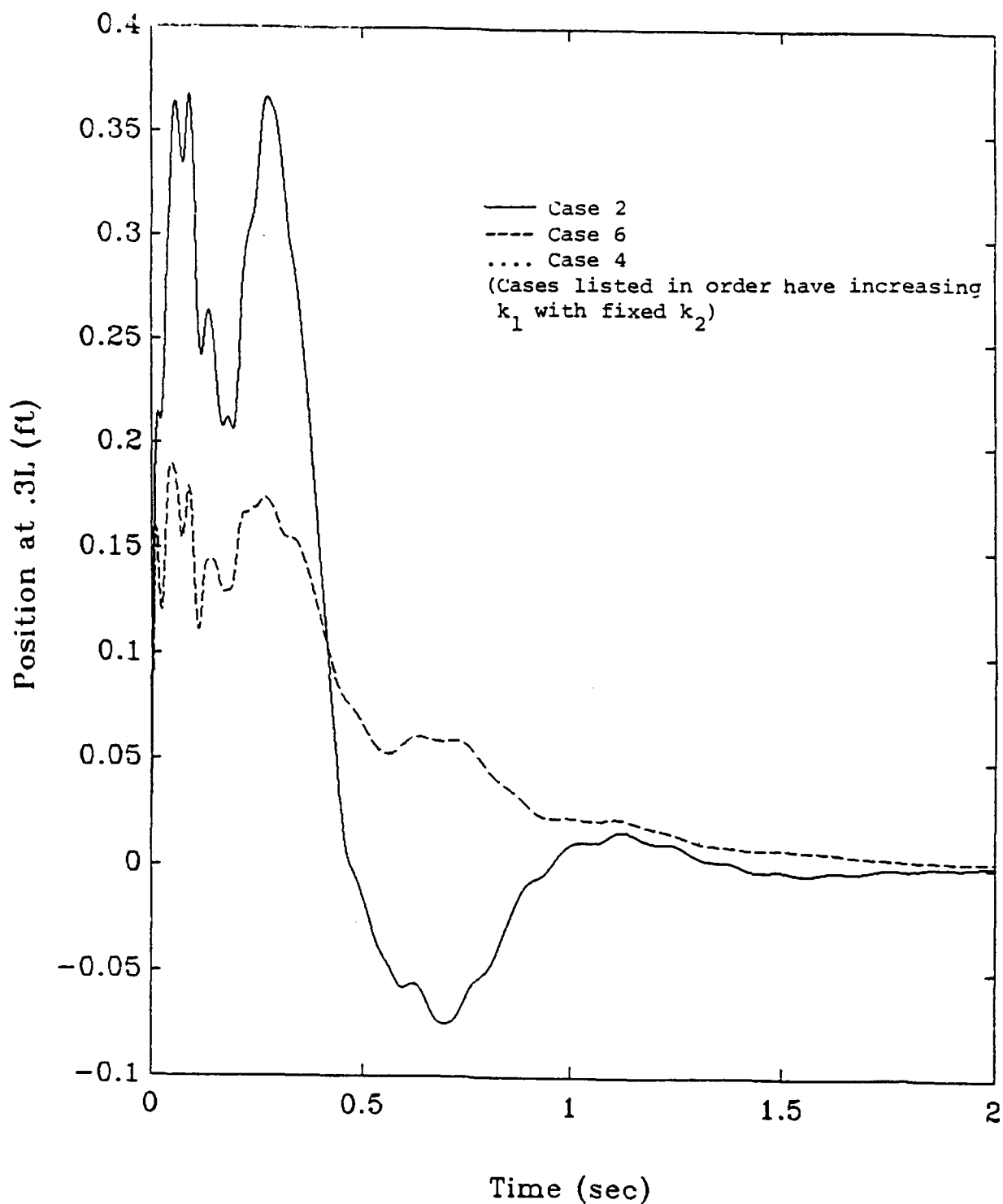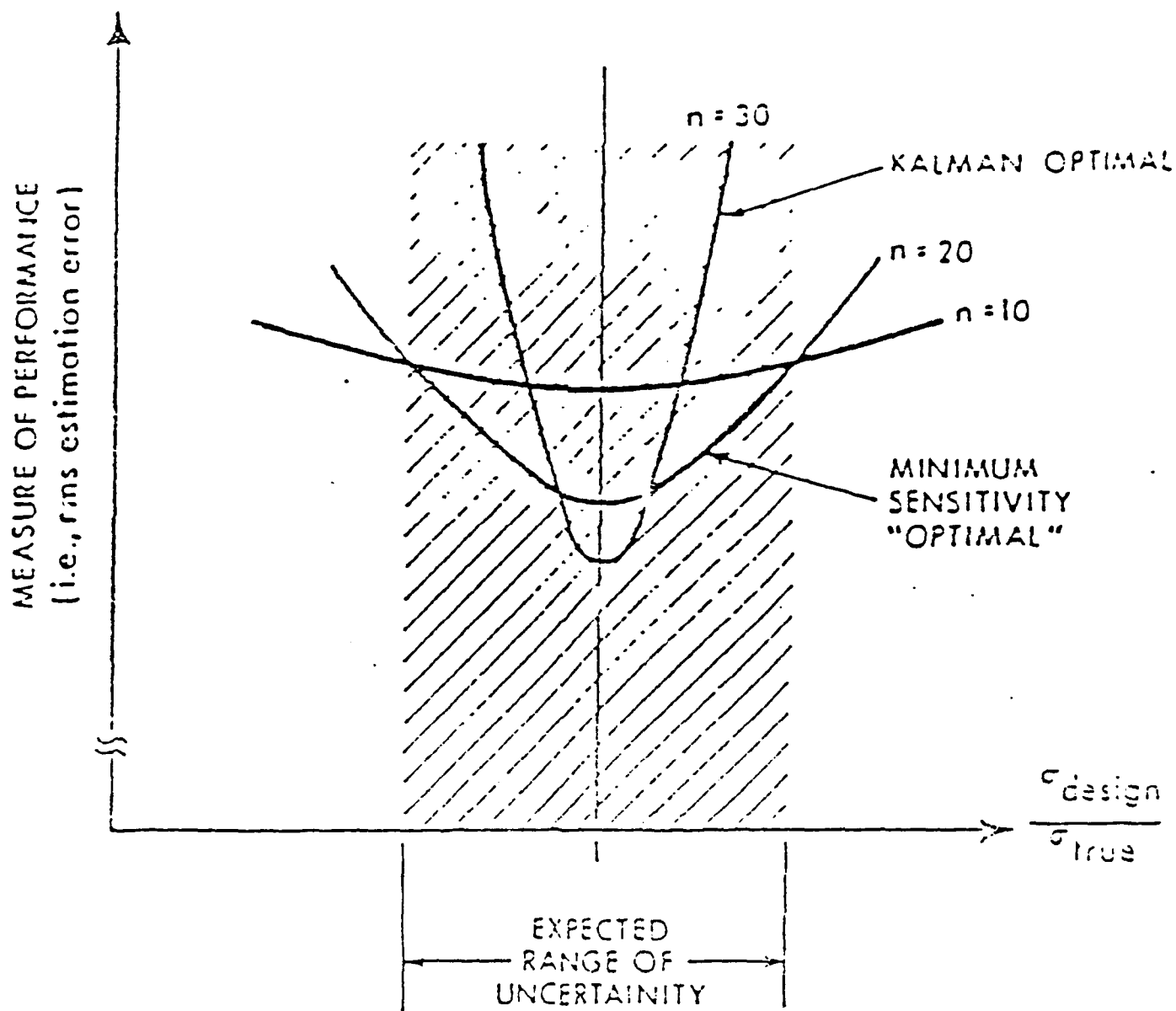
Figure 4.10: Conceptual example of designing for minimum sensitivity (σ_{true} held constant, σ_{design} is varied
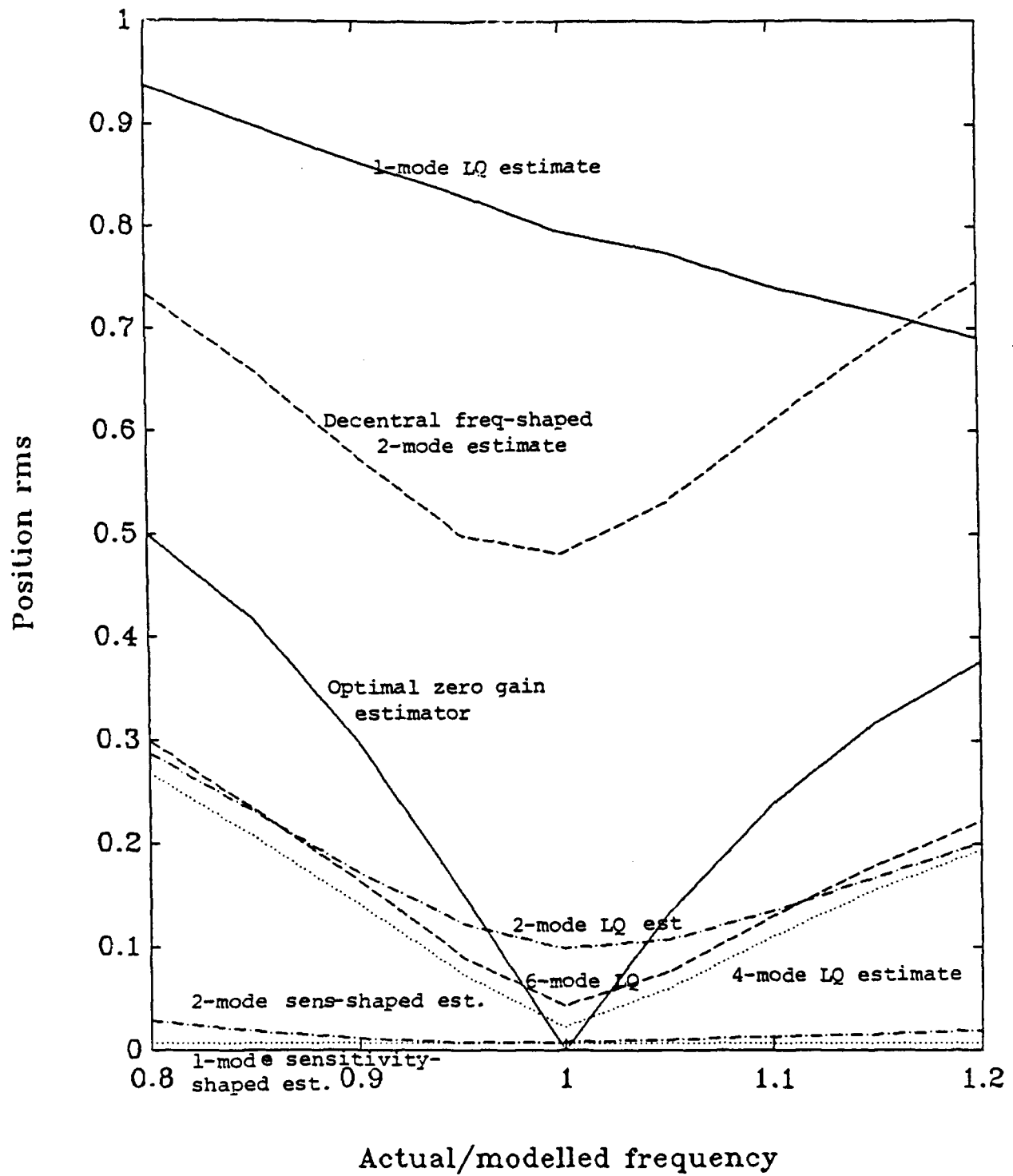
Figure 4.11a: Sensitivity of various estimators to variations in structural frequencies up to 20 %. System does not contain noise.

Figure 4.11b: Sensitivity of various estimators to variations in structural frequencies up to 20 %. System does not contain noise.

Figure 4.12a: Sensitivity of various estimators to variations in structural frequencies up to 20 %. Noise present in system.

Figure 4.12b: Sensitivity of various estimators to variations in structural frequencies up to 20 %. Noise present in system.

Chapter 5

Conclusions and Recommendations

Full and reduced-order centralized and decentralized estimators applied to a flexible structure have been evaluated. When perfect model informa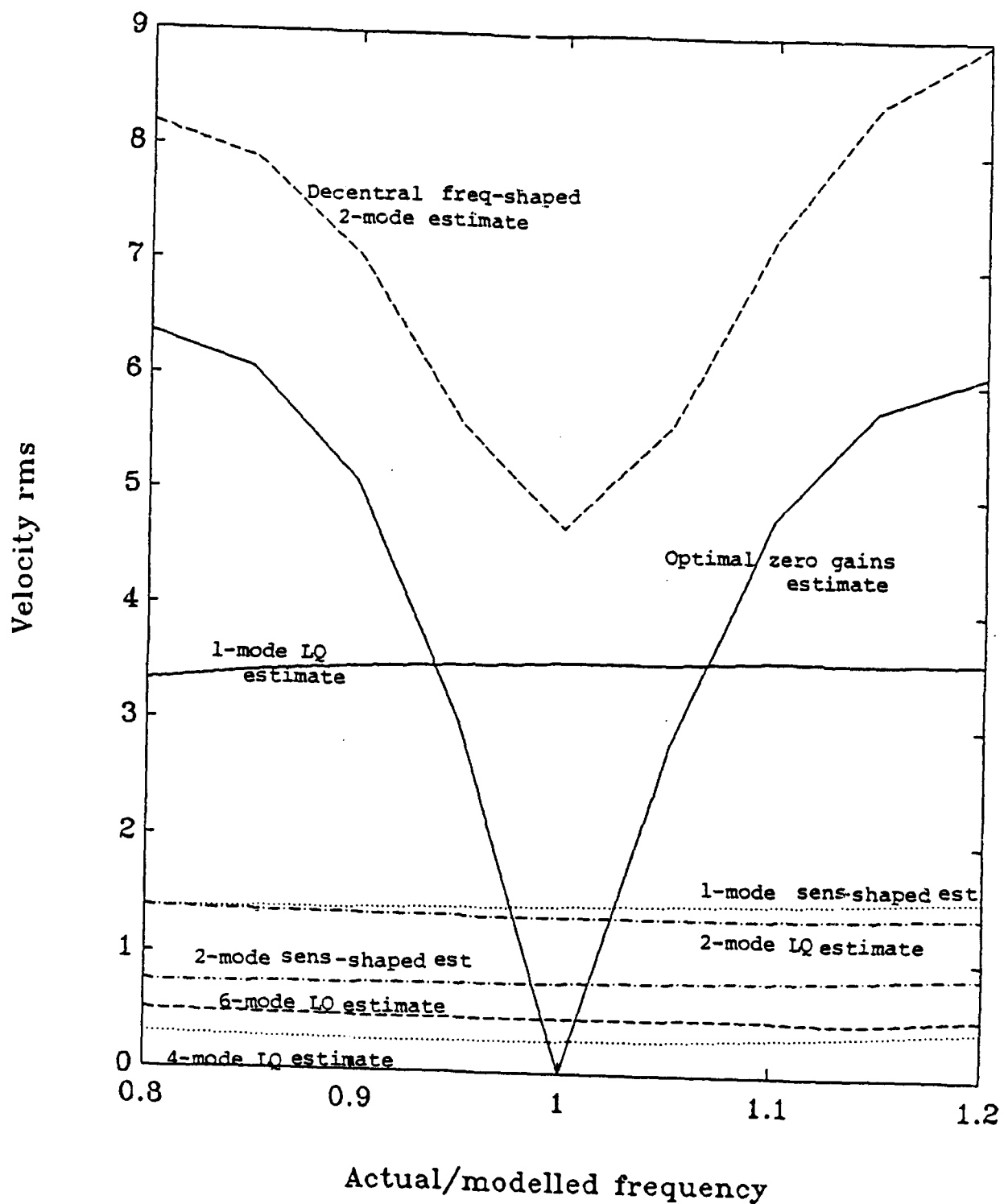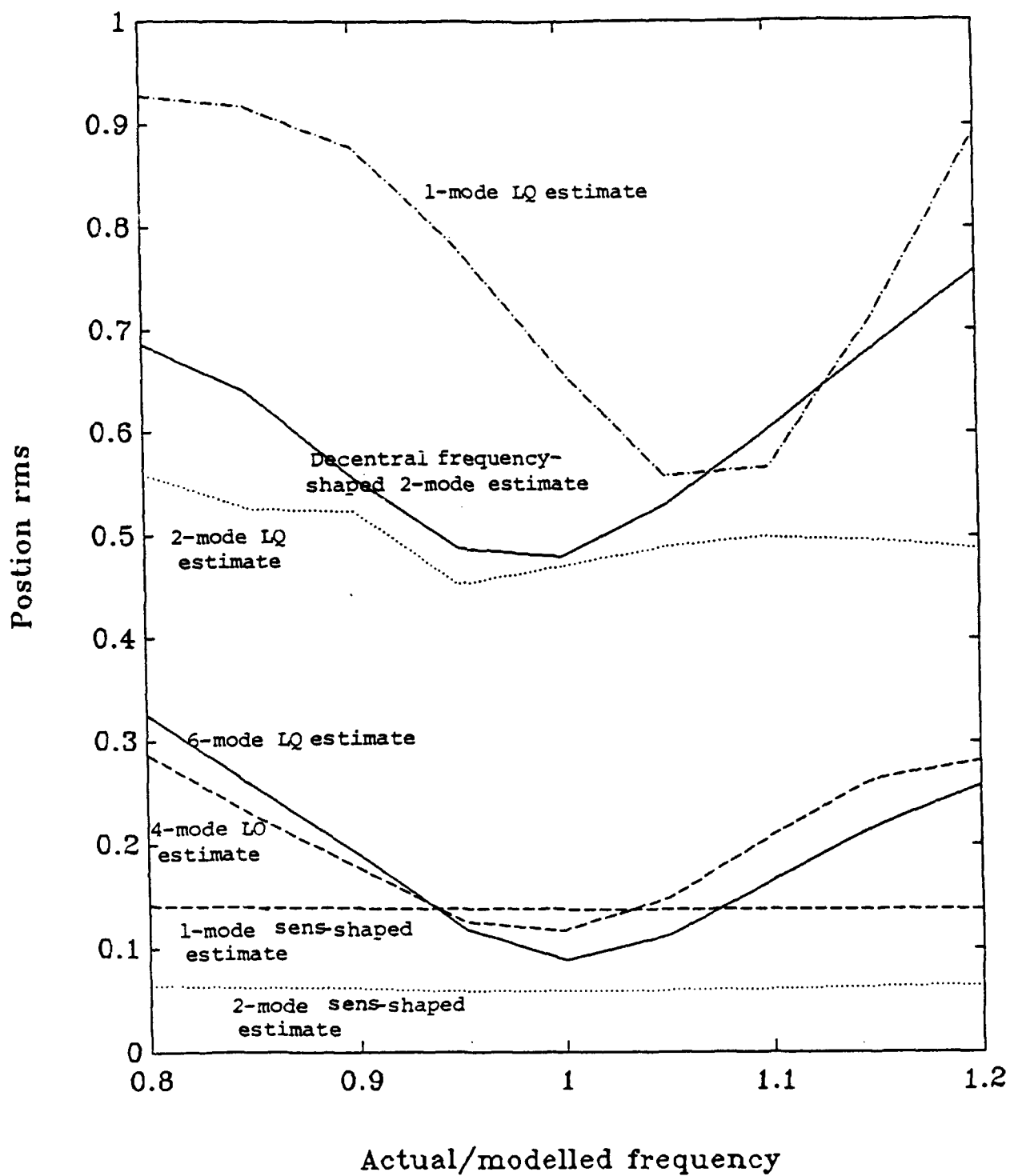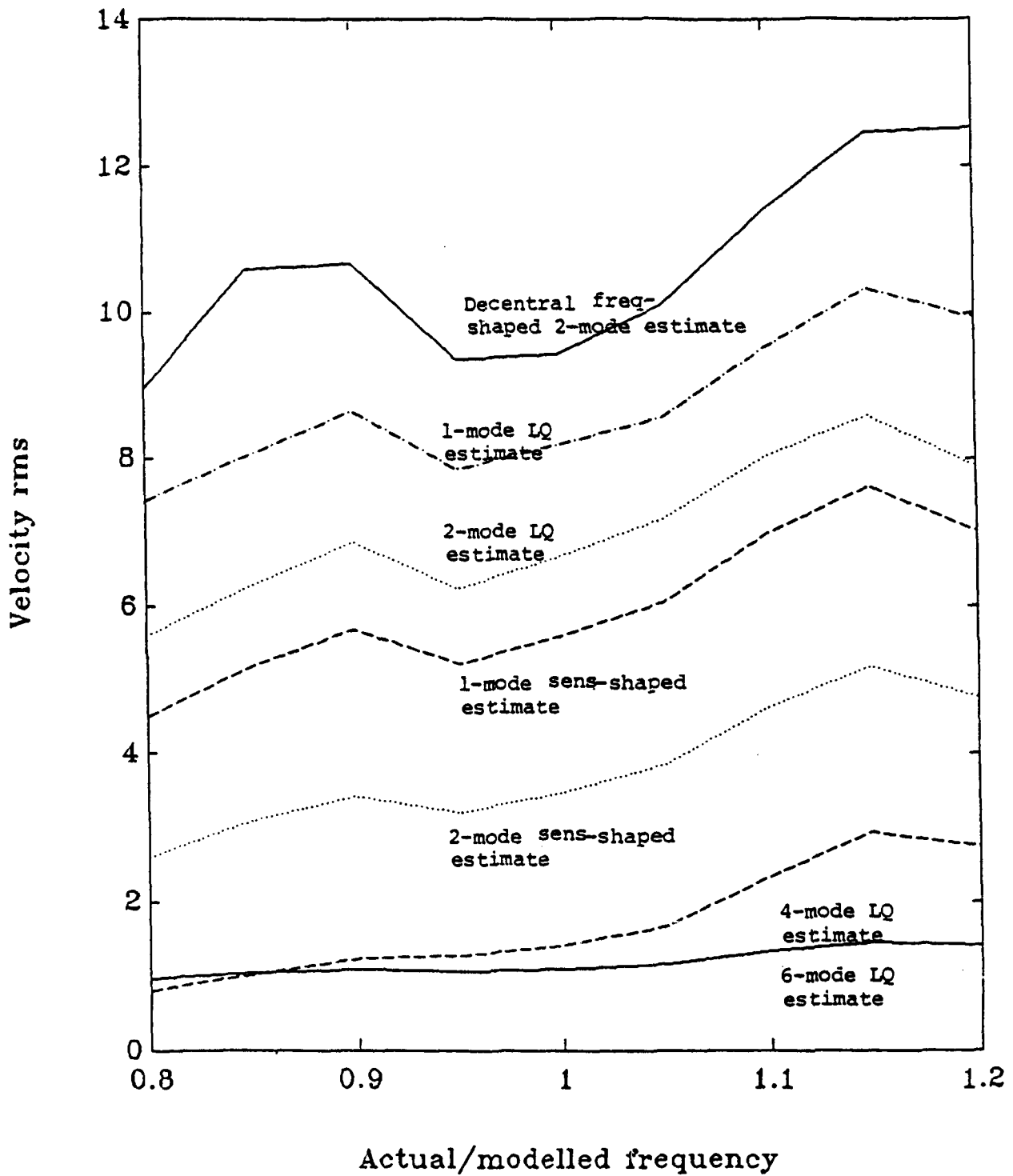tion exists, the full order Kalman filter is the optimal filter in the sense of minimizing the mean square value of the error. While errors are introduced via model order reduction and decentralization, these filters generally require less computation and design costs. A more extensive investigation into the errors introduced through decentralization, including a wider range of decentralized estimators, is suggested.

In actuality, perfect model information does not exist and the Kalman filter is no longer optimal under these modelling uncertainties. A sensitivity-shaped filter has been formulated to reduce sensitivities to variations in the structural frequencies and its estimates are compared to the centralized Linear Quadratic (LQ) filters and the decentralized frequency-shaped filter, all with 20 % structural frequency errors. The sensitivity-shaped filters' position estimates are superior to all other filters examined when modelling errors exist. The one-mode and two-mode sensitivity-shaped filters' velocity estimates are comparable to the two-mode and four-mode centralized LQ filters, respectively. Future work should include an investigation of the proposed general method to calculate gains of an n-mode filter.

Robustness of the closed-loop system with the one-mode sensitivity-shaped filter has been evaluated using a phase-shaping method which guaranteed the closed-loop system marginal stability, and using the Lyapunov method which guaranteed the closed-loop system asymptotic stability, both under structural frequency errors of 20 %. Both methods also assumed the controller gains met certain given requirements. Several controllers were investigated to examine the closed-loop system response – their gains were chosen via the Lyapunov method. The controller gains chosen via the Lyapunov method also satisfied the phase-shaping method requirements for controller gains. Preliminary studies indicate a need for further research into possible controller types and resulting closed-loop system responses.

A sensitivity to structural frequencies analysis has been conducted for all filter types introduced. Suboptimal filters are shown to be less sensitive to structural frequency variations than optimal filters. The sensitivity-shaped filters' position rms errors were lower than the centralized LQ and decentralized frequency-shaped filters when modelling errors existed. The one-mode and two-mode sensitivity-shaped filters' velocity rms errors were comparable to the two-mode and four-mode centralized filters, respectively, which indicates a saving in computation through order reduction.

Finally, the estimators evaluated in this study have been applied to a simple pinned-pinned beam. It is important to extend these results to a structure which would more closely represent a LFSS, such as a truss.

References

[1] Sridhar, Banavar, J.N. Auburn and K.R. Lorell, "Identification Experiment for Control of Flexible Structures," *IEEE Control Systems Magazine*, May 1985, pp 29-35.

[2] Wong, E.C., "In-flight Identification of the Galileo Spacecraft Flexible Mode Characteristics," *J of Guidance and Control*, Vol 9, No 1, Jan-Feb 1986, pp 92-98.

[3] Hossian, S.A. and K.Y. Lee, "System ID for Space Control Laboratory Experiment (SCOLE) Using Distributed Parameter Models," *Proc of the 26th IEEE Conf on Decision and Control*, L.A., CA, Dec 9-11, 1987, Vol 2, pp 1263-1268.

[4] Benhabib, R.J. , R.P. Iwens and R.L. Jackson, "Stability of LSS Control Systems Using Positivity Concepts", *J of Guidance and Control*, Vol 4, No 5, Sept-Oct 1981, pp 487-494.

[5] Meirovitch, L. , **Analytical Methods in Vibrations**, The Macmillan Company, New York, 1967.

[6] Kalman, R.E. , "A New Approach to Linear Filtering and Prediction Problems", *J of Basic Engineering*, Trans on ASME, Series D, Vol 82, No 1, March 1960, pp 35-45.

[7] Gelb, A. , editor, **Applied Optimal Estimation**, MIT Press, Massachusetts, 1974.

[8] Friedland, Bernard, "On the Properties of Reduced-order Kalman Filters", *Proc of the 26th Conf on Decision & Control*, Vol 2, L.A., CA, Dec 1987, pp 1601-1604.

[9] Corfmat, J.P. and A.S. Morse, "Decentralized Control of Linear Multivariable Systems", *Automatica*, Vo. 12, 1976, pp 479-495.

[10] Sandell, Nils. R. Jr. , P. Varaiya, M. Athans and M. Safonov, "Survey of Decentralized Control Methods for Large Scale Systems", *IEEE Trans on Automatic Control*, Vol AC-23, No 2, April 1978, pp 108-128.

[11] Young, K.D. and D.D. Siljak, "Robustness of Reduced order Decentralized Control Designs", *Proc of 24th Conf on Decision and Control*, Ft. Lauderdale, FL, Dec 1985, pp 1842-1843.

[12] Uskokovic, Zdravko and Juraj Medanic, "Sequential Design of Decentralized Low-Order Dynamic Regulators", *Proc of 24th Conf on Decision and Control*, Ft. Lauderdale, FL, Dec 1985, pp 837-842.

[13] Looze, D.P. , M. Athens and J.S. Eterno, "Decentralized Control of Sequentially Assembled Large Space Structures", *Proc of 24th Conf on Decision and Control*, Ft. Lauderdale, FL, Dec 1985, pp 1844-1851.

[14] Sezer, M.E. and D.D. Siljak, "Robustness of Suboptimal Control: Gain and Phase Margin", *IEEE Trans on Automatic Control*, Vol AC-26, No 4, Aug 1981, pp 907-911.

[15] Skelton, R. and C.Z. Gregory, "Measurement Feedback and Model Reduction by Modal Cost Analysis", *Proc of the JACC*, Denver, Colorado, 1979.

[16] Eitelberg, E. , "Model Reduction by Minimizing the Weighted Error", *International J of Control*, Vol 29, No 4, 1979, pp 541-556.

[17] Kabamba, P.T. , "Model Reduction by Euclidean Methods," *J of Guidance and Control*, Vol 3, No 6, 1980, pp 555-562.

[18] Pernebo, L. and L.M. Silverman, "Model Reduction via Balanced State Space Representation", *IEEE Trans on Automatic Control*, Vol AC-27, April 1982.

[19] Kwong, C.P. , "Optimal Chained Aggregation for Reduced-Order Modelling," *International J of Control*, Vol 35, No 6, 1982, pp 965-982.

[20] Lastman, G.J. and N.K. Sinha, "A Comparison of the Balanced Matrix Method and the Aggregation Method of Model Reduction," *IEEE CDC*, December 1983.

[21] Anderson, B.D.O. and J.B. Moore, **Optimal Filtering**, Prentice-Hall, Inc., New Jersey, 1979.

Appendix A

	mode 1	mode 2	mode 3	mode 4	mode 5	mode 6
frequency	7.0689	28.2757	63.6202	113.1026	176.7228	254.4809
damping ratio	.01	.02	.03	.04	.05	.06
measurement matrix	[0, 4.4501:	0, 5.2314:	0, 1.6998:	0, -3.2332:	0, -5.5007:	0, -3.2332]

pseudo noise

$Q = .5 * \mathrm{I}(\text{order } 2n)$, $R = .2 * \mathrm{I}(\text{order dim}(y))$, $n = \#$ of modes

mean of state noise (0.0)

-.011 .009 -.008 .015 .014 -.035 -.032 .026 -.004 -.081 -.014 .009

variance of state noise (.5)

.499 .510 .530 .502 .500 .431 .483 .501 .470 .449 .465 .491

standard deviation of state noise (.707)

.706 .714 .728 .708 .707 .657 .695 .708 .685 .670 .682 .701

mean of measurement noise (0.0)

-.019

variance of measurement noise (.2)

.217

standard deviation of measurement noise (.447)

.466

Filter types	Filter gains
1-mode LQ	$[-1.372, 5.741]^T$
2-mode LQ	$[-.460, 10.521, -1.502, 12.616]^T$
4-mode LQ	$[-.212, 10.829, -.784, 37.037, -.869, 61.831, 1.490, -8.485]^T$
6-mode LQ	$[-.116, 10.778, -.406, 40.362, -.267, 70.596, .446,$ $-127.575, 1.235, -109.689, 1.118, 132.774]^T$

Decentral frequency-shaped 2-mode

mode 1: $[-.01, .01]^T$

mode 2: $[-.01, .1]^T$

1-mode sensitivity-shaped

$[.2247, 30]^T$

2-mode sensitivity-shaped

$[.2247, 30, .1912, 70]^T$

Appendix B

Proof of Theorem 3:

$H_F(s)$ is, in the case of the one-mode sensitivity-shaped filter, a column matrix with transfer function elements $[H_{F_1} \; H_{F_2}]$. If the phase of a transfer function element lies between $\pm$ 90 degrees not including the endpoints, then the transfer function is a strictly positive real function. Also for this case, the controller gain matrix is given by $[k_1 \; k_2]$. If k_1 and k_2 are both positive, then the feedback transfer matrix $H(s) = K H_F(s)$ is the sum of two strictly positive real transfer functions, $k_1 H_{F_1} + k_2 H_{F_2}$. The statement to prove, then, is that the sum of strictly positive real functions is a strictly positive real function.

Let $H(s) = H_1(s) + H_2(s) + ... + H_r(s)$. Then

(a) If $H_1(s), H_2(s), ..., H_r(s)$ have real elements for real s, then $H(s)$ also has real elements for real s.

(b) If $H_1(s), ..., H_r(s)$ have elements analytic for $\Re(s) \geq 0$, then $H(s)$ has real elements for $\Re(s) \geq 0$.

(c) By the definition of a positive real function, for all $x \neq 0$, and for all real ω,

$x^*[H_1(j\omega) + H_1^*(j\omega)]x > 0, ..., x^*[H_r(j\omega) + H_r^*(j\omega)]x > 0.$

Then the sum of these functions is also positive

$x^*[H_1(j\omega) + H_1^*(j\omega)]x + ... + x^*[H_r(j\omega) + H_r^*(j\omega)]x > 0.$

This can be factored as

$x^*[H_1(j\omega) + ... + H_r(j\omega) + H_1^*(j\omega) + ... + H_r^*(j\omega)]x > 0$ or

$x^*[H(j\omega) + H^*(j\omega)]x > 0$ which states that $H(s)$ is a positive real function.